Phytoplankton Diversity in Relation to Coastal Physical Processes

by

Paula S. Bontempi
and
Denis A. Wiesenburg

Institute of Marine Sciences
University of Southern Mississippi
Stennis Space Center, MS 39529

Final Report

Prepared for

Department of the Navy
Office of Naval Research
800 North Quincy Street
Arlington, Virginia 22217-5000

Contract No. N00014-93-1-0513

Report No. IMS-97-01

February 1997

REPORT DOCUMENTATION PAGE

Form Approved
OMB No. 0704-0188

1. AGENCY USE ONLY (Leave blank)	2. REPORT DATE	3. REPORT TYPE AND DATES COVERED
	March 1997	Final 01 May 93 - 31 Jul 96

4. TITLE AND SUBTITLE
Phytoplankton Diversity in Relation to Coastal Physical Processes

5. FUNDING NUMBERS
G N00014-93-0513

6. AUTHOR(S)
Denis A. Wiesenburg
Paula S. Bontempi

7. PERFORMING ORGANIZATION NAME(S) AND ADDRESS(ES)
Texas A&M Research Foundation
Box 3578
College Station, TX 77843

8. PERFORMING ORGANIZATION REPORT NUMBER
8457

9. SPONSORING/MONITORING AGENCY NAME(S) AND ADDRESS(ES)
Office of Naval Research
800 North Quincy Street
Arlington, VA 22217-5000

10. SPONSORING/MONITORING AGENCY REPORT NUMBER

11. SUPPLEMENTARY NOTES

12a. DISTRIBUTION/AVAILABILITY STATEMENT

12b. DISTRIBUTION CODE

13. ABSTRACT *(Maximum 200 words)*

This study describes and interprets phytoplankton distributions across the Texas-Louisiana shelf, detailing relationships among the major phytoplankton groups, including diatoms (Bacillariophyceae), dinoflagellates (Dinophyceae), coccolithophorids (Prymnesiophyceae), silicoflagellates (Chrysophyceae), and microflagellates (Cryptophyceae and Prasinophyceae, and some Prymnesiophytes). Phytoplankton distributions will be related to physical processes acting on the shelf and to variable seasonal Mississippi River flows from May 1992 to May 1993. The role of phytoplankton as the basis of the oceanic food chain merits this study. The objective is to establish a 2-dimensional model for predicting dominant phytoplankton species, distributions, and biomass across the Texas-Louisiana continental shelf under a given set of hydrographic, river flow, and physical conditions. These variations in the phytoplankton community will be documented seasonally and anually. Coastal on-shore/off-shore gradients of phytoplankton are interpreted with the dominant environmental parameters. Both dynamic physical forces, such as mixing, and diffusive processes, such as nutrient regeneration from sediments, are addressed.

14. SUBJECT TERMS

15. NUMBER OF PAGES

16. PRICE CODE

17. SECURITY CLASSIFICATION OF REPORT	18. SECURITY CLASSIFICATION OF THIS PAGE	19. SECURITY CLASSIFICATION OF ABSTRACT	20. LIMITATION OF ABSTRACT
UNCLASSIFIED	UNCLASSIFIED	UNCLASSIFIED	UL

Executive Summary

Acknowledgements

Contents

List of Figures

All Figures Follow the Text of this Report

Introduction

Phytoplankton are microscopic unicellular algae that are the basis of the oceanic food chain. The majority of phytoplankton are primary producers (plants), which transfer energy necessary for survival to higher trophic levels. Changes in the phytoplankton population may affect upper trophic levels such as fish and larger filter-feeding mammals. Phytoplankton contribute about 40% of the global plant algal biomass (autotrophic) (Gould 1987) and significantly contribute to the amount of oxygen produced globally. Phytoplankton biomass and distributions respond to changing environmental conditions in oceanic and coastal waters seasonally and annually, and these changes cause subsequent responses among secondary producers and consumers in upper trophic levels. Because of the effects phytoplankton have on commercially important species and on the global ecosystem, seasonal and annual changes in phytoplankton are important to know and to understand.

Determining phytoplankton concentrations and species composition is generally important to the hierarchy of the oceanic ecosystem. Knowledge of phytoplankton species composition and concentrations is valuable as certain phytoplankton are toxic and can cause fish kills and red tide events as observed on the Texas-Louisiana continental shelf (Harper and Guillen 1989; Seagrant-Texas A&M University 1986). Knowledge of which phytoplankton species dominate continental shelf waters and of the dominant species' seasonal concentrations may allow rapid assessment of mortality event causes. The questions are how do phytoplankton, the key primary producers, respond to different environments created by changing hydrographic, physical, and riverine conditions in dynamic areas of the coastal United States, and can we

develop a predictive model for a particular ecosystem? We chose to examine the Texas-Louisiana continental shelf in the northern Gulf of Mexico (Figure 1). The Texas-Louisiana shelf is affected by seasonal Mississippi River flows (nutrient loads and buoyancy forcing), physical oceanography (circulation patterns and currents), and variable hydrographic conditions (salinity and nutrients) each year.

Objectives

Few studies have evaluated phytoplankton distributions, biomass, and species composition of the world's oceans or continental shelves. Even more scarce are studies of the phytoplankton community on the Texas-Louisiana continental shelf. Riley (1937), Thomas and Simmons (1960), and El-Sayed (1972) conducted studies based on the assessment of very few samples from restricted study areas. Fucik (1974) documented phytoplankton production from only two stations off Timbalier Bay in the Gulf of Mexico. The Texas Outer Continental Shelf Study evaluated phytoplankton abundance, diversity, and production seasonally from 12 stations in the western Gulf of Mexico (Van Baalen 1975). Lohrenz et al. (1990) conducted a study of the Mississippi River plume only, and they did not measure phytoplankton directly. No full-scale evaluation of processes that cause variations in phytoplankton abundance, species composition, and distributions over the Texas-Louisiana shelf has been conducted until now.

This study describes and interprets phytoplankton distributions across the Texas-Louisiana shelf, detailing relationships among the major phytoplankton groups, including diatoms (Bacillariophyceae), dinoflagellates (Dinophyceae), coccolithophorids (Prymnesiophyceae), silicoflagellates (Chrysophyceae), and microflagellates (Cryptophyceae and

Prasinophyceae, and some Prymnesiophytes). Phytoplankton distributions will be related to physical processes acting on the shelf and to variable seasonal Mississippi River flows from May 1992 to May 1993. The role of phytoplankton as the basis of the oceanic food chain merits this study. The objective is to establish a 2-dimensional model for predicting dominant phytoplankton species, distributions, and biomass across the Texas-Louisiana continental shelf under a given set of hydrographic, river flow, and physical conditions. These variations in the phytoplankton community will be documented seasonally and annually. Coastal on-shore/off-shore gradients of phytoplankton are interpreted with the dominant environmental parameters. Both dynamic physical forces, such as mixing, and diffusive processes, such as nutrient regeneration from sediments, are addressed.

Texas-Louisiana Continental Shelf

Different phytoplankton species proliferate in different environments, and environmental conditions and forces vary seasonally in the coastal waters of a continental shelf. The coastal ocean/continental shelf is in a state of flux due to physical processes that circulate and mix the waters. Deciphering the complex interactions between the biology and physical and hydrographic processes will lead to a better understanding of global biogeochemical cycles (Csanady, 1990); only then can accurate assessments of phytoplankton diversity be quantified and predictions of coastal ocean productivity through phytoplankton biomass estimates be made. Hydrography, physical processes, and riverine input have a significant impact on phytoplankton on the Texas-Louisiana continental shelf.

The Texas-Louisiana shelf in the northern Gulf of Mexico is an estuarine coastal system subject to changing flows of the Mississippi River and of the Atchafalaya River. The U.S. Army Corps of Engineers has diverted 30% of the Mississippi River flow down the Atchafalaya River, located 250 kilometers to the west of the Mississippi River along the Louisiana coast. The Mississippi River drains 41% of the contiguous United States (Figure 2) and delivers 300 km^3 of fresh water annually, approximately 54% of Mississippi River discharge, onto the continental shelf west of the Mississippi River Delta (Dinnel and Wiseman 1986). Changes in meteorology over the drainage basin, such as the amount of rainfall, will alter the amount of fresh water and associated riverine nutrient loads transported to the shelf.

Outflow rates of the Mississippi River system are annually variable (Figure 3). This study compares phytoplankton distributions in 1992, an average flow year for the Mississippi

River, and in 1993, a record flow year for the river (U.S. Army Corps of Engineers 1993). Time periods examined in this report are spring (April/May), summer (August), and fall (November) 1992, and winter (February) and spring (April/May) of 1993.

Nutrients and river flow

The variability of nutrient levels in river water is a well-addressed subject because of the importance of nutrients to the resident crop of phytoplankton (Riley 1937; Throndsen 1960; Sklar and Turner 1981; Lohrenz et al. 1990; Turner and Rabalais 1991). Seasonal changes in Mississippi and Atchafalaya river flow significantly alter the quantities of nutrients entering the shelf ecosystem (Sklar and Turner 1981). Nutrient levels in Mississippi River water can vary due to human dumping of wastes and fertilizers into the river. Smith et al. (1987) discovered that in the past few decades large changes have occurred in the concentrations of several compounds, especially nitrate, in the nation's rivers. This nutrient increase is important, as the types and quantities of nutrients contained in river outflow will dictate exactly where and to what extent primary production will take place on the shelf. Thus the Mississippi River, conducting the sixth largest volume of fresh water in the world, has a significant impact on the Texas-Louisiana shelf phytoplankton and on other aspects of the shelf ecosystem.

Not only nutrient concentrations but also water temperature (optimal to phytoplankton growth rates), grazing of phytoplankton by zooplankton and secondary consumers (Brown 1994), and sinking of phytoplankton cells can be limiting to primary production. Light levels have also been found to be a limiting factor for primary production, as in the Mississippi River plume (Lohrenz et al. 1990). Meteorological conditions may affect light availability, as can

phytoplankton blooms or expansive population growth, which can affect transparency to light and ocean color (Smith and Baker 1985). Nutrients have been documented as the primary limiting factor for phytoplankton growth and production in most coastal and oceanic waters.

Effects of riverine input of nutrients on phytoplankton distributions have been examined on other continental shelves. Schindler (1978) described how increases in the annual input of nutrients due to riverine input and other sources cause a proportional increase in phytoplankton production and biomass. In the North Sea, Fransz and Verhagen (1985) found increased primary production and phytoplankton concentrations due to increased nutrient availability. Hecky and Kilham (1988) found that relative proportions of nutrients supplied to the phytoplankton shaped the phytoplankton communities and affected biomass yield relative to the limiting nutrients. Utilization of silicate depended on silicate availability in Conley et al.'s (1989) study, as physiological differences in silicate use were described for different diatoms. On the Texas-Louisiana shelf, Dortch and Whitledge (1992) found that varying nutrient concentrations carried by the Mississippi River influenced phytoplankton biomass and production in the Gulf of Mexico. A result of phytoplankton biomass increases due to nutrient input may be greater competition among phytoplankton, causing light to become the limiting factor (Hecky and Kilham, 1988).

Greater phytoplankton concentrations were located near shore and decreased seaward in the Delaware and Chesapeake Bay plumes (Marshall and Cohn 1987). Edmond et al. (1981) found diatoms to dominate on the shelf in the Amazon River plume while removing nitrate and phosphate from the surface layer. The Changjiang (Yangtze) River, with the third largest river discharge in the world, affected phytoplankton communities due to the large amounts of nutrients

it transports (Xiuren et al. 1988). Inorganic nutrient input was affirmed there by Vaulot and Xiuren (1988). One of few surveys of river-borne nutrients in the northern Gulf of Mexico was the Nutrient-Enhanced Coastal Ocean Productivity (NECOP) study (1990-1994), which found that nutrients coming out of the Mississippi River greatly affected the Texas-Louisiana shelf ecosystem. Dortch and Whitledge (1992) speculated that the changing concentration of the nutrient load, i.e. silica, carried by the Mississippi River altered the phytoplankton community species composition.

The lower salinity of the Mississippi and Atchafalaya river waters can also influence the phytoplankton community. Fluctuations in salinity due to variable river flow have affected photosynthesis and growth of different phytoplankton species (Smayda 1969; Paasche 1975; Krawiec 1982; Miller and Kamykowski 1986a; Lohrenz et al. 1990). If phytoplankton are affected by salinity, primary production will be affected accordingly.

Phytoplankton requirements and growth

Each phytoplankton species has specific requirements for growth. If the nutrients necessary for growth are not present in sufficient concentrations in the resident water mass, growth will not occur. Walsh et al. (1981) found that phytoplankton populations on the continental shelves off Peru, western Mexico, and the Middle Atlantic Bight require nitrogen for growth. The major source of nitrate in these areas was river runoff. Tilman et al. (1982) also found algal uptake of nitrogen when it was available to phytoplankton. Increased nitrogen and phosphorous levels benefitted flagellates in a study by Officer and Ryther (1980). Turner and Rabalais (1991) found that diatom numbers to increase when silicate availability increased.

Riley (1937) found phosphate input from the Mississippi River was a limiting factor for phytoplankton growth across the Texas-Louisiana shelf. Nitrate and phosphate utilization have been correlated with maximum phytoplankton biomass in the Chesapeake and Delaware Bays (Fisher et al. 1988). Effects of variability in nitrate, silicate, and phosphate levels on the Texas-Louisiana shelf phytoplankton population are addressed in this study.

Phytoplankton can be nitrogen-, phosphorous-, or silica-limited based on availability. A depletion in any of these nutrients could result in a shift in phytoplankton abundance and species composition. This compositional shift will ultimately influence trophodynamics and biogeochemical processes in the ecosystem. Dortch and Whitledge (1992) found this affect of nutrient limitation on the Texas-Louisiana shelf. Phytoplankton across the shelf are subject to a changing environment due partly to salinity and nutrient fluctuations caused by variable Mississippi River input (Geyer 1950). Mixing of the fresh, nutrient-rich river water and the oligotrophic, more saline Gulf of Mexico waters moves us to address what physical forcing mechanisms drive the shelf circulation seasonally and disperse the river water.

Physical Oceanography of the Texas-Louisiana Shelf

Many physical processes influence phytoplankton distributions, abundances, and species composition in coastal environments. Fransz and Verhagen (1985) found winds, tides, and turbulent mixing to influence the biology of the North Sea. On the Texas-Louisiana shelf, these processes include a low-frequency cyclonic circulation pattern (Cochrane and Kelly 1986), turbulent vertical mixing (Neuhard 1994), wind-driven mixing (Tilman et al. 1982), shelf-edge upwelling (Sahl et al. 1993), and the presence of features such as eddies or rings (Hitchcock et al. 1987; Gould 1988; Bontempi 1995). Physical processes on the Texas-Louisiana shelf distribute fresh water and associated nutrients from the Mississippi and Atchafalaya rivers (Dortch and Whitledge 1992; Dinnel and Wiseman 1993; Sahl et al. 1993).

The phytoplankton community, and therefore primary production on the Texas-Louisiana shelf, can be enhanced or limited depending not only on the volume of riverine input and associated nutrient loads, but also by where this flow is directed by large-scale physical processes such as winds and currents after leaving the river delta. Each season the shelf is subject to different circulation patterns (Cochrane and Kelly 1986) and variable river flows (U.S. Army Corps of Engineers 1995).

Small-scale physical forcings also occur on the Texas-Louisiana shelf. Upwelling results from a shift in wind direction (Pond and Pickard 1983), transporting nutrient-rich waters to an oligotrophic area (Sahl et al. 1993). Eddies or rings form as a result of meanders in the Loop Current (Angel and Fasham 1983), and these eddies can travel across the Gulf of Mexico and affect the outer Texas-Louisiana continental shelf. Eddies can entrain nutrient-rich waters and

advect them to a nutrient-poor area (Bontempi 1995).

Earlier studies on the Texas-Louisiana shelf have shown effects of large-scale and small-scale mixing processes. Dinnel and Wiseman (1986) showed Mississippi and Atchafalaya river waters mixing with offshore waters as an indicator of rapid, large-scale diffusive mixing. Lohrenz et al. (1990) found this mixing to result in intermediate salinities and showed this mixing zone to have increased production levels. Dinnel and Bratkovich (1993) also showed Mississippi River discharge to affect circulation on the shelf, particularly in the northwest Gulf of Mexico.

The description of overall Texas-Louisiana shelf circulation patterns is from Cochrane and Kelly (1986) and has been confirmed by the Texas-Louisiana Shelf Circulation and Transport Processes Study (LATEX A) moored current meter and Acoustic Doppler Current Profiler (ADCP) data (Jochens and Nowlin 1994). Different seasonal general circulation patterns prevail on the shelf, as revealed in Figure 4, a diagram of time-averaged geopotential anomalies relative to 70 dbar for the Texas-Louisiana shelf during different months. This circulation is responsible for directing river flow and for influencing phytoplankton distributions. Circulation patterns will be described for each month that phytoplankton distributions were observed and assessed, as demonstrated by calculated geopotential anomalies from seasonal shelf cruises. Detailed accounts of circulation patterns are found in Cochrane and Kelly (1986) and LATEX A annual reports.

Seasonal shelf circulation patterns

The Texas-Louisiana continental shelf stretches from Brownsville, TX, to the Mississippi

River Delta (Figure 5). The focus for this study is the Louisiana shelf and a small part of the Texas shelf west of 94°W longitude. Unlike circulation patterns on other continental shelves in the United States, Texas-Louisiana shelf circulation is not based on the existence of one main large current near the shelf break. Circulation is driven by two major processes: Ekman transport and the geostrophic current. Ekman transport is related to wind stress, while geostrophic flow is related to density. Both of these circulatory features are affected by the Coriolis force and are described for the shelf by Neuhard (1994) and Bontempi (1995).

The wind's strength and direction are responsible for the currents along most of the coastline of Texas and Louisiana. The coastal, cross-shelf, and shelf-break currents comprise a circulation pattern that exists with little variability across the Texas-Louisiana shelf during most of the year. Coastal currents change due to the change in monthly mean alongshore components of the wind. The circulation differs with location due to geographical variations in the frequency distribution of the wind and to the orientation of the coastline. Wind direction is normal to the coast, and a convergence point of coastal currents results; convergence indicates the point toward which flows are directed from both sides. Wind direction varies seasonally, causing a seasonal migration in the convergence point of coastal currents.

The pattern of seasonal change for the convergence point is as follows (Figure 4). The convergence is located off Port Isabel, TX, during September, October, and November due to the downcoast force off Port Isabel in those months. From December to March, the convergence of coastal currents is between Port Isabel and Port Aransas, TX; from March to June, the stress components for Port Aransas and Freeport, TX, imply a current convergence between these locations. In July, the convergence is approximately off Cameron, LA. In August,

the stress and current convergences rapidly migrate downcoast as indicated by alongshore stresses for Freeport, Port Aransas, and Port Isabel (Cochrane and Kelly 1986).

Sea-surface salinity can be used as a tracer to follow Texas-Louisiana shelf circulation patterns (Figure 6). By plotting or contouring shelf salinities, the flow of the Mississippi and Atchafalaya rivers can be documented. A band of low salinity water is usually found along the coast from September to June as directed by a single current with downcoast flow prevailing annually from Port Aransas, TX, to Cameron, LA, except for a period of upcoast flow in spring and summer. Salinity usually reaches its minimum on the Texas-Louisiana shelf in May along most of the coast. The lowest salinities are usually found off of the Mississippi River delta. Salinity increases moving west and south away from the delta. However, a secondary salinity low occurs almost every month along the coast from about Cameron, LA, to Galveston, TX. The band of fresh water begins to recede upcoast in June and disappears by August. Some brackish water may remain along the coast and extend seaward over the shelf.

The location and distribution of the fresher water on the Texas-Louisiana shelf is contingent upon the quantity of river discharge. For the inner shelf, the effect of river discharge is much greater than evaporation and precipitation (Cochrane and Kelly 1986). Discharge from the Mississippi-Atchafalaya river system is 15 times the combined mean discharge of all the other rivers that empty onto the Texas-Louisiana shelf. Peak river flow is in April (spring flood), and the minimum discharge is in October (Figure 7). A small downcoast change in coastal sea-surface salinity is found in all months except July. Downcoast advection and mixing of the river water is the only explanation of the gradual change in salinity, as local river discharges are very variable. A low-salinity lens of fresher water (Mississippi-Atchafalaya river discharge) is

expected to be located along the coast during May in accordance with the April spring flood maximum discharge. Another very local freshwater lens may be apparent near the Texas coast along 94°W longitude due to freshwater input from the Sabine River (Bontempi 1995). Another major feature of Texas-Louisiana shelf circulation is a current near the shelf break that runs counter to the coastal current (Cochrane and Kelly 1986). This countercurrent seems to be connected to the downcoast current which dominates on the inner shelf almost year-round, except in summer. The countercurrent supports the theory that cyclonic, gyre-like circulation prevails on the shelf.

Monthly mean geopotential anomalies were calculated for the Texas-Louisiana continental shelf for May 1992 to May 1993 by the method of Montgomery (1941), an example displayed in Figure 15. Maps of geopotential anomaly show an elongated cyclone (low) present over a large portion of the shelf for almost all months except July and August. The downcoast current, which dominates the coastal circulation except during summer months, comprises the western arm of the gyre. Offshore flow is the gyre's southwestern arm, and the eastern arm is the shoreward flow off the coast of Louisiana, completing the cyclonic, gyre-like circulation on the shelf (Figure 4). This predominant circulation on the shelf carries fresh water and nutrients from the river discharge areas to the remainder of the Texas-Louisiana continental shelf, affecting phytoplankton abundances, distributions, and species composition over a large area.

Seasonal phenomena

The Texas-Louisiana shelf, as influenced by the Mississippi and Atchafalaya rivers, is subject to seasonal phenomena. For example, the spring is marked by peak discharge from the

Mississippi River (Dinnel and Wiseman 1986), with the river's greatest flow occurring in April and May. Larger river flow delivers greater concentrations of nutrients (nitrate, phosphate, and silicate) to the shelf area (Dinnel and Bratkovich 1993). When the river flow is high as in the spring, primary productivity and chlorophyll *a* concentrations peak (Sklar and Turner 1981).

During the summer, a coupled biological and physical process, hypoxia, develops on the Texas-Louisiana shelf. Hypoxia is decreased dissolved oxygen levels in water and is usually defined as less than 2 mg/L or 1.4 ml/L of dissolved oxygen (Rabalais et al. 1991). Hypoxia in this area is contingent on the flow of the Mississippi River. This condition can occur on the Louisiana shelf during the spring flood time of April and May and last through October, but the region of hypoxia is most extensive during the summer months of June, July, and August (Rabalais et al. 1991). During the summer, the increased amount of fresh water on the shelf discharged during spring, in conjunction with increasing temperatures, causes greater water column stability than is present in the water column during winter months. Increased water column stability inhibits mixing and, therefore, transport of oxygen to lower layers. Hypoxia may also be influenced by phytoplankton; as phytoplankton organic material sinks, respiration rates are fueled in bottom waters, potentially utilizing any available oxygen (Rabalais et al. 1991).

Large Mississippi River flow volume can correspond zones of hypoxia across the shelf due to a surface fresh water lens and the resulting stratification. Nutrients associated with high river flow may cause an increase in phytoplankton numbers which may lead to hypoxia or to anoxia, the total lack of dissolved oxygen. This phenomenon has been documented in the Chesapeake Bay, where larger algal standing stocks have been related to anoxia in bottom waters

(Fisher et al. 1988). Changes in phytoplankton stocks as a result of hypoxic or anoxic waters will affect upper trophic levels, as a hypoxic event would decrease the amount of transferrable energy produced by phytoplankton.

Synopsis of LATEX Cruises

Phytoplankton samples were collected during the Texas-Louisiana Shelf Circulation and Transport Processes Study (LATEX A) hydrography cruises. LATEX A was one component of LATEX, the Louisiana-Texas Shelf Physical Oceanography Program, funded by the Minerals Management Service. An objective of the LATEX A hydrography component was to determine water mass distributions across the shelf, i.e. horizontal and vertical physical processes occurring along the coastal margin. Hydrographic sampling included CTD (conductivity, temperature, and depth) deployments to measure temperature, salinity, depth, chlorophyll fluorescence, and light. Nutrient concentrations and oxygen values were also measured. Phytoplankton pigments were determined by high-performance liquid chromatography (HPLC) (Mantoura and Llewellyn 1983) on filtered water samples. LATEX A data will be used to resolve the circulation spatially and temporally on the shelf. In addition to the host of hydrographic parameters studied, wind, current, and meteorological data were also gathered across the shelf as well.

The first four LATEX hydrography cruise, H01 (May 1992-spring), H02 (August 1992-summer), H03 (November 1992-fall), and H04 (February 1993-winter), surveyed the Louisiana continental shelf from about 90°30' to 94°0' W longitude. Cruise information is listed in Table (Cruise,dates,vessel,station number,pytopl stations, stations examined). The May 1992 cruise track (Figure 5) covered the Louisiana continental shelf and a small portion of the Texas shelf along 94°W longitude. The H01-H04 survey tracks were divided into 4 cross-shelf transects (vertical lines) that extend from the 10 to the 200 m isobath. Cross-shelf transects are labeled with Line 1 as the easternmost transect, then Lines 2, 3, and 4 progressively to the west. Two

along-shelf transects were conducted, one located along the 50 m isobath (Line 0), and one along the 200 m isobath (Line 9). These station and transect locations were determined based on physical oceanographic analyses, specifically the Cochrane and Kelly (1986) description of the Texas-Louisiana shelf circulation discussed previously. The location and spacing of stations was based on knowledge of spatial scales in the study region and on the Rossby radius of deformation (Nowlin et al. 1991- Latex proposal).

The May 1993, cruise H05, LATEX A hydrography cruise track covered the entire Texas-Louisiana continental shelf (Figure 8). A full-shelf survey was decided upon based on the need to discern circulation and transport processes over the entire Texas-Louisiana shelf. Cruise H05 occupied 215 stations in eight cross-shelf transects labeled from east to west in the same manner as the H01-H04 cruises and two along-shelf transects. The cross-shelf transects extended from Line 1 at about 90°30' W longitude, south of Terrebonne Bay, LA, to Line 8 extending due east of Brownsville, TX. For this study, the focus of the May 1993 cruise is Line 1 to Line 4.

At each of these stations, a Sea-Bird 911*plus* CTD cast was done. The CTD was mounted on a Rosette, which was outfitted with 12 10-liter Lever Action Niskin Bottles for collecting discrete water samples throughout the water column. The CTD-Rosette (General Oceanics 12-place frame) system was outfitted with a Datasonics PSA-900 altimeter, a SeaTech 3000 m fluorometer, a D&A Instruments OBS-3 optical-backscatter sensor, a SeaTech 2000 m transmissometer, and a Biospherical QSP-200L photosynthetically active radiation (PAR) sensor. Profiles of each parameter were collected along the entire coast. Conductivity (salinity),

temperature, and dissolved oxygen profiles from the CTD itself were collected as well.

Niskin bottles attached to the Rosette were tripped to collect water samples during the upcast at depths determined from fluorescence profiles observed during the CTD downcast. Discrete water samples for nutrients were collected at each hydrographic station; measurements were made of six (6) different nutrients: nitrate, nitrite, phosphate, silicate, ammonia, and urea. Other hydrographic samples were collected at predetermined stations including dissolved oxygen, salinity, pigments, and suspended particulate material. Complimentary programs on the LATEX hydrography cruises measured zooplankton grazing rates and primary production. A Secchi depth was taken on daylight stations.

Phytoplankton Sample Collection and Analyses

There are many advantages to microscopic enumeration of phytoplankton which other methods of observing phytoplankton do not provide (Smayda 1978). Microscopic analyses allow detection of phytoplankton species that remote sensing and phytoplankton pigment analyses do not. The taxonomic structure of the phytoplankton community can be detailed because species identifications are made. Species identification and discernment of the community structure coupled with detailed hydrographic measurements can lead to insight into strategies for species succession and possibly ecosystem succession.

An ideal phytoplankton study should detect, enumerate, and identify to species level (where possible) all cells in one size fraction present in a sample. Often the intactness and general condition of the cell will aid in identification (Smayda 1978). Cells that were unidentifiable were recorded and can be found in the actual counts as cells, monads, flagellates, centric diatoms, etc. Since it is possible to determine that an object under the microscope is actually a cell (or was), it should be represented in the individual count. Several times in this study dimensions of unidentifiable cells were measured, sketched, and recorded in the general grouping "cell", only to later be identified to the generic or species level once a different view or more intact cell was found. The Scanning Electron Microscope (SEM) helped in the identification process as well. Proper identification of organisms provided a better opportunity to determine its niche in the phytoplankton community.

Sampling locations

Phytoplankton samples were collected from about 40% of the total stations surveyed for each cruise included in this study. Phytoplankton samples from approximately one-quarter of these stations were chosen for enumeration, about 22-25 stations per cruise. These stations are marked as dark circles on the maps of the LATEX H01 through H05 cruises (Figure 9). Stations chosen for phytoplankton identification and enumeration were determined after examining shelf-wide distributions of chlorophyll *a*, *b*, and *c* contours, salinity profiles, and vertical fluorescence profiles from the LATEX data set. The shelf-wide distribution of stations is broken down into the inner, middle, and outer shelf, as shown in Figure 10. On each of the four transect lines used in this study, one station was chosen on the inner shelf, two to three on the middle shelf, and one station on the outer shelf. Each station had a surface and chlorophyll maximum sample determined by continuous fluorescence profiles recorded on CTD casts. The same stations for examination for all five cruises were chosen where possible; otherwise the adjacent station on the cross-shelf transect was substituted.

Collection and storage of samples

Phytoplankton water samples were collected in Niskin bottles attached to a CTD-Rosette system as previously described. Water samples for phytoplankton determinations (250 ml) were collected from the surface and from the chlorophyll maximum. Samples were transferred from the Niskin bottles to opaque Nalgene bottles at stations where pigment samples were collected on the LATEX A hydrography cruises. Each sample was preserved in a 1% glutaraldehyde solution, kept in a refrigerator on board the ship at about 4.5 to 8°C, and transported from the

ship in coolers to maintain a maximum number of organisms. Samples were then stored in a laboratory refrigerator at 4.5 to 8 °C until removed for counting.

Phytoplankton preparation and counting

Phytoplankton species composition, abundance, and distributions were determined using the inverted-microscope technique (observation and enumeration) and the Utermöhl method (Utermöhl 1958; Hasle 1978). These methods have been employed in several phytoplankton distribution studies, including studies of the south Texas outer continental shelf (Van Baalen 1975), a warm core ring off the East coast of the United States in the northwestern Atlantic Ocean (Gould 1987), the western Atlantic off cape Henry and Cape May, including the New York Bight (Marshall and Cohn 1987), the northwestern Atlantic Ocean (Gould 1988), and in the Antarctic marginal ice zone (Kang 1992). The inverted-microscope method is one of the most widely used methods for quantitative analyses of phytoplankton (Crumpton 1987); this method permits analysis of phytoplankton ranging from fragile nanoplankton to larger species. In this study, dominant phytoplankton groups including families, genera, and species were identified wherever possible and have been compared with LATEX A pigment samples to aid in understanding the phytoplankton community on the shelf.

Prior to microscopic analysis, phytoplankton were concentrated on a perspex plate for counting and identification, as illustrated in Figures 11 and 12. Concentrations were done according to the Utermöhl technique (Utermöhl 1958; Semina 1978; Bontempi 1995). A settling or sedimentation chamber size is selected depending on the amount of the biomass or abundance expected at a particular station. If the station was on the inner shelf and was assumed to have a

dense phytoplankton population or high detritus concentration, a 10 ml sample was settled and observed. When samples were so heavily sedimented or thickly settled, dilutions were necessary for assessment of the phytoplankton community. In this case, a 2 ml aliquot of sample was placed on the settling plate and covered with a top plate. The sample was counted and a correction made in the abundance calculation for the altered volume. Middle and outer shelf samples usually require a 50 ml aliquot to be settled, as these areas have smaller population numbers and less detritus. Phytoplankton from these regions are seen better in a chamber where the bottom area is smaller relative to the volume (Utermöhl 1958).

The settling apparatus is assembled according to Bontempi (1995) (Figure 11). The perspex plate containing the settled material is placed under an inverted microscope, in this case a Zeiss IM-35. The actual methodology for counting was done according to the guidelines in Bontempi (1995). Dr. Greta Fryxell, a phytoplankton taxonomist at Texas A&M University, was consulted with the proposed methodology before any final decisions were made or when any problems in identification were encountered.

For the actual enumeration processes, a Planapo 16x Phase-Contrast Lens was used, while species were identified using a Planapo 40x Phase-Contrast Lens or a Planapo 40x Bright field Lens (Semina 1978). These methods allow for both determination of the phytoplankton species on the shelf and provide for a better estimate of their biomass.

Abundance

Abundance concentrations (cells L^{-1}) were calculated for each major group of phytoplankton (diatoms, dinoflagellates, coccolithophorids, silicoflagellates, microflagellates,

and other) at each station, depth, and cruise examined for this study. The calculation was done according to Bontempi (1995). An analysis of phytoplankton abundance at the surface and at the chlorophyll maximum will be presented in the discussion. Also, a comparison of their on-shore/off-shore gradients during different river flow regimes will be made between phytoplankton abundance data from all cruises.

Synopsis of Phytoplankton Results

The Texas-Louisiana shelf phytoplankton distributions were examined from two different views: the proximity of the stations to the Mississippi and Atchafalaya river outflows and in the regions of the inner, middle and outer shelf based on a phytoplankton pigment study completed by Neuhard (1994). Each region of the shelf has specific phytoplankton groups, hydrography, and physical processes associated with it (Bontempi 1995) and will be discussed accordingly.

May 1992

The flow year of 1992 was an average one for the Mississippi River (Figure 7). In the spring of 1992, overall abundance numbers of phytoplankton were highest on the inner shelf, particularly near the Mississippi and Atchafalaya river outflows (Figure 13 and Figure 14). Concentrations of phytoplankton were in the millions of cells per liter (1to 9 million cells L^{-1}). The predominant downcoast flow in the spring (Cochrane and Kelly 1986) is the primary physical process affecting the phytoplankton distributions on the inner shelf. The inner shelf also receives the majority of the Mississippi River outflow and its associated nutrients and low salinity waters (Figure 15). The eastern inner shelf waters were more stratified (Figure 16) due to the presence of the lower density, fresher Mississippi River waters in this portion of the shelf. The western part of the inner shelf was well-mixed. Diatoms were dominant on the inner shelf, composing about 95% of the phytoplankton population. The two most dominant diatoms shelf-wide were the chain-formers *Leptocylindrus danicus* and *Rhizosolenia delicatula.*

On the middle shelf, overall concentrations of phytoplankton decreased with distance

from the Mississippi River both at the surface (Figure 17) and at the chlorophyll maximum (Figure 18). This trend of decreasing phytoplankton numbers reflects the decreasing effects of riverine input and its associated nutrients loads, and is easily seen in the nutrient (Figures 19 and 20) and salinity (Figure 21) contours from the Texas-Louisiana shelf in May 1992. Surface waters of the middle shelf were oligotrophic. Diatoms still composed the majority, about 60-70%, of the phytoplankton population. At the surface of the middle shelf, a shift occurred in dominant phytoplankton groups to dinoflagellates and microflagellates, which are smaller and more motile cells having lower nutrient requirements or the ability to migrate into areas that are nutrient or light-enriched. A species shift is a response of the phytoplankton to the hydrographic and physical conditions on the shelf. Dominance of a species with a growth rate or light requirements more suitable to the environment would most likely occur due the changing conditions on the shelf. The oligotrophic, middle-shelf water column qualities create an environment that supports a higher percentage of dinoflagellates and microflagellates.

Waters at the chlorophyll maximum of the middle shelf were fairly low in nutrients as well (Figures 20 and 22), but a slightly larger diatom was population present. The chlorophyll maximum was found at or near the bottom of the middle shelf in the spring of 1992 and 1993. It was hypothesized by Flint and Kamykowski (1984) and Neuhard (1994) that benthic regeneration of nutrients and resuspension of these nutrients into the upper water column may be taking place. This resuspension would support the phytoplankton population, particularly the diatoms, at the middle shelf chlorophyll maximum. Confirmation of this theory is seen in the phytoplankton species composition. Examination of the dominant diatom species at the chlorophyll maximum of the middle shelf revealed the presence of tychopelagic diatom species.

Tychopelagic diatoms are those species that live the majority of their life cycle attached to a bottom substrate until forcibly torn from their environment and advected into the upper water column (Hendey 1964). Their presence in the upper water column provides evidence that benthic resuspension processes may be taking place on the middle shelf, supporting the phytoplankton population there. The tychopelagic species include a *Nitzschia* species, a *Navicula* species, and *Thalassiosira decipiens* (Admiraal 1984).

On the outer shelf, the upper water column (about 50-70 m) was oligotrophic (Figure 20 and 22), and the overall concentrations of phytoplankton decreased even more moving away from the middle shelf (Figures 17 and 18). Diatoms composed only 30-40% of the phytoplankton population at the outer shelf surface. Due to the oligotrophic nature of the water column, dominant phytoplankton groups shifted from diatoms to dinoflagellates, microflagellates, and coccolithophorids. These phytoplankton, again, are smaller or more motile cells with lower nutrient requirements or with migratory abilities that allow them to survive in a nutrient-poor environment created by the hydrography and by physical processes.

At the chlorophyll maximum, a greater contribution of dinoflagellates, microflagellates, and coccolithophorids to the phytoplankton population due to the oligotrophic water column was seen, as was observed at the surface. Upwelling processes may have occurred in some regions of the outer shelf (Figures 20 and 22) and advected nutrient-rich waters into an area of the shelf that is nutrient-poor. This influx of higher nutrient water along the outer shelf would help support the phytoplankton population in a typically oligotrophic region.

In 1992, the dominant dinoflagellates were of the family Gymnodiniaceae, the majority under 20 μm in length. The majority of the microflagellates were cryptomonads, and the most

dominant coccolithophorid shelf-wide was *Emiliania huxleyi*. There was one area on the outer shelf where an elevated population of diatoms, more typical of an inner shelf or coastal area, was found amidst an overall elevated abundance of phytoplankton (Figures 17 and 18). At the time prior to sampling, a Loop Current eddy, Eddy Triton, was in the study area (Figure 23). Eddy Triton entrained waters from a coastal area and advected these waters and their associated nutrients, lower salinities, and elevated phytoplankton and diatom population (all characteristic of near-shore water masses) into the study area. This biological response of the outer shelf phytoplankton to the presence of a Loop Current eddy is reflected in the outer shelf phytoplankton distributions.

The middle shelf was found to be a transitional zone for phytoplankton species composition, particularly diatoms, for both May 1992 and May 1993. Particular species dominated the inner shelf, and other specific species dominated on the outer shelf. The middle shelf diatoms were a compilation of these two groupings. The middle shelf also displayed hydrographic characteristics resulting from mixing between coastal waters (high nutrients, low salinity) and open ocean Gulf of Mexico waters (low nutrients, high salinity).

August 1992

Summer is a period during which lower volumes of river water and associated nutrients are delivered to the Texas-Louisiana shelf (Figure 7). Circulation patterns are somewhat reversed from springtime current and wind regimes (Cochrane and Kelly, 1986) (Figure 24). During the summer, changes in wind direction alter the cyclonic circulation pattern. The freshest water is found on the eastern part of the study area near the Mississippi River delta, and salinities

increase radially from that area (Line 1) (Figure 25). The lowest salinities, 26-29, are found on the innermost part of the shelf near Line 1 (Mississippi River delta) and Line 2 (Atchafalaya River outflow), and the lowest salinities were higher than the lowest salinities observed in the spring. Lower flow occurred for the Mississippi and Atchafalaya rivers for the month prior to the August 1992 cruise (Figure 7). These changes in winds, currents, and river flow are environmental factors which influence phytoplankton distributions and abundances across the shelf.

The overall pattern of summertime phytoplankton abundance is similar to the spring pattern, with highest numbers on the inner shelf and decreasing numbers moving off-shore (Figures 26 and 27). Overall summertime abundances were 5-10 times lower at the surface and at the chlorophyll maximum than abundances observed during spring. Surface summer phytoplankton abundances ranged from 22,000 to 885,000 cells L^{-1}, and chlorophyll maximum abundances ranged from 24,000 to 1.06 million cells L^{-1}. Few stations had phytoplankton abundances in the hundreds of thousands of cells L^{-1}, and only one station had a concentration of phytoplankton of 1 million cells L^{-1}. This lower summer 1992 abundance could be due to lessened riverine influence, to a complete population shift in phytoplankton from the spring, or to the influence of vertical stratification, water column stability, and resultant lower light levels.

The inner shelf area was greatly affected by the changing riverine and wind dynamics. Neuhard (personal comm.) has shown that the average depth of the subsurface chlorophyll maximum increased across the shelf in the summer as the water column became more stratified, particularly on the inner shelf. The chlorophyll maximum was located near the bottom in the summertime, except on Line 2, illustrating the increased stratification in the summer.

A significant component of phytoplankton greater than 3 μm during August 1992 on the Texas-Louisiana shelf was composed of dinoflagellates and microflagellates (Figures 26 and 27), particularly moving off-shore. Overall, less diatoms were present in summer than in the spring. Lower nutrient levels may explain the decrease in diatoms and the increase in dinoflagellate and microflagellate numbers, but even though river flows were lower, nutrient levels were higher (D. Wiesenburg, personal comm). A decrease in nutrients cannot be used as an explanation for the shift in phytoplankton group dominance. The grazing rate of phytoplankton by zooplankton may also have been higher in the summer, reducing the number of phytoplankton present on the shelf.

Diatoms dominated the inner shelf, composing 50% or more of the inner shelf phytoplankton population, during August 1992 as in May 1992 both at the surface and at the chlorophyll maximum, except for one station nearest the Mississippi River delta on Line 1 (Figure 26). Higher nutrients and phytoplankton abundances were located on Lines 2 and 4 at the surface and chlorophyll maximum near the areas of river outflow also (the Atchafalaya and Sabine rivers, respectively). Nutrients from the Atchafalaya and Sabine rivers may influence stations on these transects (Figures 28 and 29) causing increased phytoplankton growth before the river water is transported from the inner shelf. The abundance of phytoplankton in the less than 3 μm size fraction may also have increased. Concentrations of phytoplankton at the surface of the inner shelf were significantly lower than in the spring, except on Line 2. The most dramatic differences were on Line 1, where concentrations of phytoplankton in the summer were about an order of magnitude lower than springtime abundances, and on Line 4 where August abundances were about 2-5 times lower than in the spring. However, average Line 4 inner shelf

abundances were highest of any transect, most likely due to stratification of the water column and sufficient light levels for growth.

During August 1992, silicate levels were fairly high, above 2-3 μmol/L (Figure 30), and nitrate levels were fairly low, below 1μmol/L, on the inner shelf (Figure 31) and. Extremely high values of silicate, around 5-20 μmol/L, were seen at the surface of the inner shelf on Line 1, Line 2, and Line 4, the highest values being on Lines 2 and 4, where diatoms dominated at the surface and at the chlorophyll maximum. Some resuspension, advective, or regenerative process may have occurred on Line 4 that would supply phytoplankton with the nutrients necessary for growth, as the water column is well-mixed. A study needs to be conducted on the Sabine River, its outflow, and the effect of its outflow on the local phytoplankton population to help explain the high levels of nutrients and the elevated phytoplankton numbers observed in this region.

Phytoplankton abundances decreased moving from the inner to the middle shelf in August 1992 (Figure 26), as in spring. No group of phytoplankton dominated middle shelf surface waters; variable levels of diatoms, dinoflagellates, and microflagellates were observed. More dinoflagellates and microflagellates were present at the surface of the middle shelf than at the inner shelf. The middle shelf area is characterized by higher salinities (Figure 25) and slightly lower nutrients (Figure 30 and 31) than the inner shelf due to the lessened riverine influence and circulation pattern. Slightly lower silicate levels were present in middle shelf waters, and average nitrate concentrations were below 0.3 μmol/L. Lower levels of silicate may correspond to lower numbers of diatoms, while dinoflagellates and microflagellates are smaller and more motile cells that may survive better in oligotrophic environments as is typical of middle

shelf surface waters. Interestingly, the dominant species of phytoplankton across the surface of all middle shelf stations was the diatom *Nitzschia closterium*. Other phytoplankton that were dominant but less so at the middle shelf surface are several dinoflagellates of the family Gymnodiniaceae, a few cryptomonad species and other flagellates, and the diatom *Leptocylindrus danicus*.

At the chlorophyll maximum of the middle shelf, diatoms composed the majority, generally greater than 60%, of the phytoplankton population except for one station near the outer shelf (32%) (Appendix A). The contribution of diatoms to the phytoplankton population at the chlorophyll maximum was greater than at the surface, as during the spring. On Line 1, evidence exists in vertical contours of nitrate and silicate that advective processes may be occurring and resuspending phytoplankton or nutrients from the bottom and supplying diatoms with nutrients necessary for growth. A shift in the dominant species of diatoms at the chlorophyll maximum occurred. *Nitzschia closterium* was still dominant at some stations, but several other diatoms dominated including *Thalassiothrix frauenfeldii, Thalassiosira minima*, and *Bacteriastrum varians*. These other species were dominant at only one station, while *Nitzschia closterium* is present in the top three dominant phytoplankton at several stations, except on Line 1.

Outer shelf, phytoplankton abundances were similar in magnitude to those observed during the spring, with abundances in the tens of thousands of cells L^{-1} at the surface and chlorophyll maximum (Figures 32 and 33). The highest abundances across the outer shelf were located along Line 1. Even though concentrations of silicate were extremely high, the percent composition of diatoms present was much less than in the spring. At the surface, diatoms composed more of the phytoplankton population on the eastern part of the shelf than the western

shelf. More microflagellates than diatoms were observed at the surface, the majority being tiny, unidentified flagellates. The coccolithophorid *Emiliania huxleyi* dominated at one station. More smaller, motile cells were present on the outer shelf in high salinity, lower nutrient waters as during spring.

Phytoplankton concentrations at the outer shelf chlorophyll maximum were similar to those found at the surface (Figures 32 and 33). Diatoms still contributed to the phytoplankton but composed less of the population moving offshore. Dinoflagellates and microflagellates were fairly dominant, together composing 20-70% of the phytoplankton, in the outer shelf chlorophyll maximum higher salinity, lower-nutrient waters as they were in the spring. Dominant phytoplankton include several *Nitzschia* species and Gymnodiniaceae.

In August 1992, no definitive influence of the overall circulation pattern on the phytoplankton distributions seemed to be present as was determined in the spring, except for riverine influence. Atchafalaya River water may be transported from the inner shelf of Line 2 to the middle shelf of Line 1, as the geopotential anomaly dictates (Figure 24). The chlorophyll maximum phytoplankton species supported this transport, because the dominant diatoms at the chlorophyll maximum of Line 1 at the middle shelf, *Bacteriastrum* and *Chaetoceros* species, were similar to those species dominating the inner shelf at Line 2.

The lessened influence of the Mississippi and Atchafalaya river water during the summer was reflected in the overall lower abundances of phytoplankton on the Texas-Louisiana shelf. Higher abundances were found on the inner shelf and decreased seaward. Vertical stratification and water column stability may play a role in dictating which phytoplankton groups dominate a shelf area, as the chlorophyll maximum was located near the bottom, particularly where fresher

river water was located (C. Neuhard, pers. comm.) on the inner shelf. The density gradient may be important to summer phytoplankton distributions. The summertime phytoplankton regime revealed that diatoms were dominant across the inner shelf. Dinoflagellates and microflagellates dominate across the middle and outer shelf, even though one species of diatom was usually dominant at any particular station at the surface and chlorophyll maximum. Overall, Line 1 had the highest abundances of phytoplankton of any transect. Dominant phytoplankton species were not chain-forming as in the spring but were single cells of the diatom *Nitzschia closterium*, several unidentified microflagellates and cryptomonads, and dinoflagellates of the family Gymnodiniaceae that were generally small (less than 20 μm in diameter).

November 1992

Winter winds in November 1992 mixed the waters on the Louisiana shelf. The vertical nutrient sections reflected this (Figures 34 and 35), as did the vertical salinity contours (Figure 36). Nitrate concentrations seemed to be low overall on the shelf (<1 μmol/L), which may indicate that phytoplankton on the Louisiana shelf were nitrate-limited. Overall silicate concentrations were very high, but total diatom numbers were much lower than in the summer or in the spring. Total phytoplankton abundances at the surface and chlorophyll maximum were also lower in November 1992 than in May or August (Figures 37 and 38).

The circulation present during November (Figure 39) consisted of an alongshore current that carried fresher, nutrient-rich Mississippi and Atchafalaya river waters to the west along the coast. Thus, the highest silicate levels (Figure 40) and phytoplankton abundances were seen on the inner shelf, where the freshest water was located (Figure 41). Nitrate levels were depleted

along the entire shelf throughout the upper 50 m of the water column (Figure 34), until below the nitracline at about 50-60 meters depth on the outer shelf. The inner shelf at the surface was diatom-dominated (Figure 37), with a fairly high contribution to the phytoplankton population from microflagellates and some dinoflagellates. The chlorophyll maximum phytoplankton population was also composed mainly of diatoms (Figure 38), with a more significant contribution from microflagellates and dinoflagellates than was seen at the surface. Phytoplankton on the inner shelf were in an environment that supported the greatest phytoplankton growth in the overall low-nitrate shelf waters present during November. November was the period of lowest river flow (Figure 7), so less riverine nutrients were discharged to the shelf. This low riverine nutrient discharge probably contributed to the low shelf nutrients and low phytoplankton abundances during November 1992. The areas nearest the Mississippi and Atchafalaya river outflows, Line 1 and Line 2...(comment on phyto abund and composition).

Middle shelf nutrient levels were lower than inner shelf levels. Nitrate concentrations were still low overall, but silicate levels were high (about 2-3 μmol/L), although lower than on the inner shelf. Overall phytoplankton numbers decreased moving from the inner to the middle shelf (Figures 37 and 38); numbers were in the tens of thousands of cells L^{-1}, whereas phytoplankton concentrations were in the hundreds of thousands of cells L^{-1} on the inner shelf. The middle shelf was an area of higher salinity and less riverine influence during this time period as well. Phytoplankton at the surface and at the chlorophyll maximum had a large population of diatoms , particularly on the eastern shelf. This large contribution of diatoms to the phytoplankton population was most likely due to influence from the Mississippi River. Eastern

middle shelf waters had more phytoplankton than western shelf waters had (316,000 cells L^{-1} at the surface and 279,000 cells L^{-1} at the chlorophyll maximum to 50,000-90,000 cells L^{-1} at the surface and 32,000-71,000 cells L^{-1} at the chlorophyll maximum), similar to observations made during spring and summer. The greater phytoplankton numbers found on the eastern shelf were likely again due to riverine influence. Moving towards the western shelf, coccolithophorids, dinoflagellates and microflagellates became greater constituents of the population. This abundance trend supports the theory that in an oligotrophic water column, smaller cells with lower nutrient requirements dominate. Overall phytoplankton abundances might have been lower in November due to increased turbulence, to lower light levels, and to oligotrophic waters.

Overall phytoplankton abundances decreased even more moving away from the middle shelf (Figures 37 and 38). Outer shelf abundances at the surface averaged 25,000 cells L^{-1}, while abundances at the chlorophyll maximum were between 9,700 and 30,000 cells L^{-1}. Coccolithophorids, diatoms, dinoflagellates, and microflagellates seemed to contribute approximately equal numbers to the phytoplankton populations. Phytoplankton numbers were probably much lower at the outer shelf, because the water column was depleted in nitrate for the upper 50 m and had the lowest silicate of this cruise (Figures 34 and 35). The outer shelf is the region of the shelf furthest from the Mississippi-Atchafalaya river input, so these waters feel little influence of nutrient concentrations from the rivers. Outer shelf waters are more influenced by high salinity Gulf of Mexico waters, which are typically nutrient-poor.

November 1992 phytoplankton distributions on the Louisiana shelf seemed to reflect phytoplankton distributions and overall trends in abundances similar to those determined for in the spring and summer. Higher levels of phytoplankton were found on the inner shelf, numbers

decreased towards the middle shelf, and abundances were lowest on the outer shelf. The November 1992 phytoplankton at the surface and chlorophyll maximum of the Louisiana shelf were dominated by *Nitzschia* and *Pseudo-nitzschia* species, as seen in the middle shelf phytoplankton population, particularly on Lines 2-4. Line 1 was dominated by other chain-forming diatoms, including *Skeletonema costatum*, *Chaetoceros* spp., and *Leptocylindrus danicus*. Moving towards the outer shelf, cryptomonads and the coccolithophorid *Emiliania huxleyi* become dominant. Several monoflagellates become dominant at the outer shelf, particularly at the chlorophyll maximum. The microflagellates, dinoflagellates (Gymnodiniaceae), and coccolithophorids that dominate the shelf were very small (<10μm diameter). Cells smaller than 3 μm, such as cyanobacteria, may possibly have had very high concentrations due to the oligotrophic waters present in November 1992. Pigment data in the study area ...

February 1993

February analyses are preliminary, based on observance of a series of net tows, until more extensive work can be done on the phytoplankton samples. A bloom of diatoms abounded in February 1993, elevating the phytoplankton population even though river flow was generally lower (Figure 7). The bloom was of the diatom *Leptocylindrus minimus*. High numbers of several *Coscinodiscus* species were also present. The bloom of diatoms dominated the phytoplankton greater than 3 μm in diameter, particularly on the inner shelf; *Coscinodiscus* species were the largest diatoms found across the Texas-Louisiana shelf. These observations of phytoplankton blooms may allow us to conclude that phytoplankton biomass will be greatest in

the winter. Unfortunately, we do not have data from a following February that would allow us to probe further into fluctuating phytoplankton abundances on the shelf.

Overall phytoplankton abundance seems to have decreased moving off-shore as it did for all of the other seasons observed in this study. This decrease in number was most likely due to the lessened effect of riverine influence and associated nutrient loads.

Say something about mixing, ga, nutrients, etc.

May 1993

The same general trends in hydrography, physical processes, and phytoplankton distributions, abundances, and species composition were seen in the spring shelf regimes of 1992 and 1993, a record flow year for the Mississippi River, as were observed during May 1992, an average river flow year. Each region of the shelf in 1993 had hydrographic and physical processes similar to those previously described for May 1992. The inner shelf was diatom-dominated and had the highest phytoplankton abundances overall (Figure 42 and 43). The inner shelf was subject to increased Mississippi River flow of 1993 (Figure 7) and its associated nutrients loads. This increased volume of river water influenced the shelf ecosystem through the middle shelf , as is evident in surface nutrient (Figures 44 and 45) and salinity contours (Figure 46) for the shelf region.

Middle shelf surface waters were fairly oligotrophic (Figures 47 and 48), supporting more microflagellates, dinoflagellates, and coccolithophorids, similar to abundance trends in May 1992. The middle shelf area in 1993 had the presence of tychopelagic diatoms, supporting the theory of benthic regeneration and resuspension of nutrients into the near-bottom chlorophyll maximum (Neuhard 1994; Bontempi 1995). Vertical nutrient contours confirmed the presence of

these benthic processes (Figure 48). Outer shelf waters were also oligotrophic, supporting the smaller or more motile dinoflagellates, microflagellates, and coccolithophorids at the surface and chlorophyll maximum (Figures 49 and 50). Some evidence of upwelling processes was present in the vertical nutrient contours at the chlorophyll maximum.

Overall in the spring of 1993, areas that had increased phytoplankton abundances across the Texas-Louisiana shelf delineated the area occupied by the increased volume of fresh water from the Mississippi River. This was one main difference in the two spring regimes of phytoplankton. Another major difference in the two phytoplankton regimes was found in the species composition of inner shelf waters in 1993. The inner shelf dominants in May 1992 were *Leptocylindrus danicus* and *Rhizosolenia delicatula*. In May 1993, the inner shelf was dominated almost exclusively by the diatom, *Skeletonema costatum*, particularly in the area nearest the Mississippi River. *Skeletonema costatum* is a cosmopolitan species of diatom found to inhabit the neritic waters of the world in a range of salinity, temperature, and nutrient regimes (Winsborough and Ward 1979; Malone et al. 1983; Marshall and Cohn 1987; Xiuren et al. 1988; Medlin et al. 1991). *Skeletonema*'s dominance on the inner shelf in the area occupied by the increased volume of fresh water indicated the possibility that the shelf environment was so radically altered by the volume of fresh water that this environment may have almost exclusively supported *Skeletonema costatum*'s dominance. This shift in phytoplankton species dominance was a response of the phytoplankton community to the physical processes and to hydrography on the Texas-Louisiana shelf.

Conclusions

Phytoplankton abundances, distributions, and species composition on the Texas-Louisiana continental shelf reflected the hydrographic and physical environment present during each particular season and river flow year of the study period. Abundance was greatest, as was species richness, during times of peak river discharge in the spring. Summer was a time of lower river flow and of lower overall phytoplankton abundance. The lowest overall phytoplankton abundances and species richness occurred in the fall, reflecting the Mississippi River flow minimum and the mixing of shelf waters from winds. The wintertime phytoplankton regime, in this case February 1993, showed a potential influence of the increased river flow of 1993 in the form of a large phytoplankton bloom which may or may not take place annually. February may be the time of greatest phytoplankton abundance on the Texas-Louisiana shelf instead of the spring as was previously thought.

The increased river flow of 1993 was reflected by the phytoplankton when comparing spring 1992 and spring 1993 phytoplankton abundances and species composition. Shifts in species composition to the dominance of a single diatom species in May 1993 may be a result of increased fresh water flow and lower salinity water on the shelf. Increased nutrient loads related to peak river flow in the spring, particularly nitrate, may also have influenced the abundance of phytoplankton species.

Although each season seemed to have different overall relationships between the phytoplankton and the variable hydrographic and physical forces, the inner, middle, and outer shelf areas each had certain general hydrography, physical processes, and phytoplankton

distributions associated with them. The inner shelf seemed to be diatom-dominated in all seasons, with the spring having the highest abundances. We cannot be sure that the February 1993 phytoplankton regime was typical for the winter on the shelf, as the high abundance of phytoplankton may be a result of the increased river flow. The inner shelf was subject to the greatest nutrient loading from the Atchafalaya river, about 50% of the Mississippi River, and probably locally on the western shelf from the Sabine River. The inner shelf was also subject to the lowest salinities due to riverine influence.

The middle shelf seemed to have been dominated by diatoms also but less so than the inner shelf. In all seasons, particularly the summer and fall, the middle shelf had more dinoflagellates, microflagellates, and cocccolithophorids. These smaller, more motile cells, can survive in environments that are oligotrophic, such as the middle and upper outer shelf. Nitrate seems to be the limiting nutrient. When nitrate abounds on the shelf, silicate may be limiting to the diatom population, and diatoms were less abundant on the middle and outer shelf where nutrient levels tend to decrease with distance from the rivers. Resuspension of nutrients from bottom waters may have been fueling some of the productivity at the middle shelf, particularly during May as evidenced by the tychopelagic diatoms in the upper water column. Upwelling from bottom waters may have provided outer shelf phytoplankton with the nutrients necessary for growth.

This study was conducted over a one year period, taking into account the variable annual flows of the Mississippi and Atchafalaya rivers. We have begun to resolve some issues regarding the hierarchy of the seasonal coastal food web of the Texas-Louisiana shelf. By calculating biomass and species diversity indices, the role this size class of phytoplankton play in

the oceanic ecosystem will become more apparent. The model will attempt to predict what the different phytoplankton regimes will be for different flow years of the river. We are determining to what extent phytoplankton greater than 3 μm contribute to carbon cycling on the shelf and what role they play in biogeochemical processes. As regional issues such as the hypoxia question become more cavalier on the coastal oceanographic agenda, phytoplankton research will prove invaluable as a tool for determining the vulnerability of coastal industries such as fisheries to potential problems. Future research in phytoplankton will give us insight into precisely how environmental conditions, including hydrography, physical forces, and changes in meteorological conditions, influence phytoplankton. A determination of how phytoplankton, in turn, reflect and respond to these parameters and influence the upper trophic levels can then be made.

References

Admiraal W. (1984) The ecology of estuarine sediment-inhabiting diatoms. In: *Progress in Phycological Research*, Round/Chapman, editors, Biopress Ltd., New York, **3**, pp. 269-322.

Angel M. V. and M. J. R. Fasham (1983) Eddies and biological processes. In: *Eddies in Marine Science*, A. R. Robinson, editor, Springer-Verlag Berlin, pp. 492-524.

Bontempi P. S. (1995) Phytoplankton distributions and species composition across the Texas-Louisiana continental shelf during two flow regimes of the Mississippi River. Master's Thesis, Texas A&M University.

Brown S. (1993) Microzooplankton grazing along the northwestern continental shelf of the Gulf of Mexico. Master's Thesis, University of Texas-Austin.

Cochrane J. D. and F. J. Kelly (1986) Low-frequency circulation on the Texas-Louisiana continental shelf. *Journal of Geophysical Research*, **91**(C9), 10645-10659.

Conley D. J., S. S. Kilham, and E. Theriot (1989) Differences in silica content between marine and freshwater diatoms. *Limnology and Oceanography*, **34**(1), 205-213.

Crumpton N. G. (1987) A simple and reliable method for making permanent mounts of phytoplankton for light and fluorescence microscopy. *Limnology and Oceanography*, **32**(5), pp. 1154-1159.

Csanady G. T. (1990) Physical basis of coastal productivity: the SEEP and MASAR experiments. *Eos*, **71**(36), 1060-1061, 1064-1065.

Dinnel S. P. and W. J. Wiseman (1986) Fresh water on the Louisiana Texas shelf. *Continental Shelf Research*, **6**(6), 765-784.

Dinnel S.P. and A. Bratkovich (1993) Water discharge, nitrate concentration and nitrate flux in the lower Mississippi River. *Journal of Marine Systems*, **4**, pp. 315-326.

Dortch Q. and T. E. Whitledge (1992) Does nitrogen and silicon limit phytoplankton production in the Mississippi River and nearby regions? *Continental Shelf Research*, **12**(11), 1293-1309.

Edmond J. M., E. A. Boyle, B. Grant and R. F. Stallard (1981) The chemical mass balance in the Amazon plume I: The nutrients. *Deep-Sea Research*, **28A**(11), 1339-1374.

El-Sayed S. Z. (1972) Primary productivity and standing crop of phytoplankton. In: *Chemistry, primary productivity, and benthic algae of the Gulf of Mexico*, V. C. Bushnell, editor, American Geographic Society, New York, Folio **22**, pp. 8-13.

Fisher T. R., L. W. Harding, Jr., D. W. Stanley and L. G. Ward (1988) Phytoplankton, nutrients, and turbidity in the Chesapeake, Delaware, and Hudson estuaries. *Estuarine, Coastal and Shelf Science*, **27**, 61-93.

Flint R. W. and D. Kamykowski (1984) Benthic regeneration of nutrients in South Texas coastal waters. *Estuarine, Coastal and Shelf Science*, **18**, 221-230.

Fransz H. G. And J. H. G. Verhagen (1985) Modeling research on the production cycle of phytoplankton in the Southern Bight of the North Sea in relation to river borne nutrient loads. *Netherlands Journal of Sea Research*, **19**(3/4), 241-250.

Fucik K. W. (1974) The effect of petroleum operations on the phytoplankton ecology of the Louisiana coastal water. Unpublished Master's Thesis, Texas A&M University.

Gould R. W. (1987) The horizontal and vertical distribution of phytoplankton in warm core ring 82B: A five month time series. Doctoral Dissertation, Texas A&M University.

Gould R. W. (1988) Net phytoplankton in a Gulf Stream warm-core ring: species composition, relative abundance, and the chlorophyll maximum layer. *Deep-Sea Research*, **35**(9), 1595-1614.

Harper D. E., Jr. and G. Guillen (1989) Occurrence of a dinoflagellate bloom associated with an influx of low salinity water at Galveston, Texas, and coincident mortalities of demersal fish and benthic invertebrates. *Contributions in Marine Science*, **31**, pp. 147-161.

Hasle G. R. (1978) Settling and the inverted-microscope method. In: Phytoplankton Manual, A. Sournia, editor, United Nations Educational, Scientific, and Cultural Organization (UNESCO), pp. 88-122.

Hecky R. E. And P. Kilham (1988) Nutrient limitation of phytoplankton in freshwater and marine environments: A review of recent evidence on the effects of enrichment. *Limnology and Oceanography*, **334**, 796-822.

Hendey N. I. (1964) An introductory account of the smaller algae of British coastal waters. Part V. Bacillariophyceae (Diatoms). *Ministry of Agriculture, Fisheries and Food, Fishery Investigation Service*, **IV**., pp. xxii-317.

Hitchcock G. L., C. Langdon, and T. J. Smayda (1987) Short-term changes in the biology of a Gulf Stream warm-core ring: Phytoplankton biomass and productivity. *Limnology and*

Oceanography, **32**(4), 919-928.

Jochens A. E. and W. D. Nowlin, Jr., eds. (1994) Texas-Louisiana Shelf Circulation and Transport Processes Study: Year 1- Annual Report. Volume II: Technical Summary. OCS Study MMS-94-0030, U. S. Dept. Of the Interior, Minerals Management Service, Gulf of Mexico OCS Region, New Orleans, LA. 207 pp.

Kang S. H. (1992) Phytoplankton in the Antarctic marginal ice zone. Doctoral Dissertation, Texas A&M University.

Krawiec R. W. (1982) Autecology and clonal variability of the marine centric diatom, *Thalassiosira rotula* (Bacillariophyceae) in response to light, temperature and salinity. *Marine Biology*, **69**, 79-89.

Lohrenz S. E., M. J. Dagg and T. E. Whitledge (1990) Enhanced primary production at the plume/oceanic interface of the Mississippi River. *Continental Shelf Research*, **10**(7), 639-664.

Malone T. C., P. G. Falkowski, T. S. Hopkins, G. T. Rowe and T. E. Whitledge (1983) Mesoscale response of diatom populations to a wind event in the plume of the Hudson River. *Deep-Sea Research*, **30**(2A), 149-170.

Mantoura R. F. C. and C. A. Llewellyn (1983) The rapid determination of algal chlorophyll and carotenoid pigments and their breakdown products in natural waters by reverse-phase high-performance liquid chromatography. *Analytica Chimica Acta*, **151**, 297-314.

Marshall H. G. and M. S. Cohn (1987) Phytoplankton distributions along the eastern coast of the USA. Part VI. Shelf waters between Cape Henry and Cape May. *Journal of Plankton Research*, **9**(1), 139-149.

Medlin L. K., H. J. Elwood, S. Stickel and M. L. Sogin (1991) Morphological and genetic variation within the diatom *Skeletonema costatum* (Bacillariophyta): evidence for a new species, *Skeletonema pseudocostatum*. *Journal of Phycology*, **27**, 514-524.

Miller R. L. and D. L. Kamykowski (1986a) Effects of temperature, salinity, irradiance and the diurnal periodicity on growth and photosynthesis in the diatom Nitzschia americana: light-limited growth. *Journal of Plankton Research*, **8**, pp. 215-228.

Montgomery R. B. (1941) Transport of the Florida current off Habana. *Journal of Marine Research*, **4**, pp. 198-220.

Neuhard C. A. (1994) Phytoplankton distributions across the Texas-Louisiana continental shelf in relation to coastal physical processes. Master's Thesis, Texas A&M University.

Officer C. B. and J. H. Ryther (1980) The possible importance of silicon in marine eutrophication. *Marine Ecology- Progress Series*, **3**, 83-91.

Paasche E. (1975) The influence of salinity on the growth of some plankton diatoms from brackish waters. *Norwegian Journal of Botany*, **22**, pp. 209-215.

Pond S. and G. L. Pickard (1983) Numerical models: models with mesoscale eddies. In: *Introductory Dynamical Oceanography*, Pergammon Press, **5**, 198-204.

Rabalais N. N., R. E. Turner, W. J. Wiseman and D. F. Boesch (1991) A brief summary of hypoxia on the northern Gulf of Mexico continental shelf: 1985-1988. In: *Modern and Ancient Continental Shelf Anoxia*, Geological Society Special Publication, **58**, pp. 35-47.

Riley G. A. (1937) The significance of the Mississippi River drainage for biological conditions in the northern Gulf of Mexico. *Journal of Marine Research*, **1**(1), 60-74.

Sahl L. E., W. J. Merrell and D. C. Biggs (1993) The influence of advection on the spatial variability of nutrient concentrations on the Texas-Louisiana continental shelf. *Continental Shelf Research*, **13**(2/3), 233-251.

Schindler D. W. (1978) Factors regulating phytoplankton production and standing crop in the world's freshwaters. *Limnology and Oceanography*, **23**(3), 478-486.

Semina H. J. (1978) Estimating cell numbers. Using the standard microscope. Treatment of an aliquot sample. In: *Phytoplankton manual*, A. Sournia, editor, United Nations Educational, Scientific, and Cultural Organization (UNESCO), pp. 181-182.

Sklar F. H. and R. E. Turner (1981) Characteristics of phytoplankton production off Barataria Bay in an area influenced by the Mississippi River. *Contributions to Marine Science*, **24**, 93-106.

Smayda T. J. (1969) Experimental observations on the influence of temperature, light, and salinity on cell division of the marine diatoms *Detonula confervacea* (Cleve) Gran. *Journal of Phycology*, **5**, 150-157.

Smayda T. J. (1978) Estimating cell numbers. General principles. What to count? In: *Phytoplankton manual*, A. Sournia, editor, United Nations Educational, Scientific, and Cultural Organization (UNESCO), pp. 165-166.

Smith R. A., R. B. Alexander and M. G. Wolman (1987) Water-quality trends in the nation's rivers. *Science*, **235**, pp. 1607-1615.

Smith and Baker (1985)

Texas A&M University Sea Grant Publication (1986) Red tide in Texas- an explanation of the phenomenon. Texas A&M University Sea Grant College Program.

Thomas W. H. and E. G. Simmons (1960) Phytoplankton production in the Mississippi delta. In: *Recent sediments, Northwest Gulf of Mexico*, F. P. Shepard, editor, American Association of Petroleum Geologists, pp. 103-116.

Throndsen J. (1993) The planktonic marine flagellates. In: *Marine Phytoplankton: a guide to naked flagellates and coccolithophorids*, C. R. Thomas, editor, Academic Press, Inc., San Diego, California, pp. 7-21.

Tilman D., S. S. Kilham, and P. Kilham (1982) Phytoplankton community ecology: The role of limiting nutrients. *Annual Review of Ecological Systems*, **13**, pp. 349-372.

Turner R. E. and N. N. Rabalais (1991) Changes in Mississippi River water quality this century. *BioScience*, **41**(3), 140-147.

U. S. Army Corps of Engineers (1993) Mississippi River flow data. New Orleans, Louisiana.

U. S. Army Corps of Engineers (1995) Mississippi River flow data. New Orleans, Louisiana.

Utermöhl H. (1958) Zur Vervollkominnung der quantitativen Phytoplankton-methodik. *Mitt. Int. Ver. Theor. Angew. Limnol.*, **9**, 1-38.

Van Baalen C. (1975) Phytoplankton and phytoplankton biomass. In: *Environmental Assessment of the South Texas Outer Continental Shelf Chemical and Biological Survey Component*, P. L. Parker, editor, Port Aransas, Texas, pp. 46-54.

Vaulot D. and N. Xiuren (1988) Abundance and cellular characteristics of marine *Synechococcus* spp. In the dilution zone of the Changjiang (Yangtze River, China). *Continental Shelf Research*, **8**(10), 1171-1186.

Walsh J. J., G. T. Rowe, R. L. Iverson and C. P. McRoy (1981) Biological export of shelf carbon is a sink of the global carbon dioxide cycle. *Nature*, **291**, 196-201.

Winsborough B. M. and G. H. Ward (1979) Phytoplankton distributions and community structure in Trinity Bay, Texas. Submitted by Espey, Huston and Associates, Inc., Presented at First Winter Meeting, American Society of Limnology and Oceanography, Corpus Christi, Texas.

Xiuren N., D. Vaulot, L. Zhensheng and L. Zilin (1988) Standing stock and production of

phytoplankton in the estuary of the Changjiang (Yangtze River) and the adjacent East China Sea. Marine Ecology-Progress Series, 49, 141-150.

Appendix I- Data Table

Appendix II- Species List

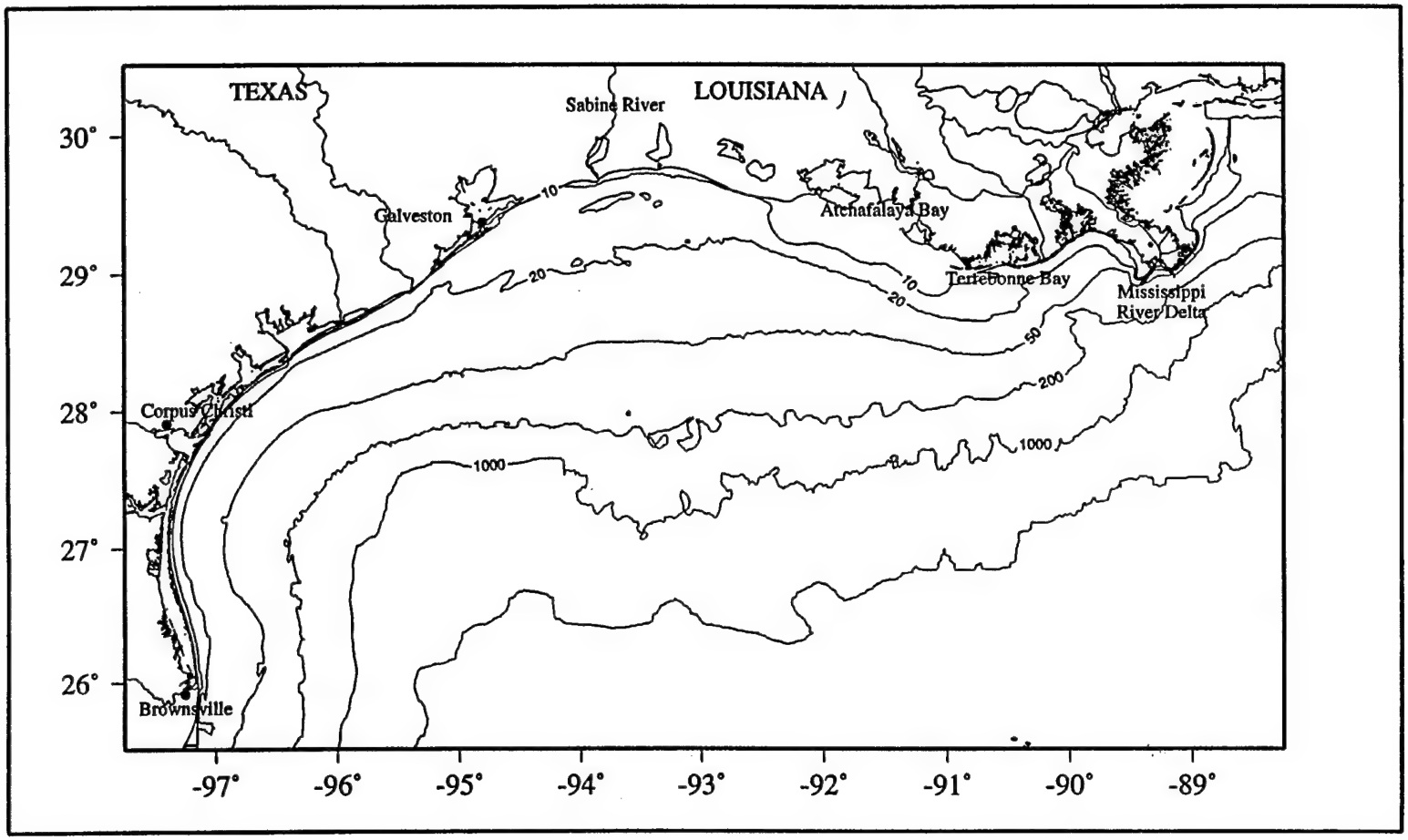

Figure 1. The Texas-Louisiana Continental Shelf in the northern Gulf of Mexico. Isobaths in meters.

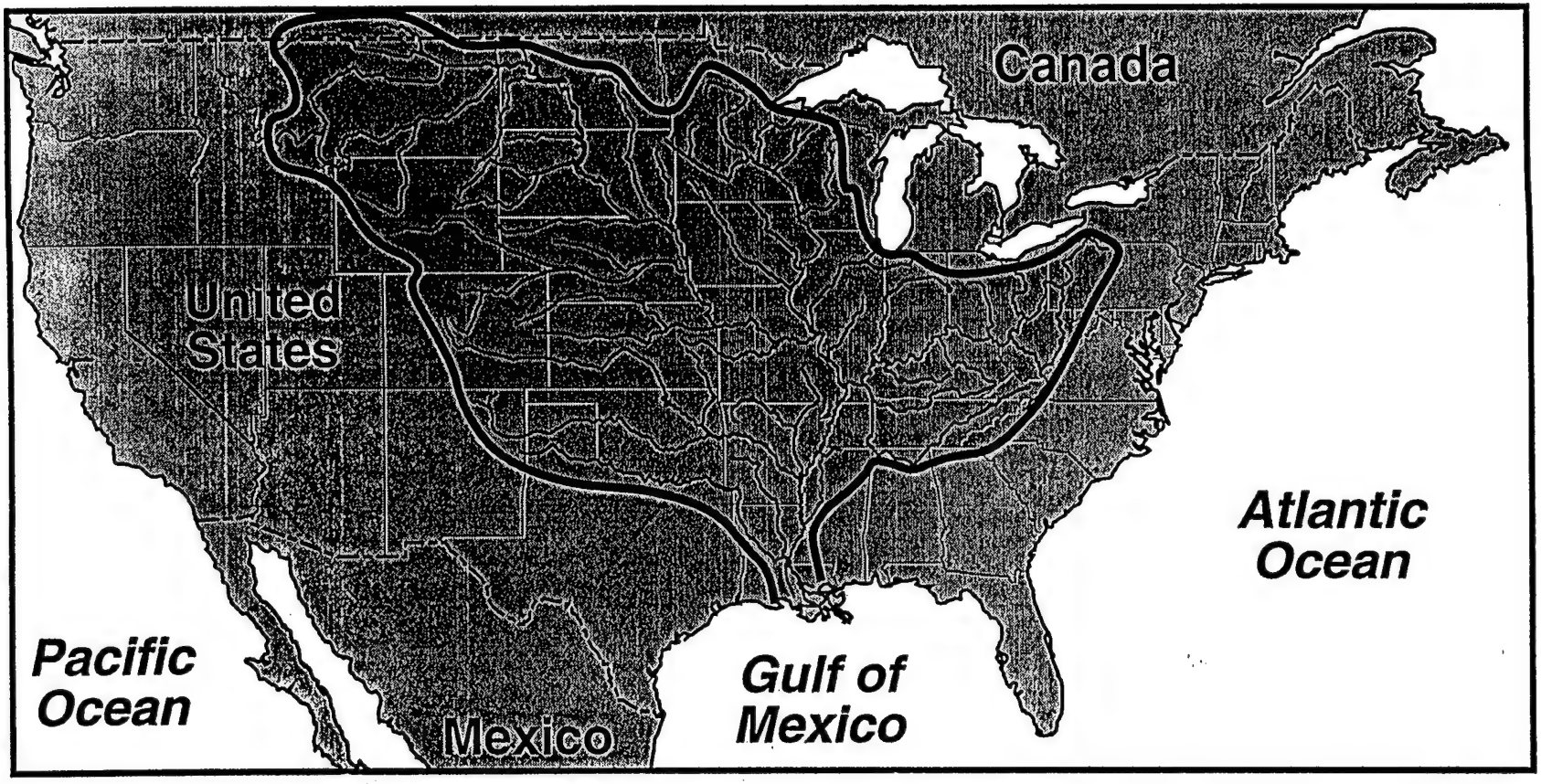

Figure 2. Drainage basin of the Mississippi River.

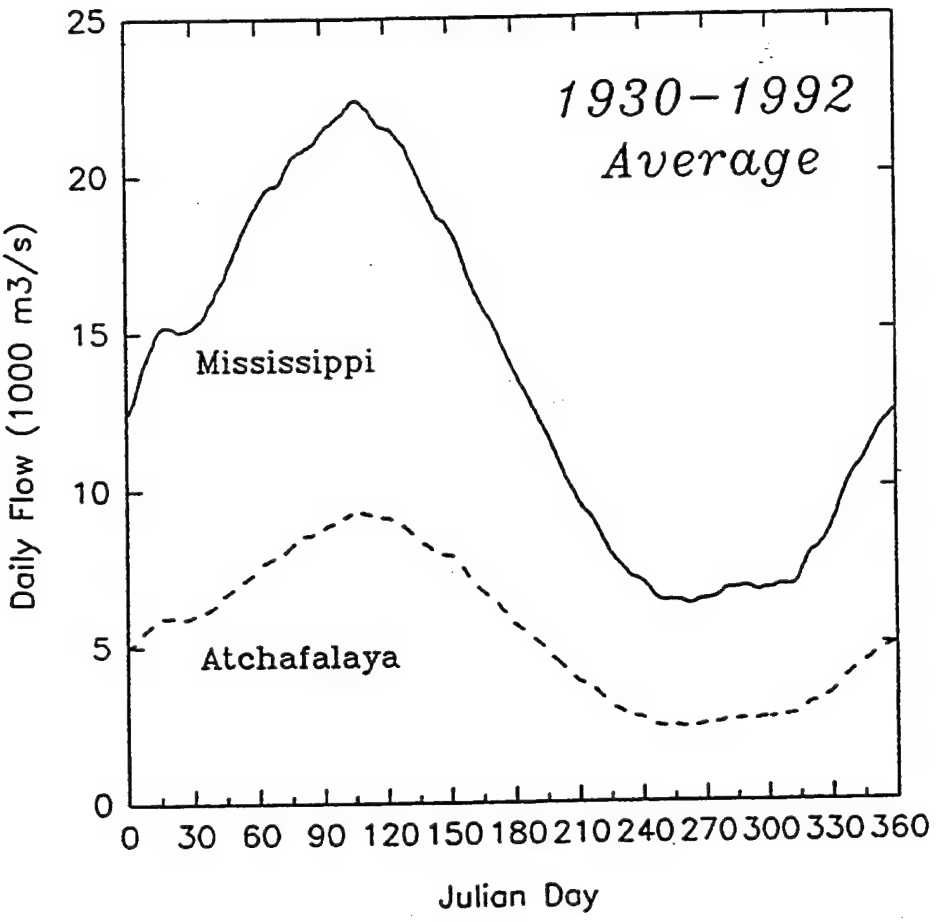

Figure 3. Average annual discharge from the Mississippi and Atchafalaya rivers from 1930 to 1992 (1000 $m^3 s^{-1}$). Daily river flow data gathered from the Army Corps of Engineers, New Orleans, Louisiana.

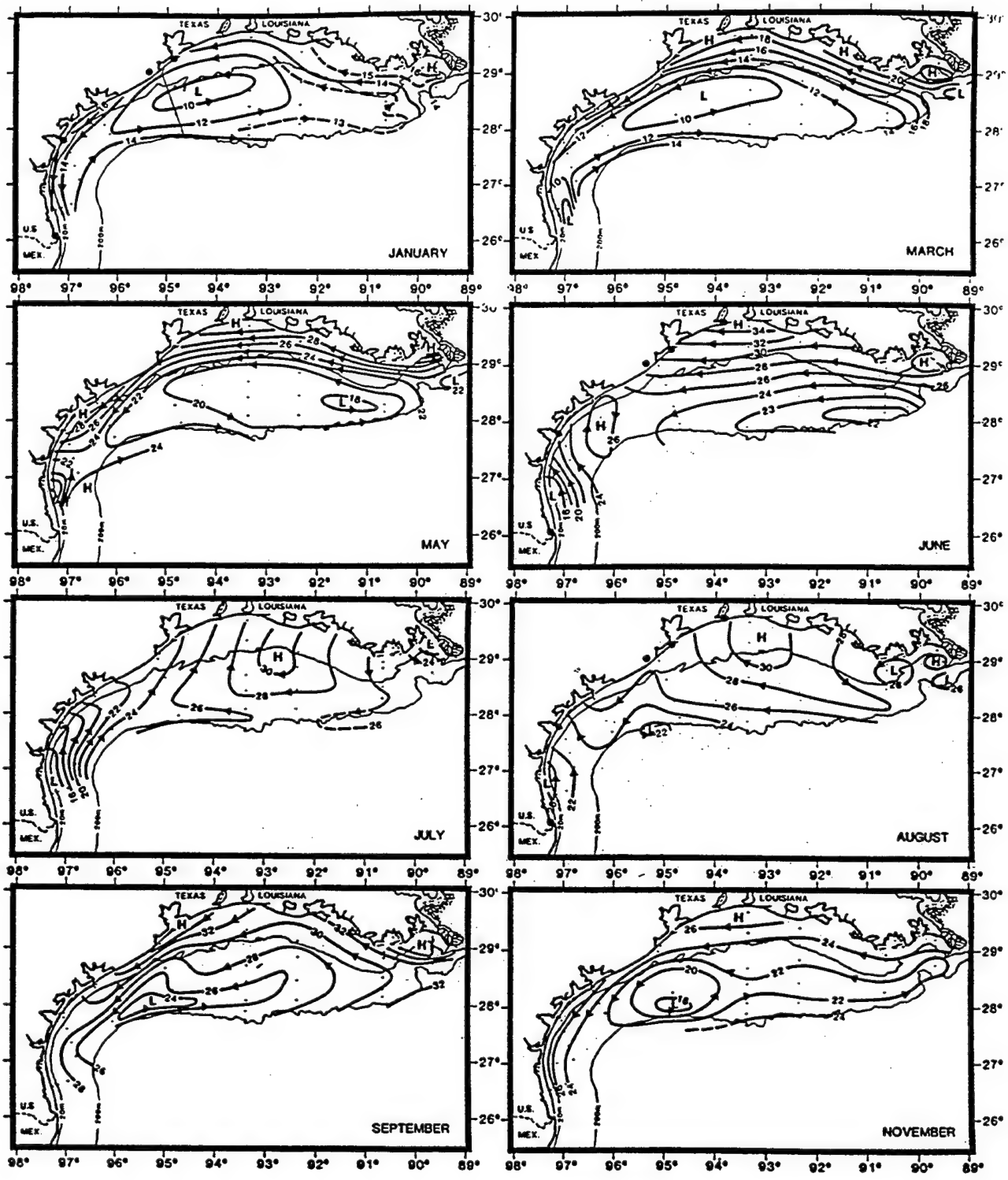

Figure 4. Monthly mean geopotential anomaly (dyn cm or 10^{-1} J kg^{-1}) of the sea surface relative to 70 dB or 0.70 MPa for representative months based on data taken aboard M/V Gus II in 1963-1965 (after Cochrane and Kelly 1986).

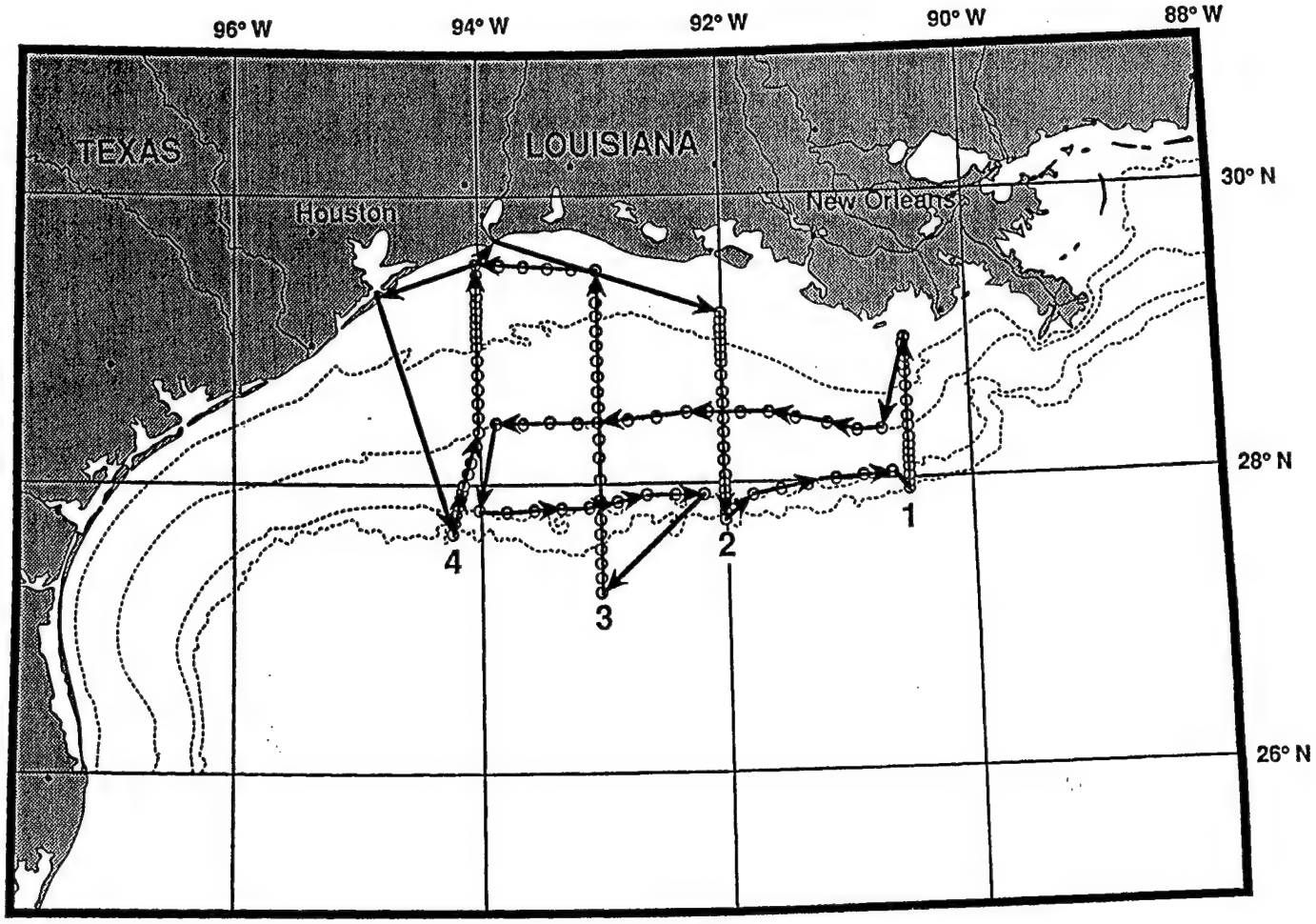

Figure 5. May 1992 LATEX A hydrographic cruise track and station locations (Cruise H01). Cruises H02-H04 had similar tracks.

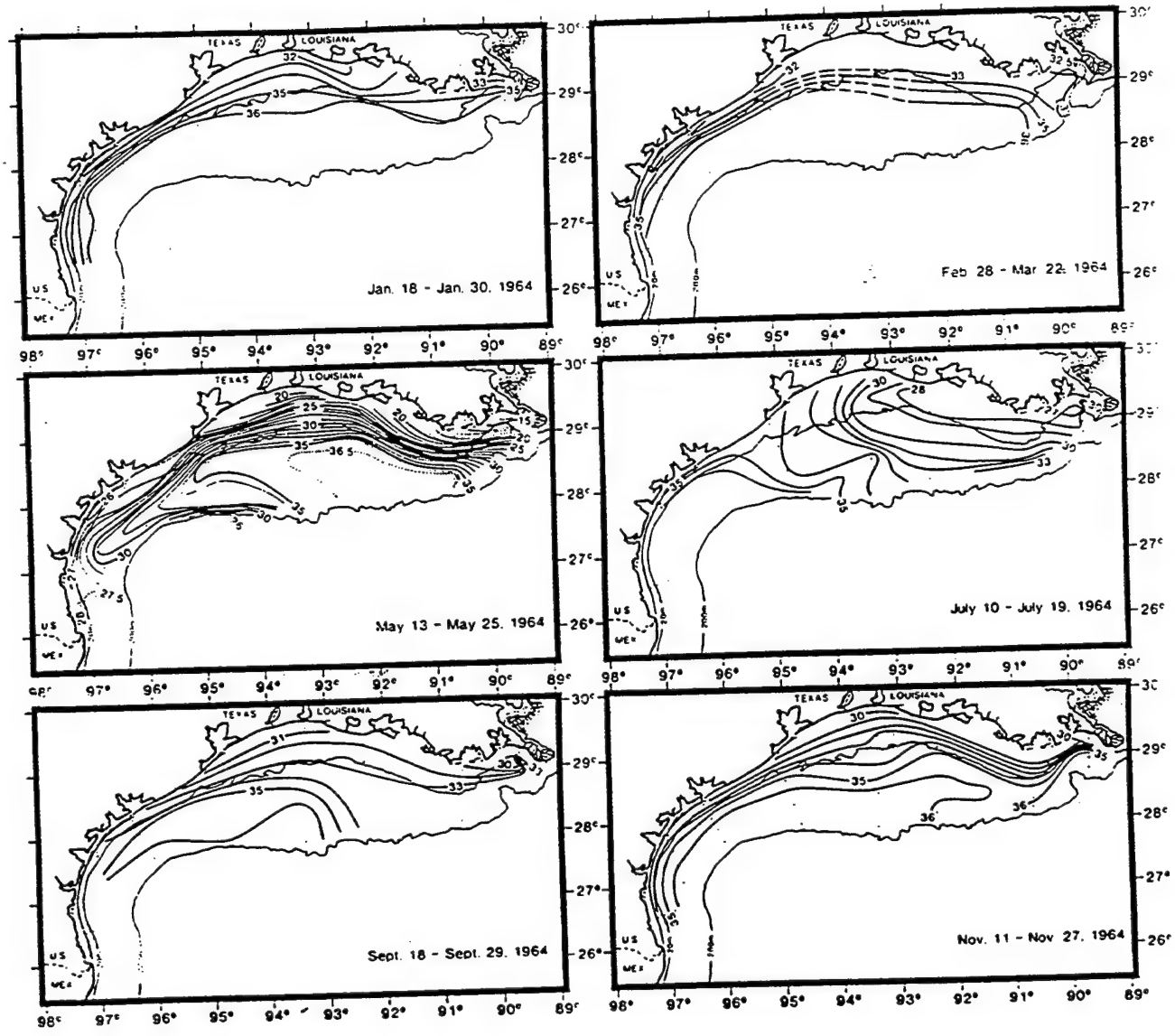

Figure 6. Sea-surface salinity for M/V Gus III cruises in 1964 (after Cochrane and Kelly 1986).

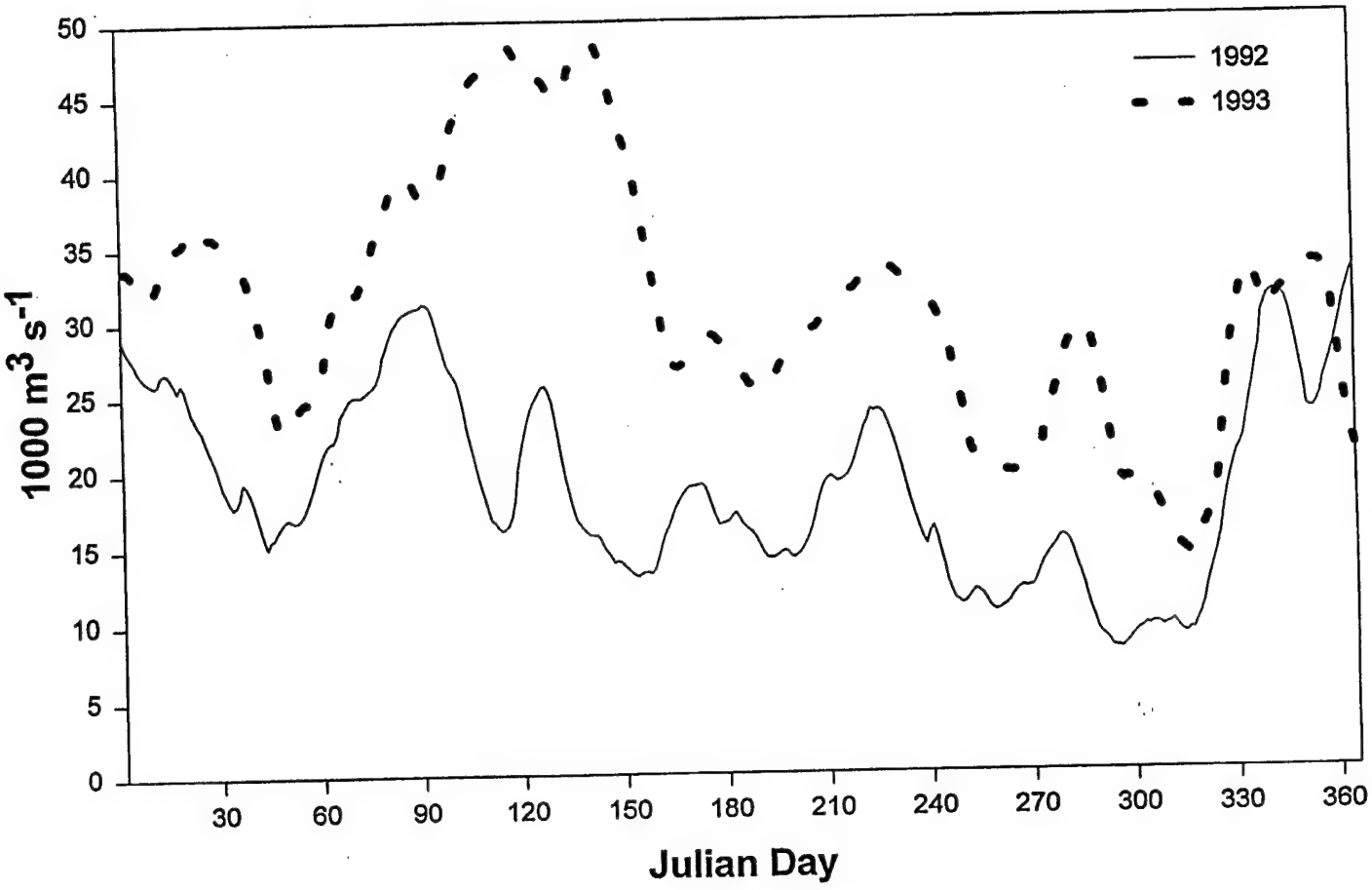

Figure 7. Annual flow (1000 m^3 s^{-1}) for the Mississippi and Atchafalaya rivers during 1992 and 1993.

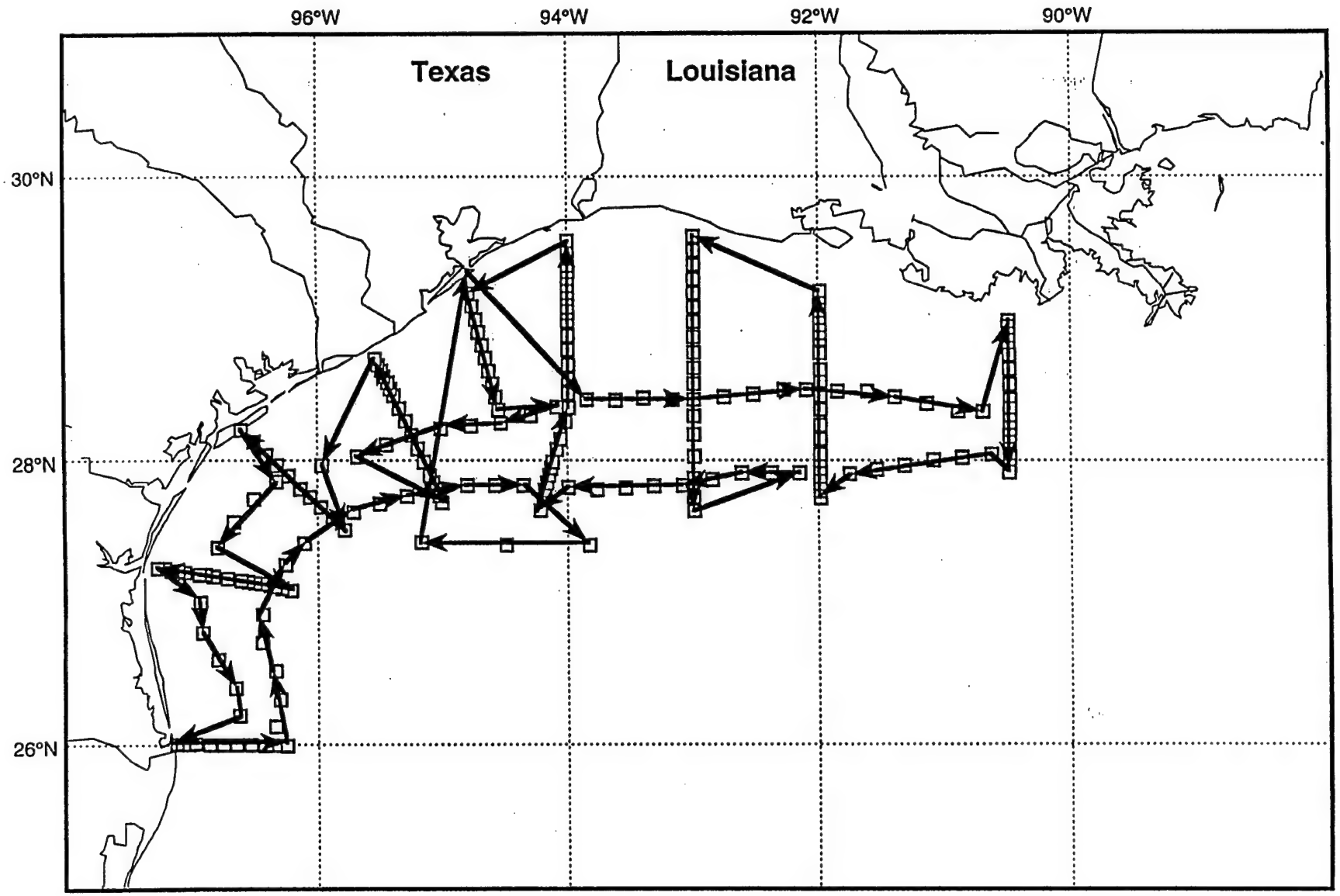

Figure 8. May 1993 LATEX A hydrographic cruise track and station locations (Cruise H05).

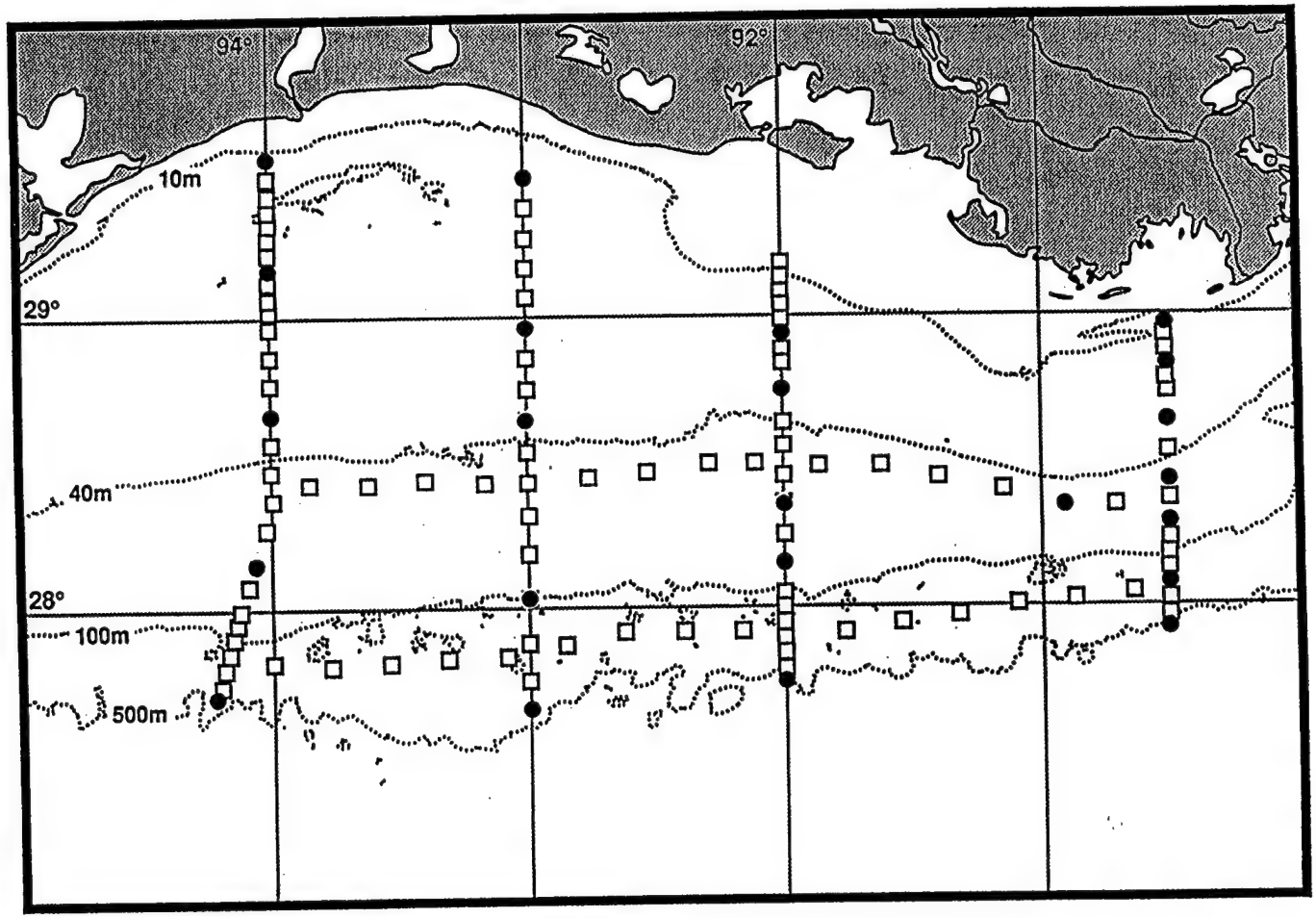

Figure 9. Map of stations chosen for phytoplankton identification for May 1992. Identical stations were examined for subsequent cruises.

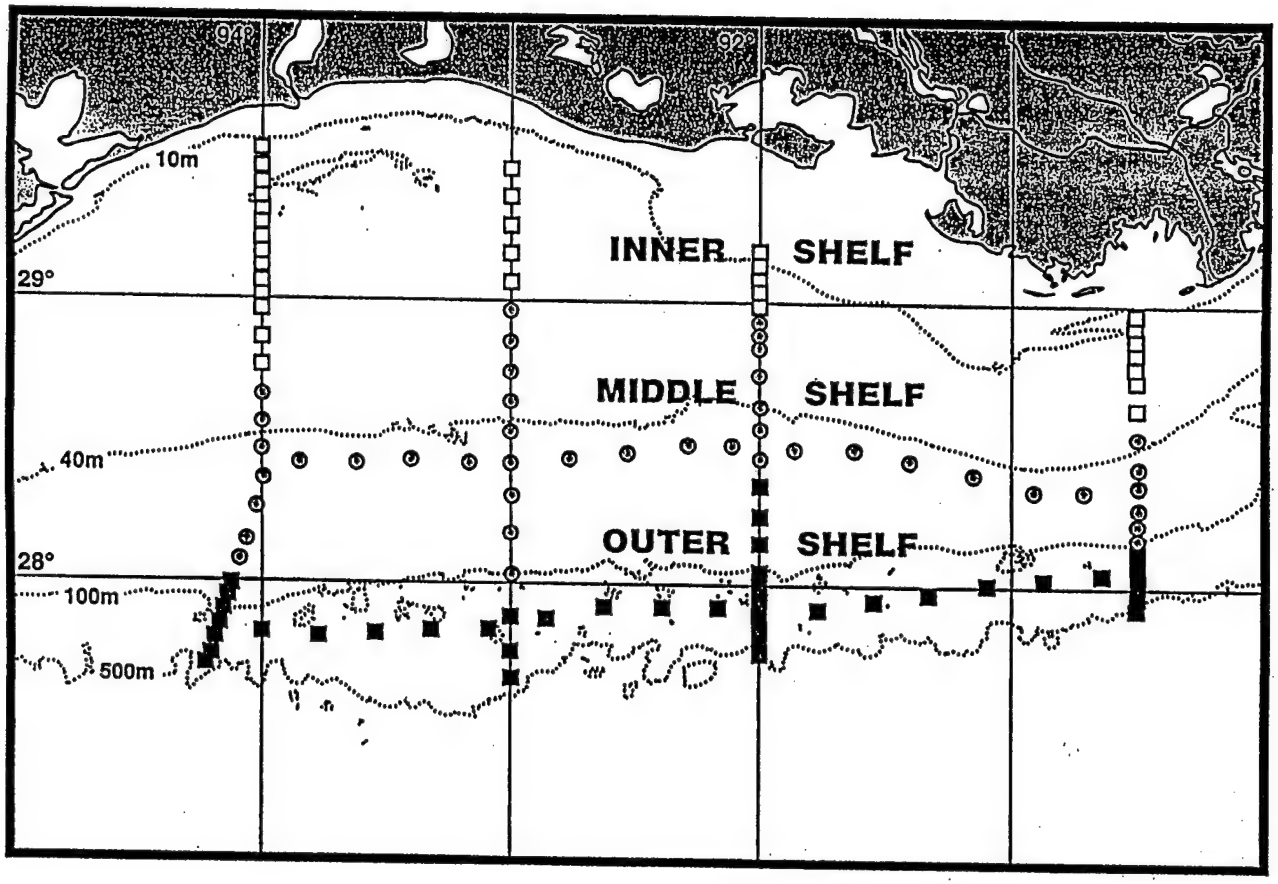

Figure 10. Inner, middle, and outer Louisiana shelf station distribution for Cruises H01-H05.

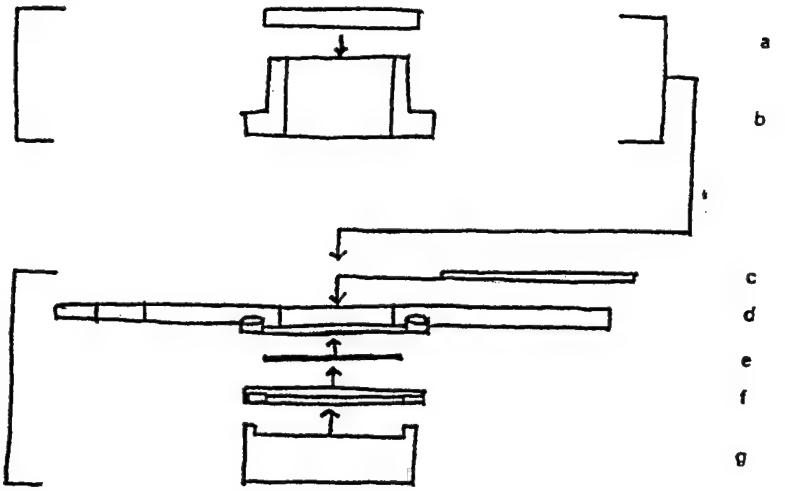

Figure 11. Bottom part of plate chamber. a. perspex plate with larger opening for column or cylinder and smaller drainage hole, b. ring to support bottom or base plate, c. key which fastens ring to bottom of perspex plate, d. top plate used to remove column or cylinder after sedimentation (after Hasle 1978).

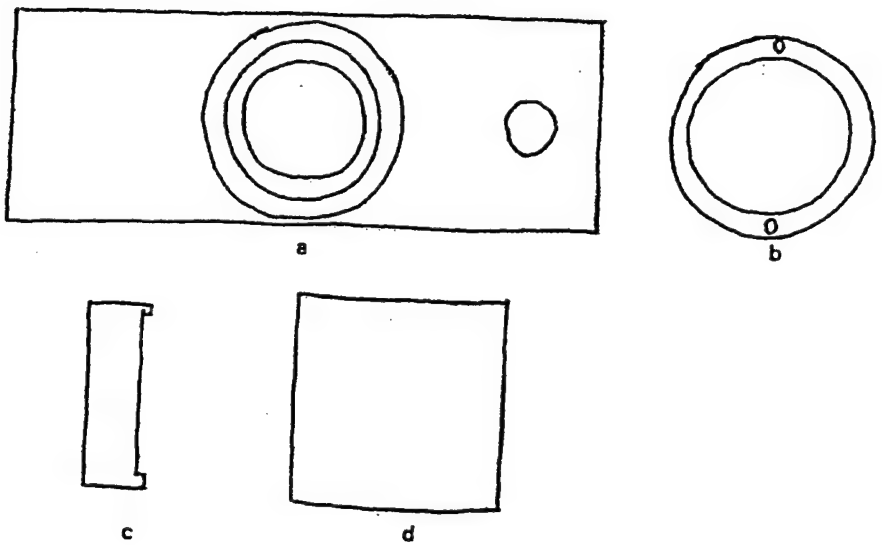

Figure 12. Vertical view of a combined plate chamber. a. top plate of sedimentation cylinder or settling column, b. sedimentation cylinder or chamber, c. top plate, d. perspex plate, e. bottom or base plate, f. ring, g. key (after Hasle 1978).

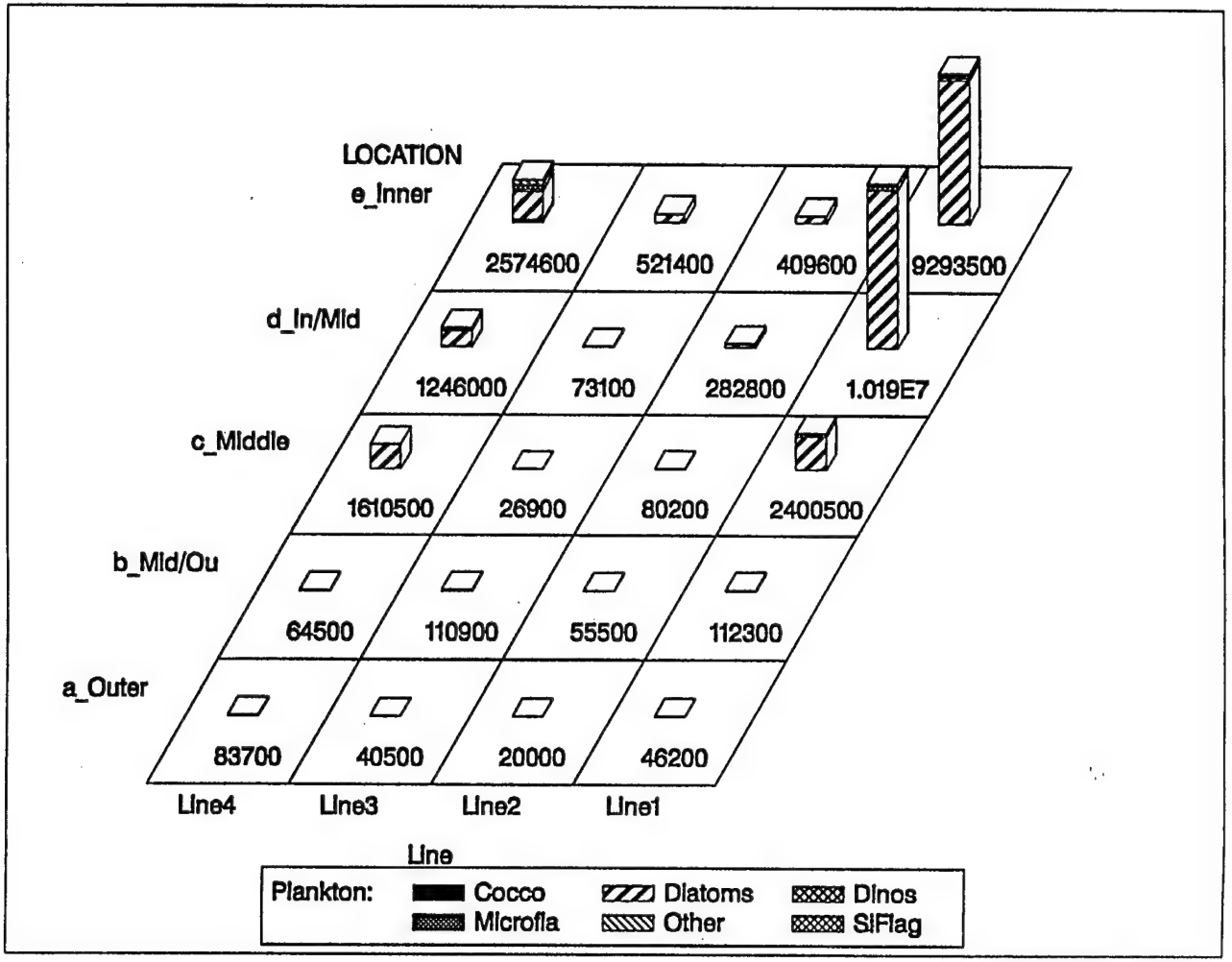

Figure 13. May 1992 (H01) Louisiana shelf surface phytoplankton distributions and abundances.

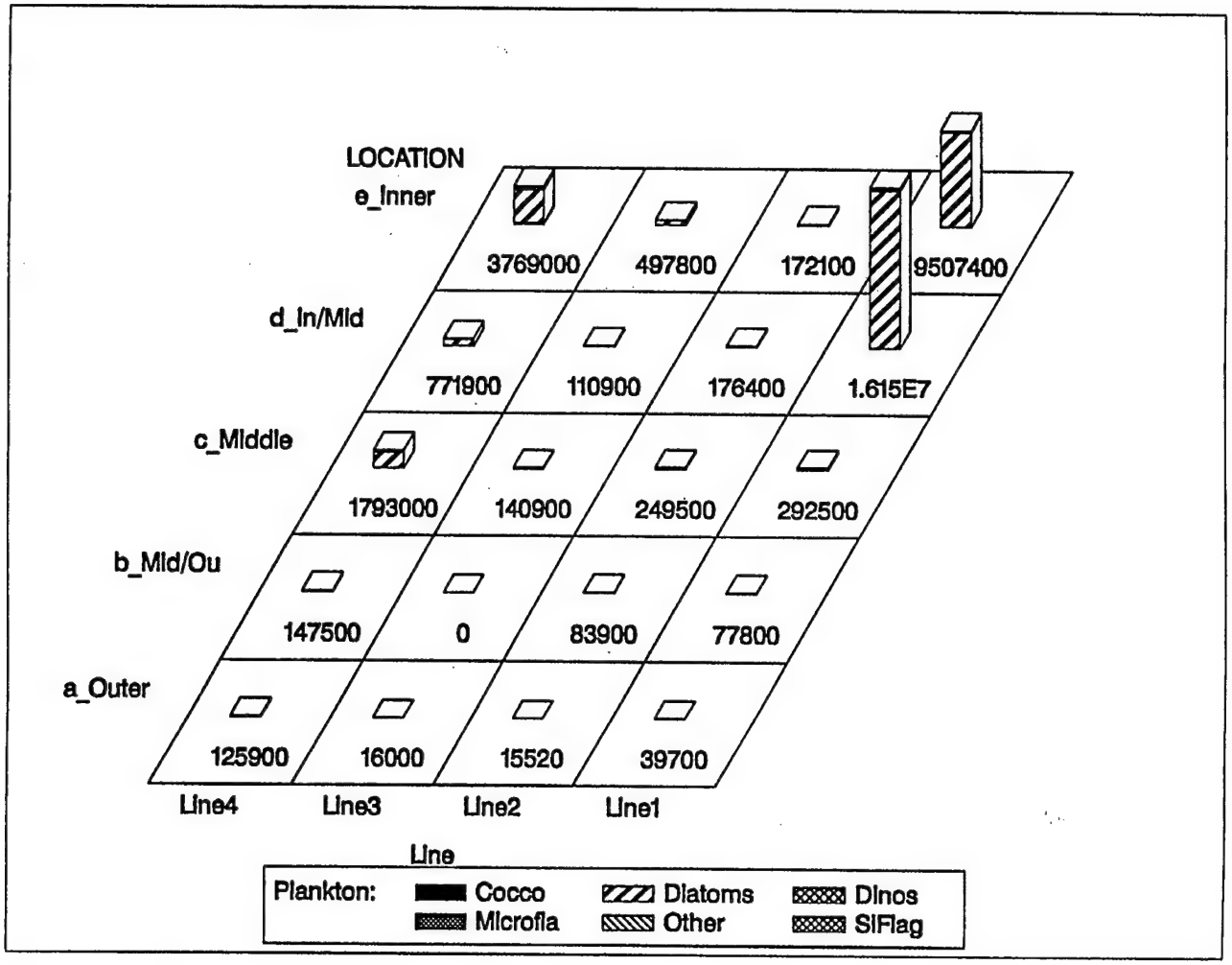

Figure 14. May 1992 (H01) Louisiana shelf chlorophyll maximum phytoplankton distributions and abundances.

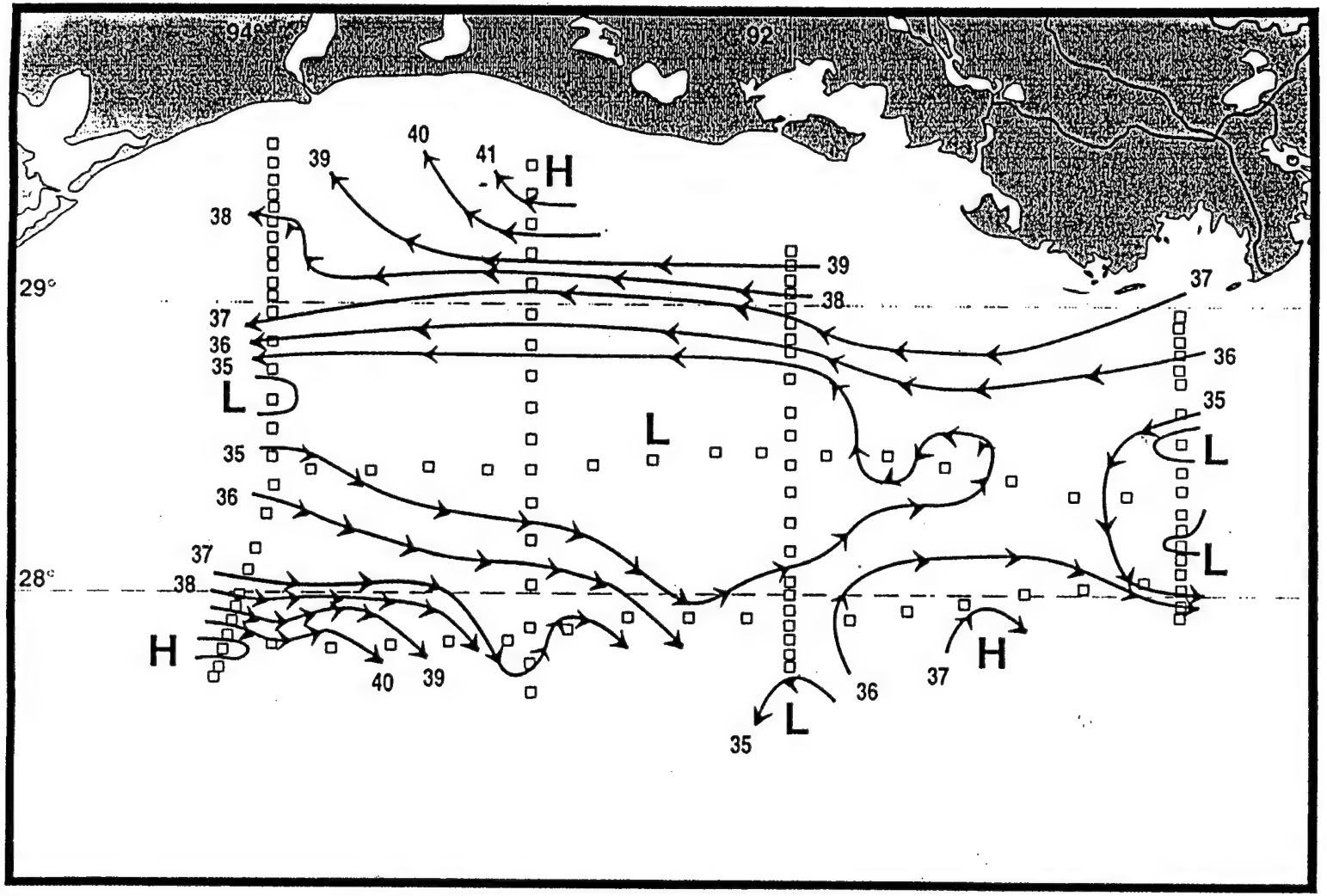

Figure 15. May 1992 (H01) geopotential anomaly for the Louisiana shelf for 3 over 160 decibars in dynamic centimeters (after Jochens and Nowlin 1994).

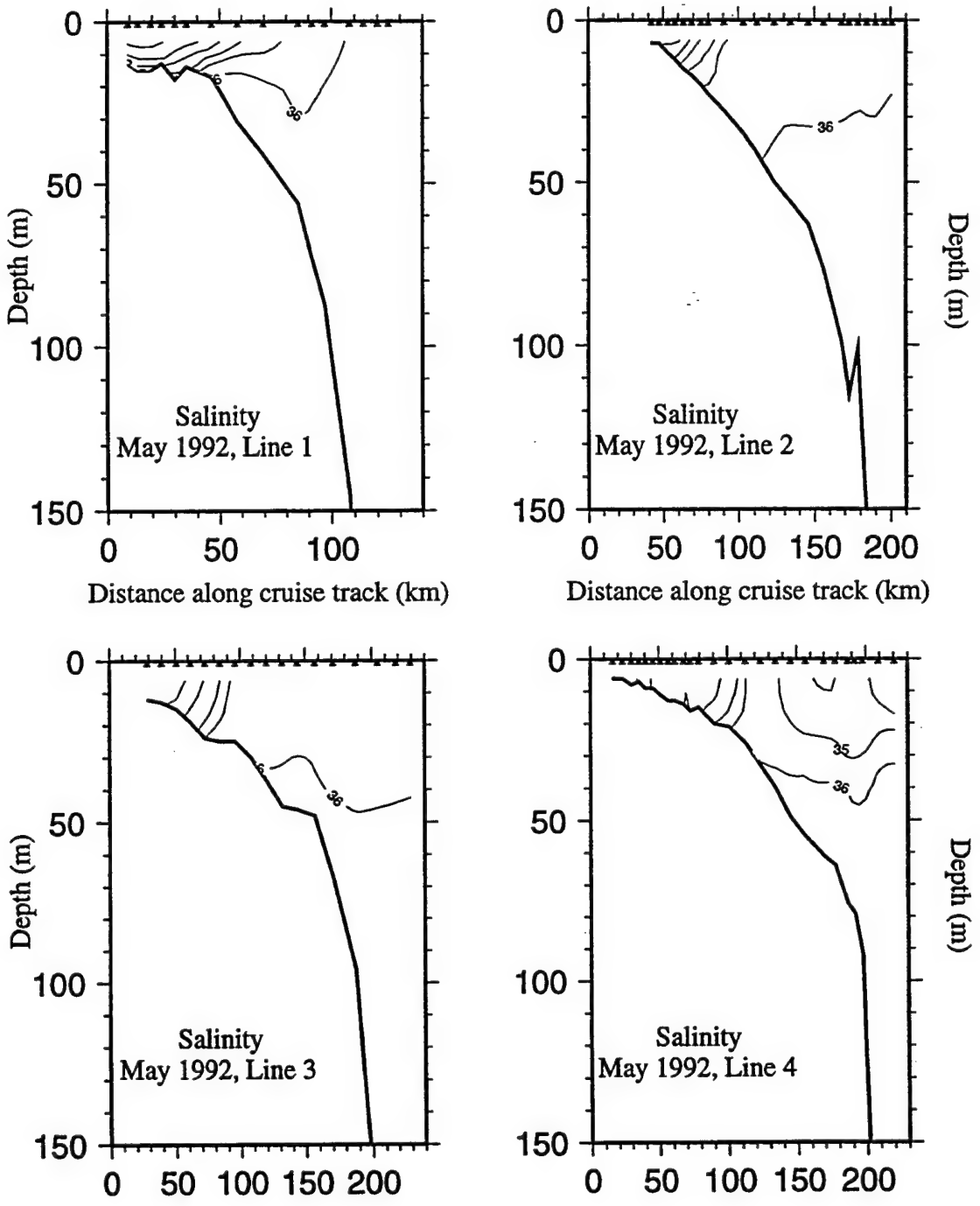

Figure 16. Vertical sections of salinity for Lines 1-4 during May 1992 (H01).

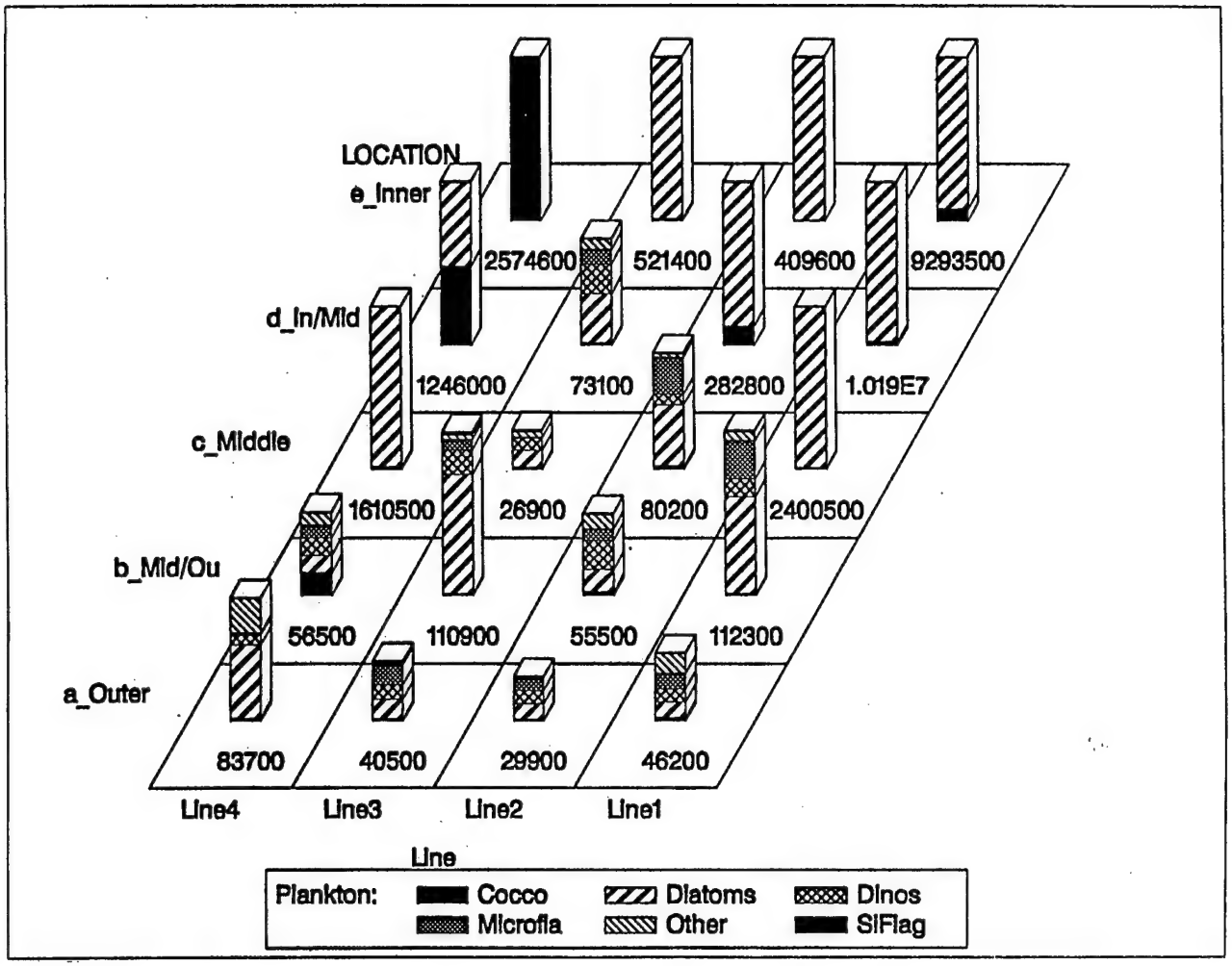

Figure 17. May 1992 (H01) Louisiana shelf surface phytoplankton distributions and abundances. Plot normalized for outer shelf distributions to box of 112,300 cells L^{-1} on Line 1.

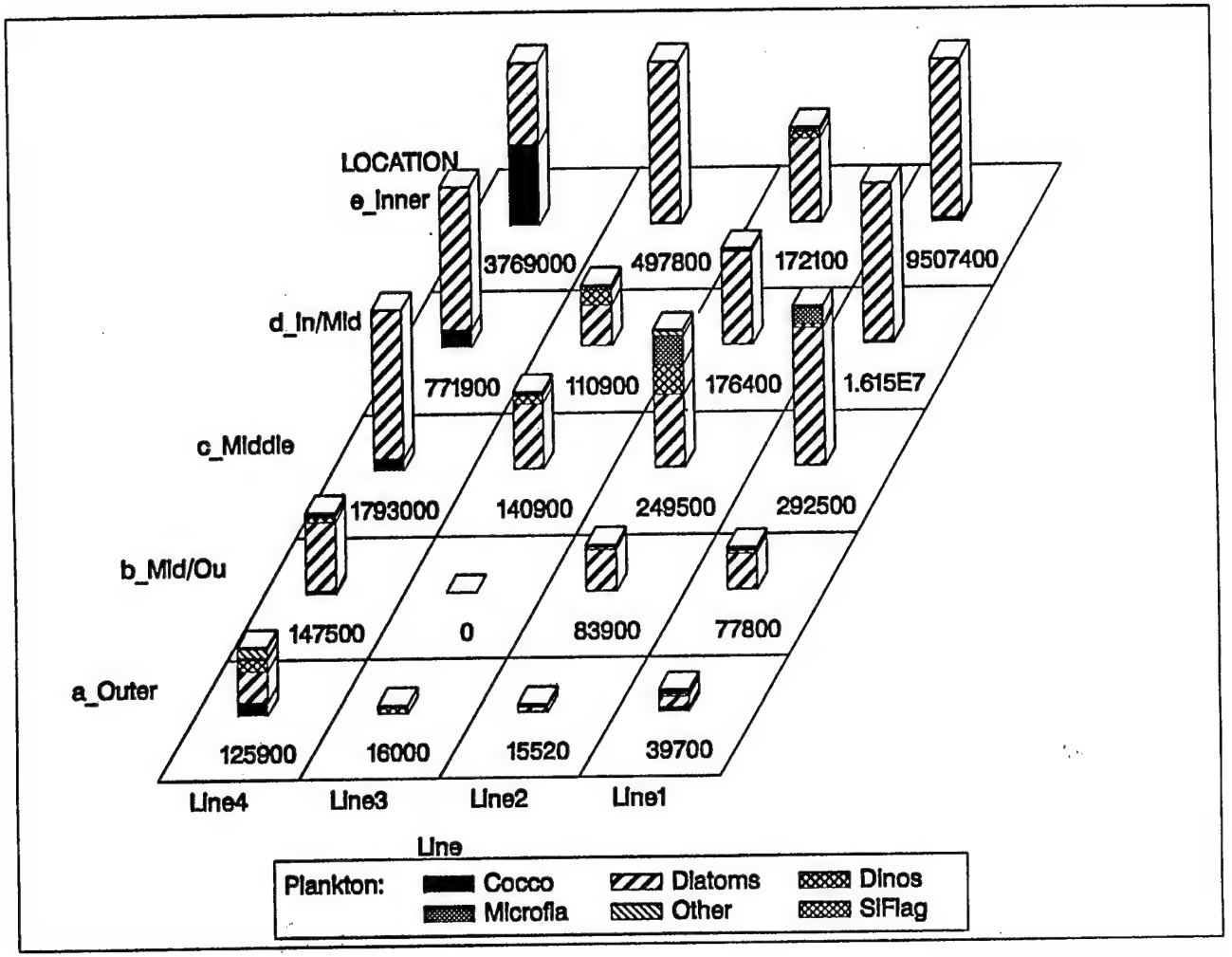

Figure 18. May 1992 (H01) Louisiana shelf chlorophyll maximum phytoplankton distributions and abundances. Plot normalized for outer shelf distributions to box of 292,500 cells L^{-1} on Line 1.

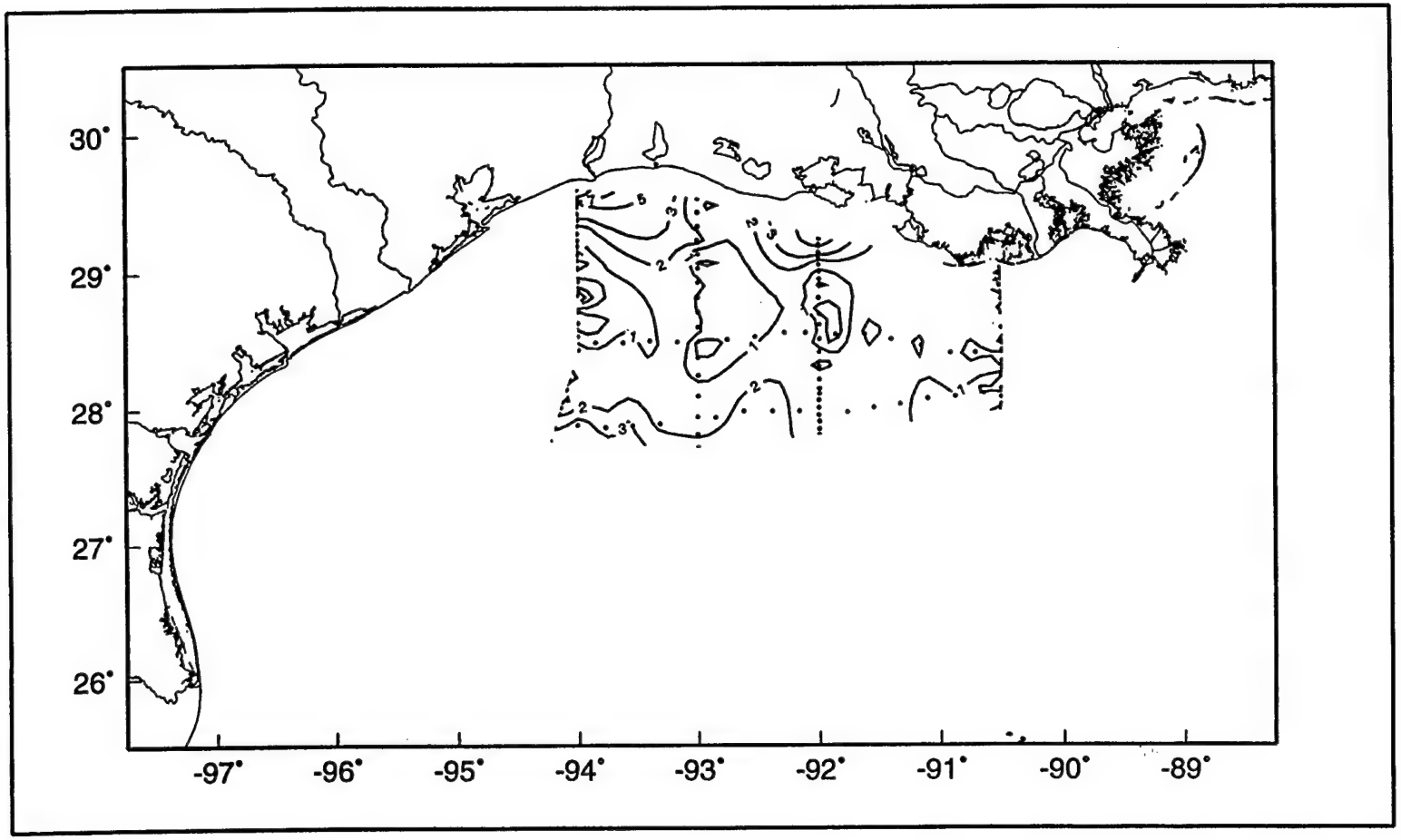

Figure 19. Surface silicate concentrations (μmol L^{-1}) on the Louisiana shelf during May 1992 (H01).

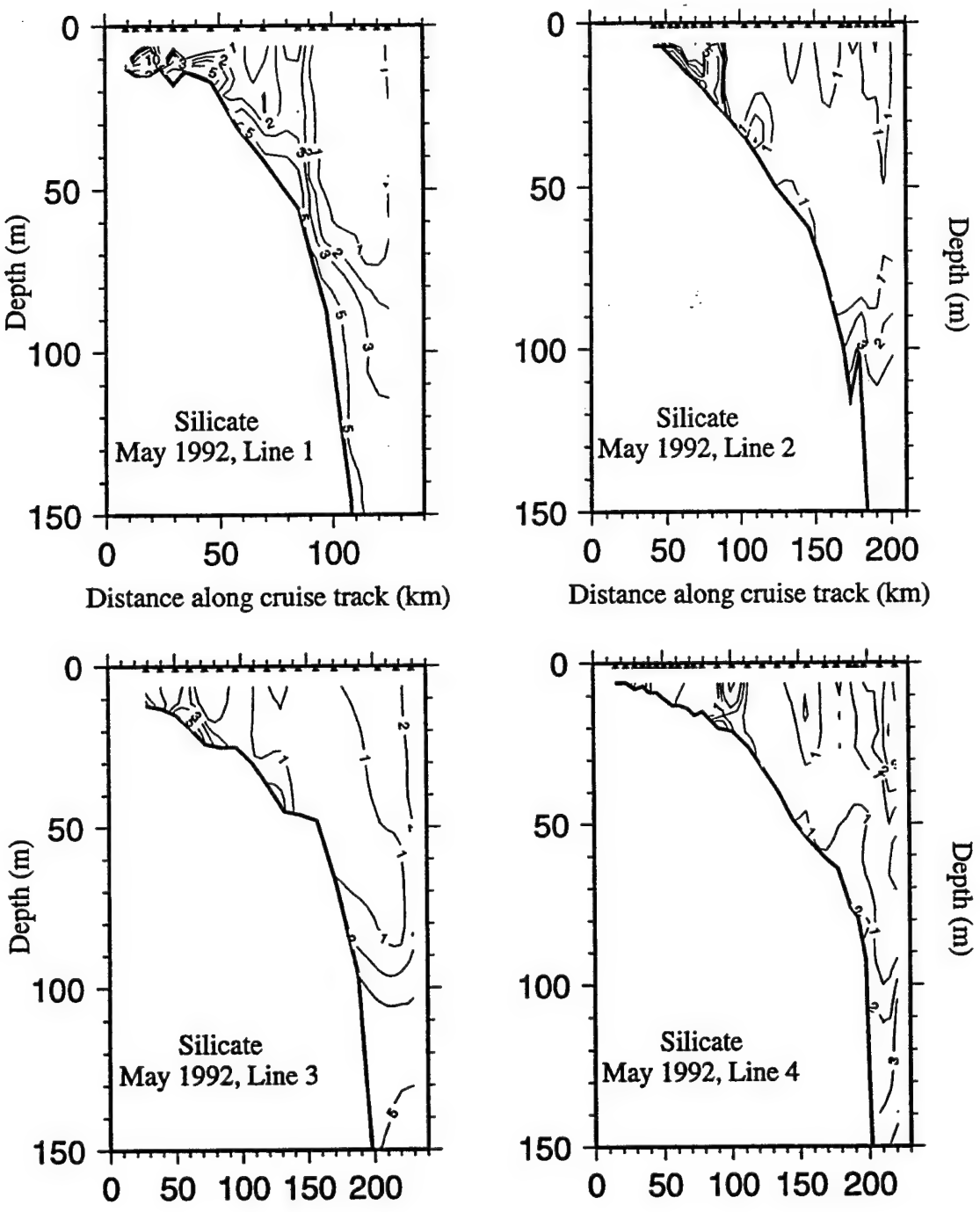

Figure 20. Vertical sections of silicate concentration (µmol L^{-1}) for Lines 1-4 during May 1992 (H01).

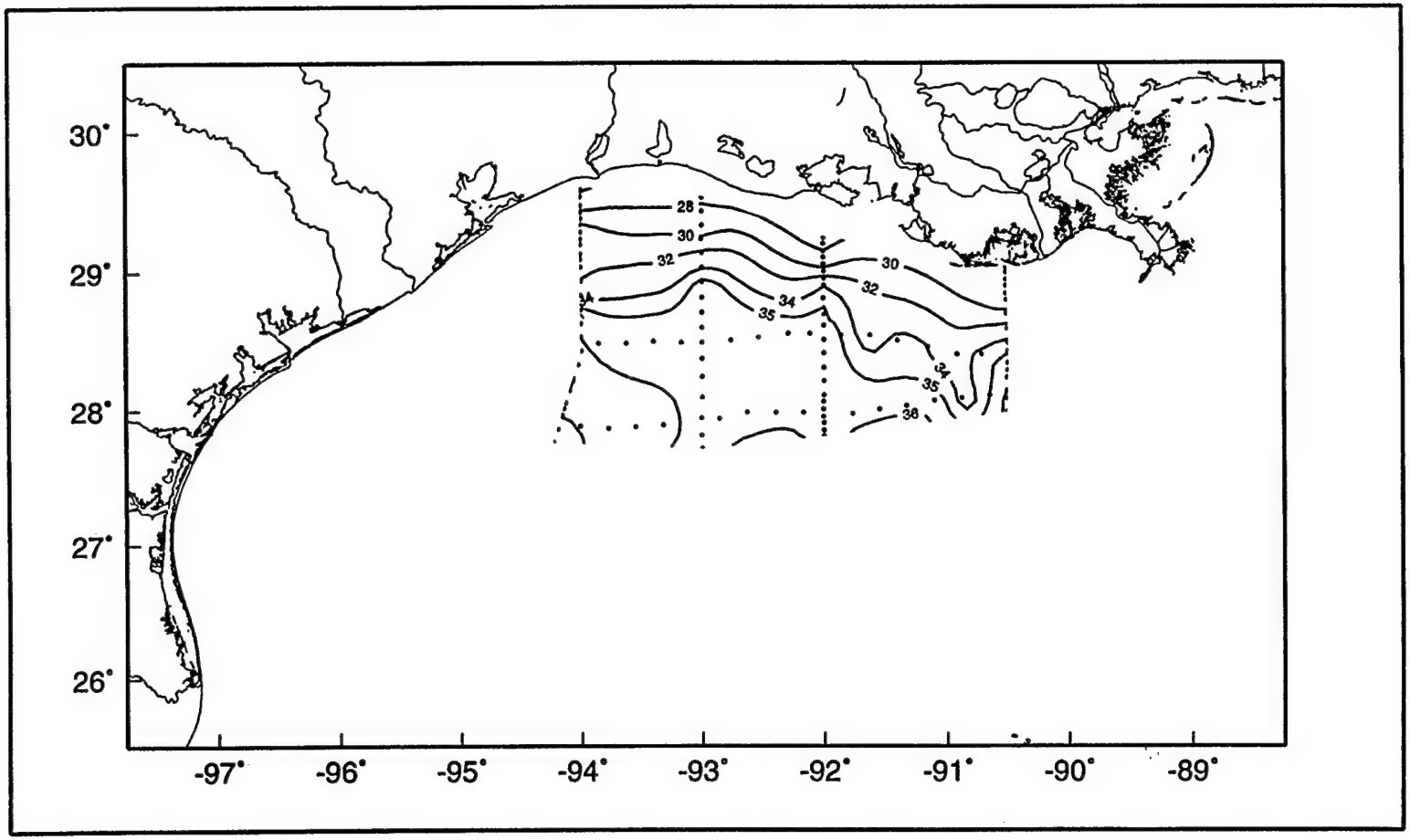

Figure 21. Surface salinity on the Louisiana shelf during May 1992 (H01).

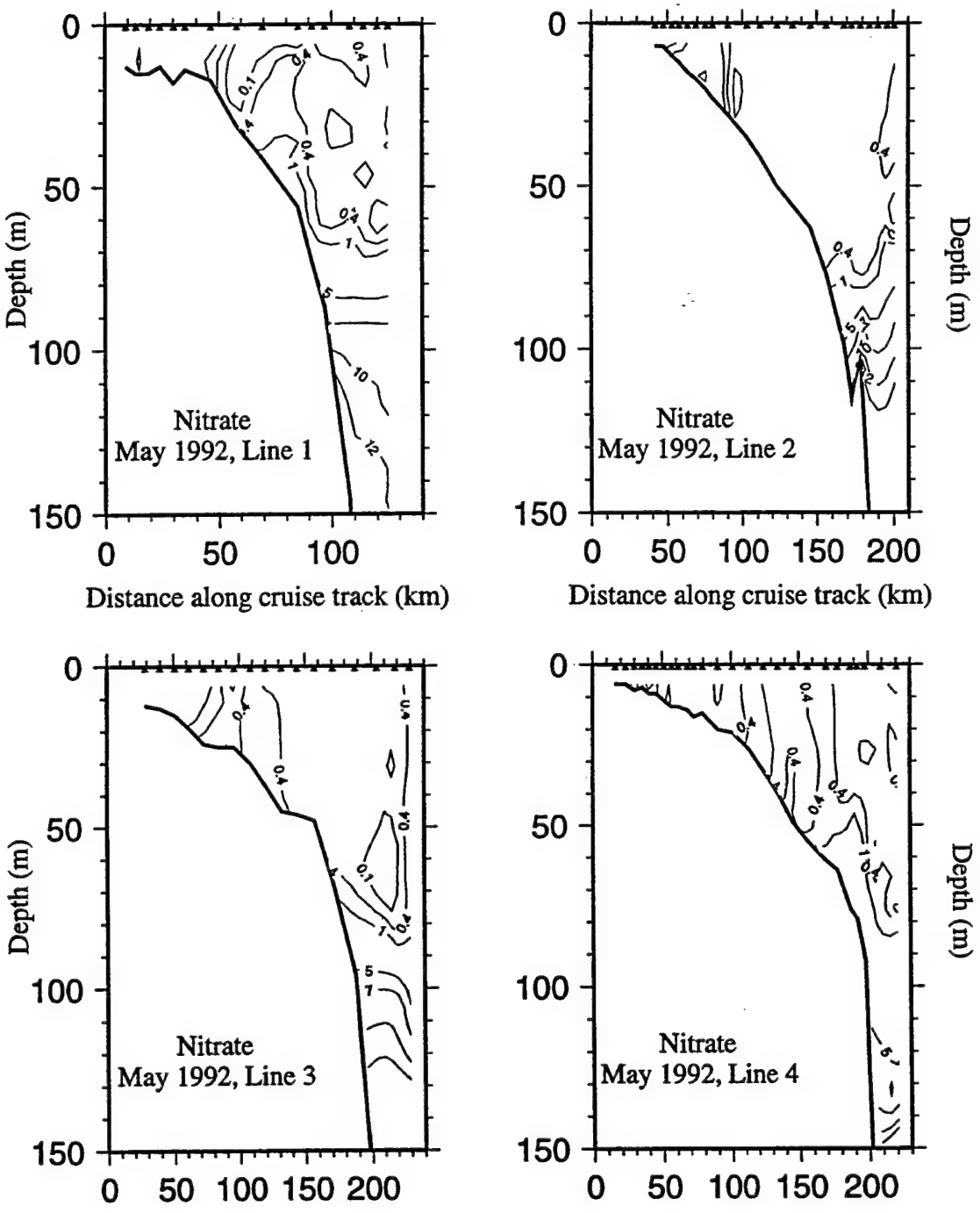

Figure 22. Vertical sections of nitrate concentration (μmol L^{-1}) for Lines 1-4 during May 1992 (H01).

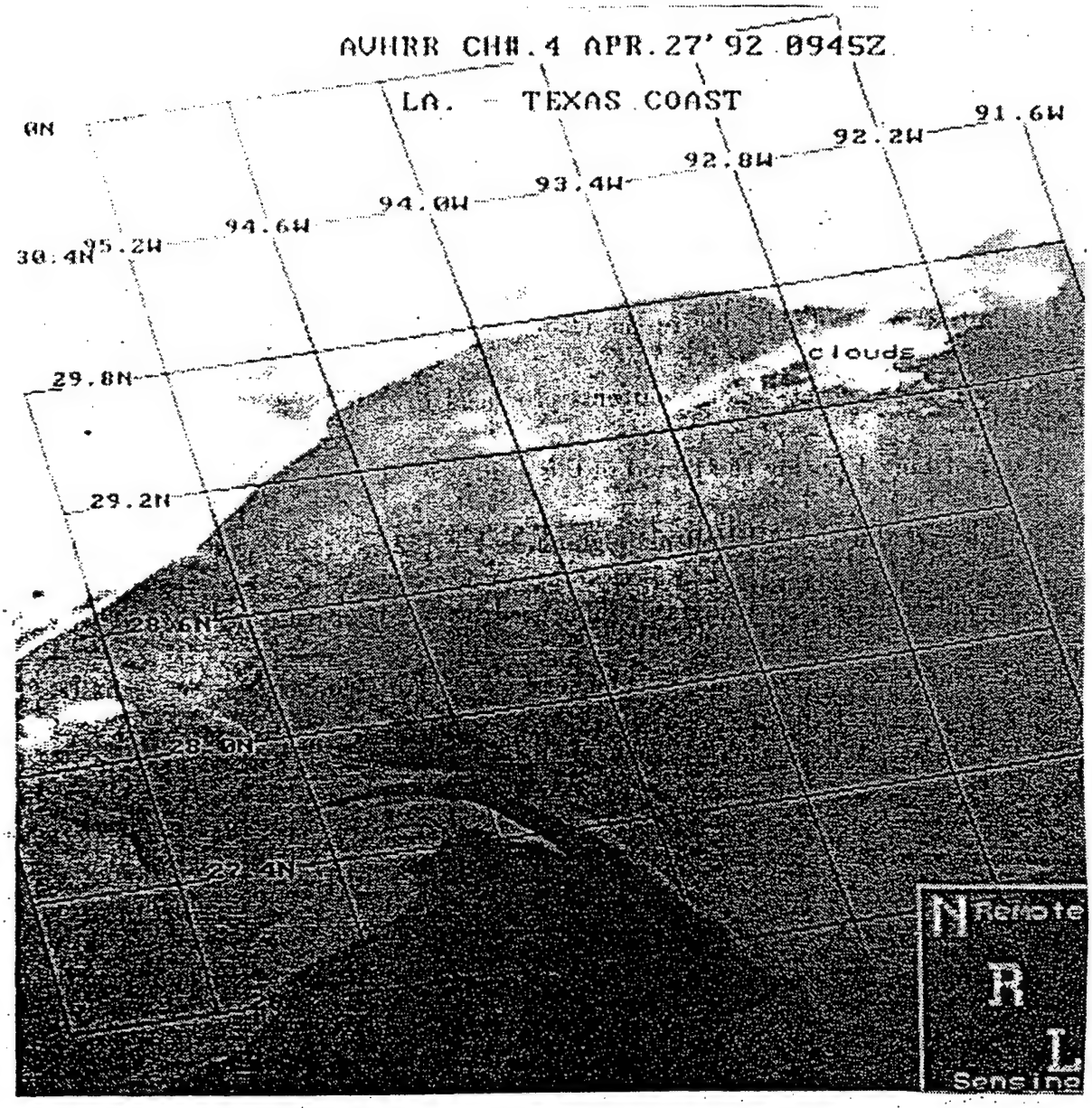

Figure 23. AVHRR image of sea surface temperature on the Texas-Louisiana continental shelf defining Eddy Triton in May 1992.

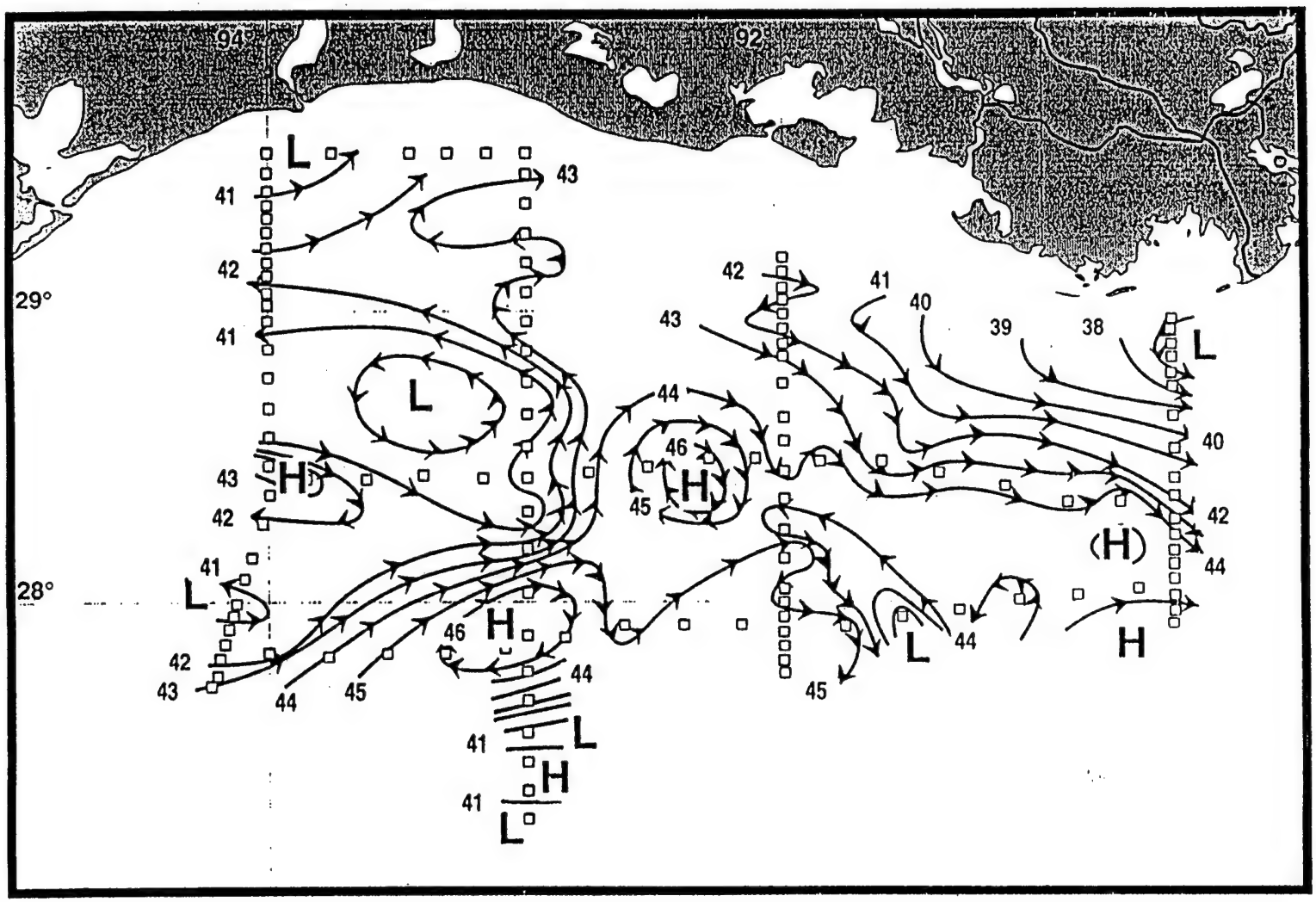

Figure 24. August 1992 (H02) geopotential anomaly for the Louisiana shelf for 3 over 160 decibars in dynamic centimeters (after Jochens and Nowlin).

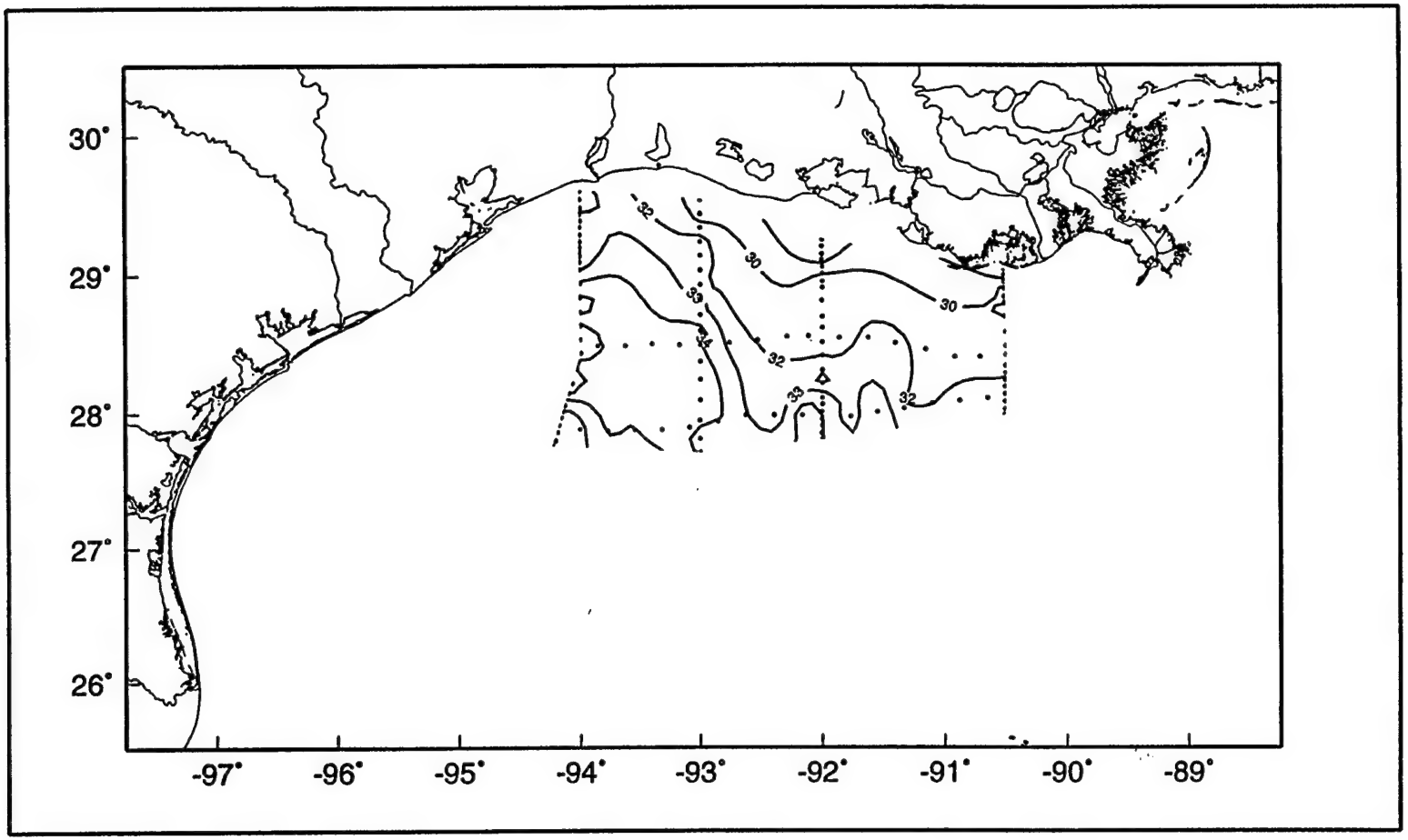

Figure 25. Surface salinity on the Louisiana shelf during August 1992 (H02).

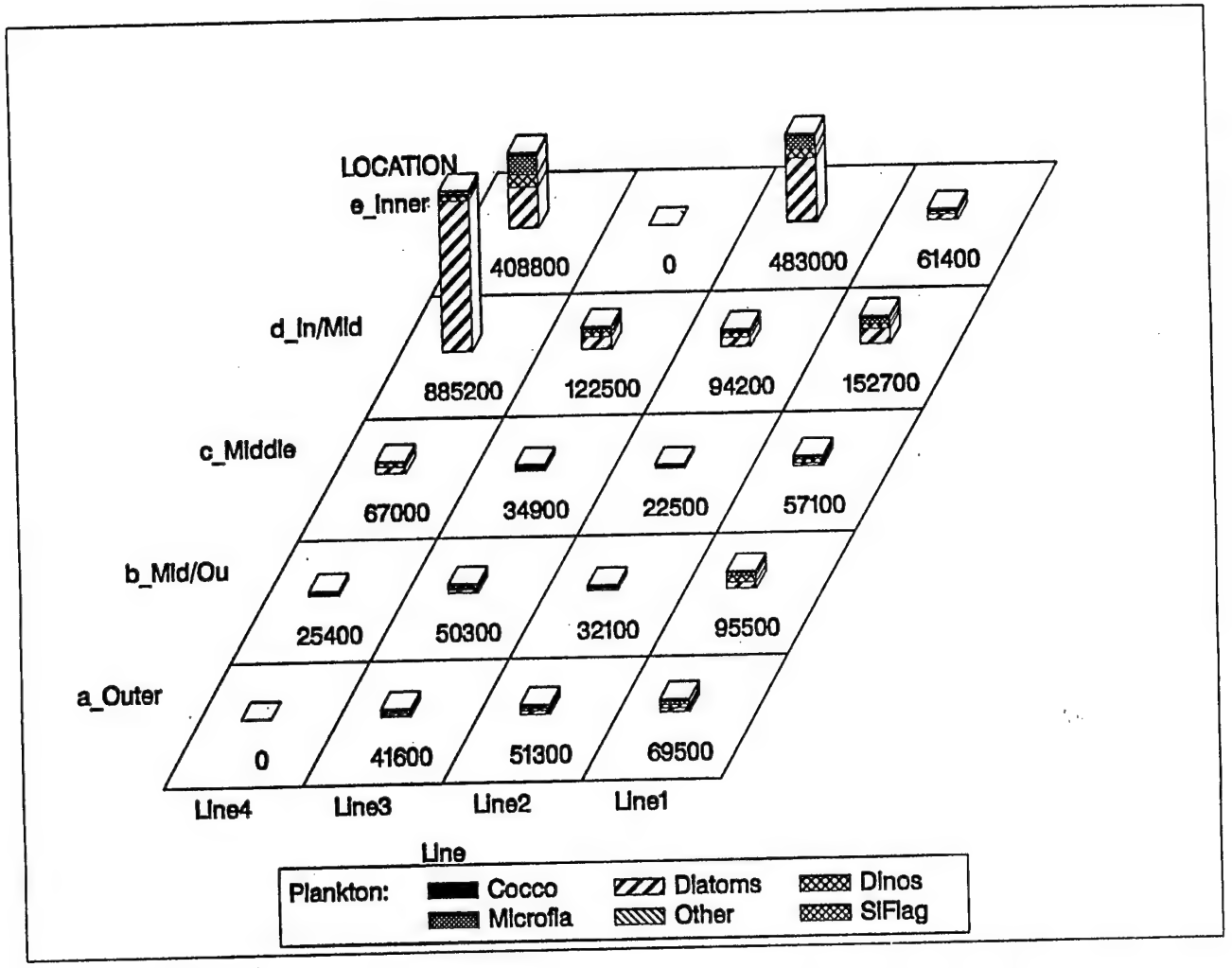

Figure 26. August 1992 (H02) Louisiana shelf surface phytoplankton distributions and abundances.

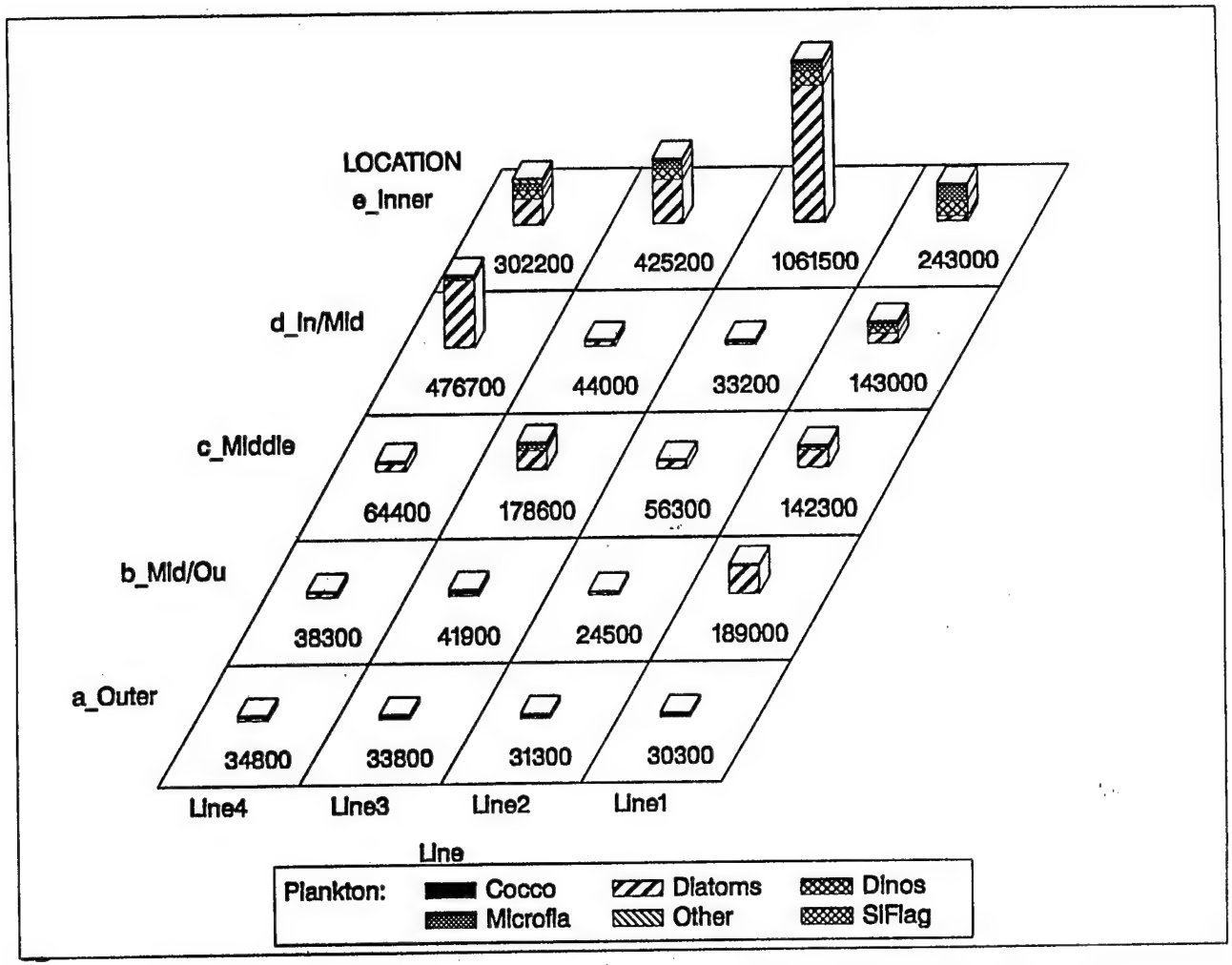

Figure 27. August 1992 Louisiana shelf chlorophyll maximum phytoplankton distributions and abundances.

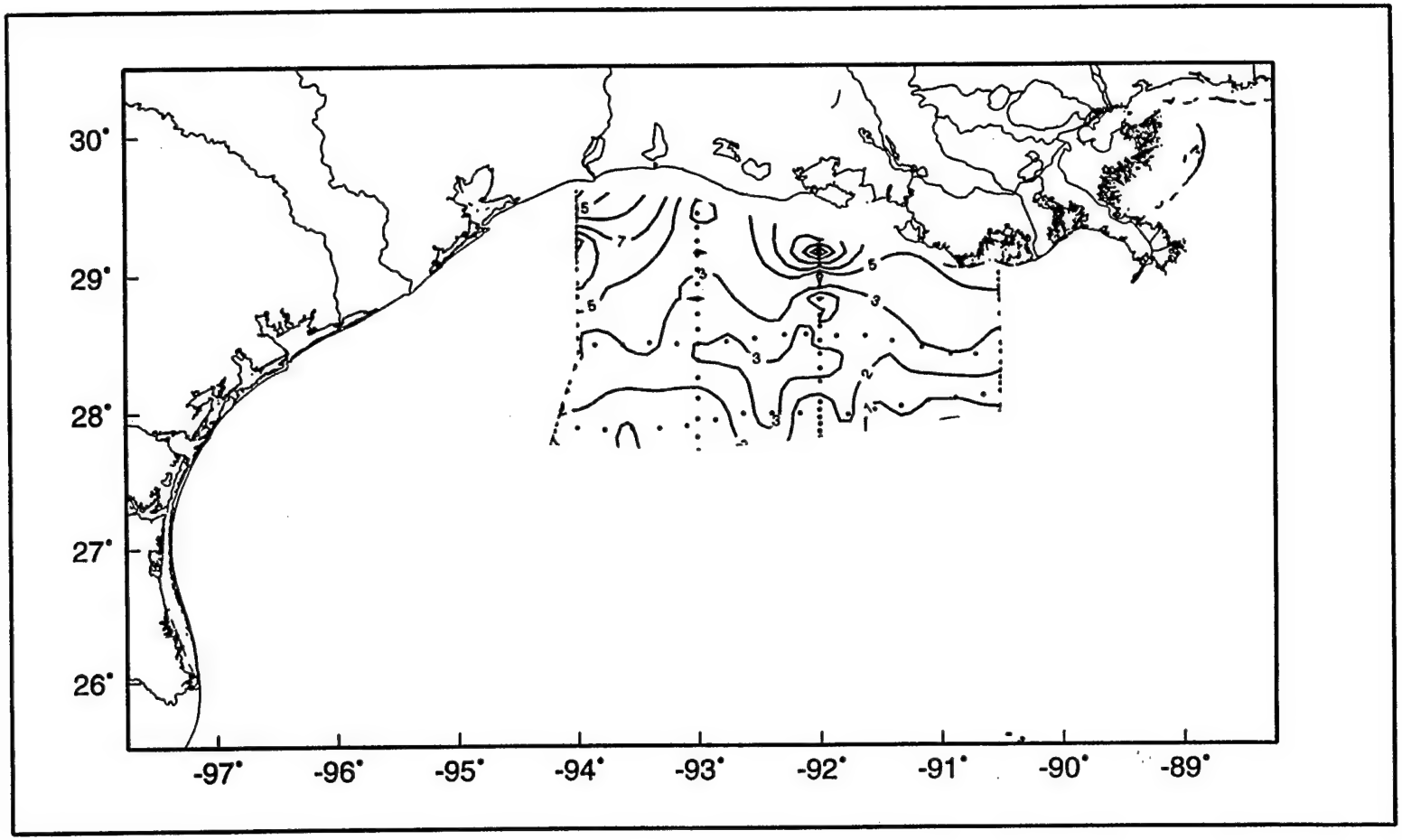

Figure 28. Surface silicate concentrations (μmol L^{-1}) on the Louisiana shelf during August 1992 (H02).

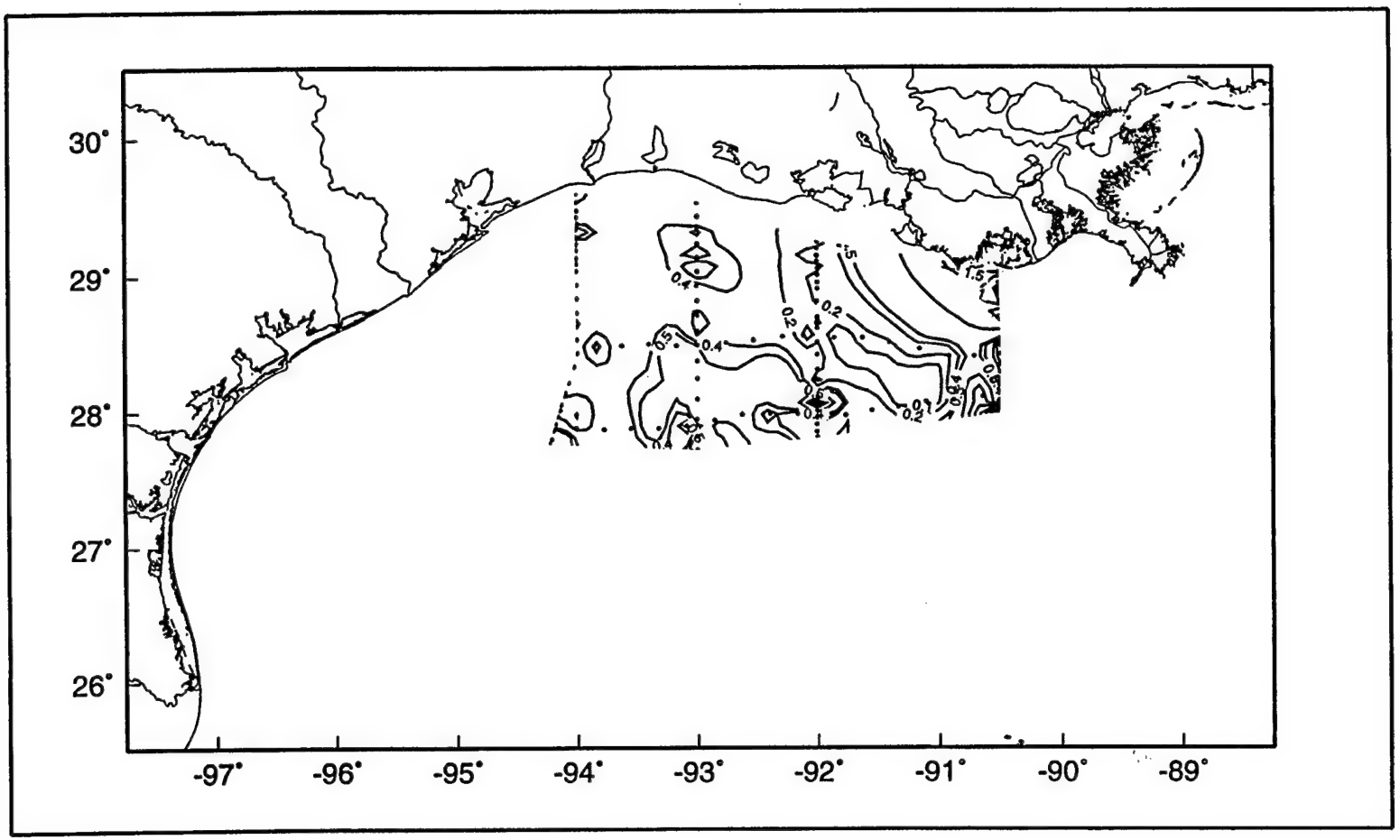

Figure 29. Surface nitrate concentrations (µmol L^{-1}) on the Louisiana shelf during August 1992 (H02).

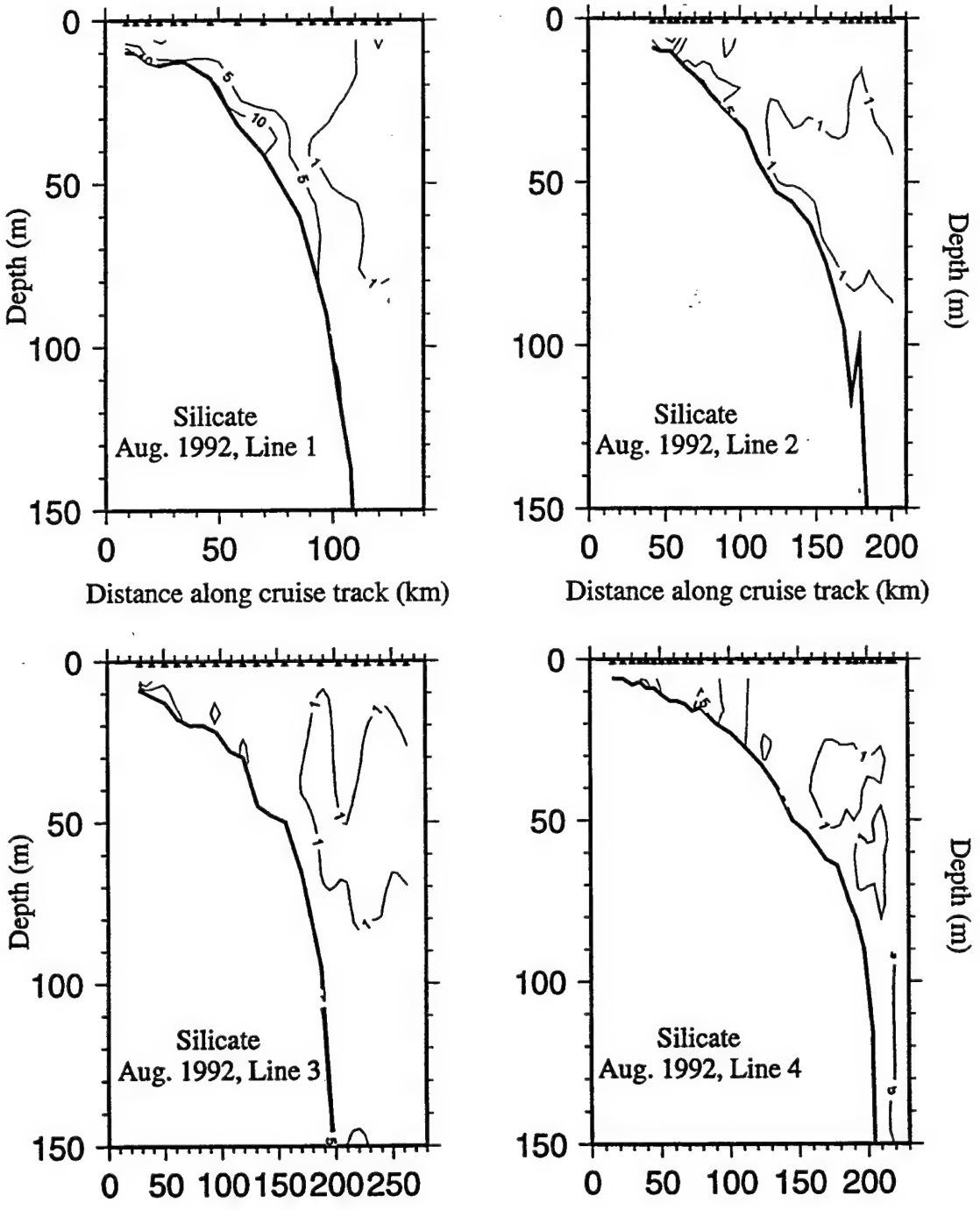

Figure 30. Vertical sections of silicate concentration (μmol L^{-1}) for Lines 1-4 during August 1992 (H02).

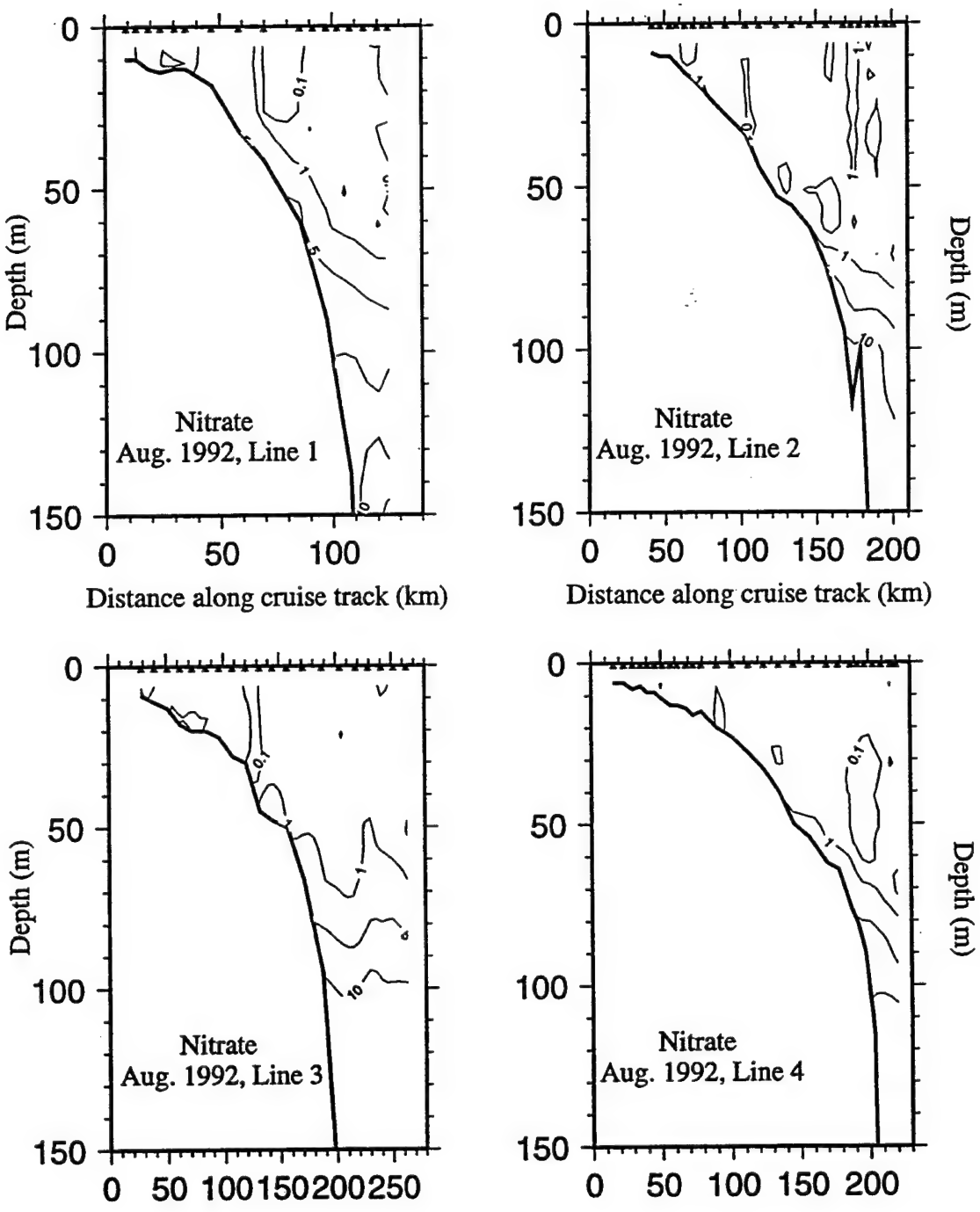

Figure 31. Vertical sections of nitrate concentration (μmol L^{-1}) for Lines 1-4 during August 1992 (H02).

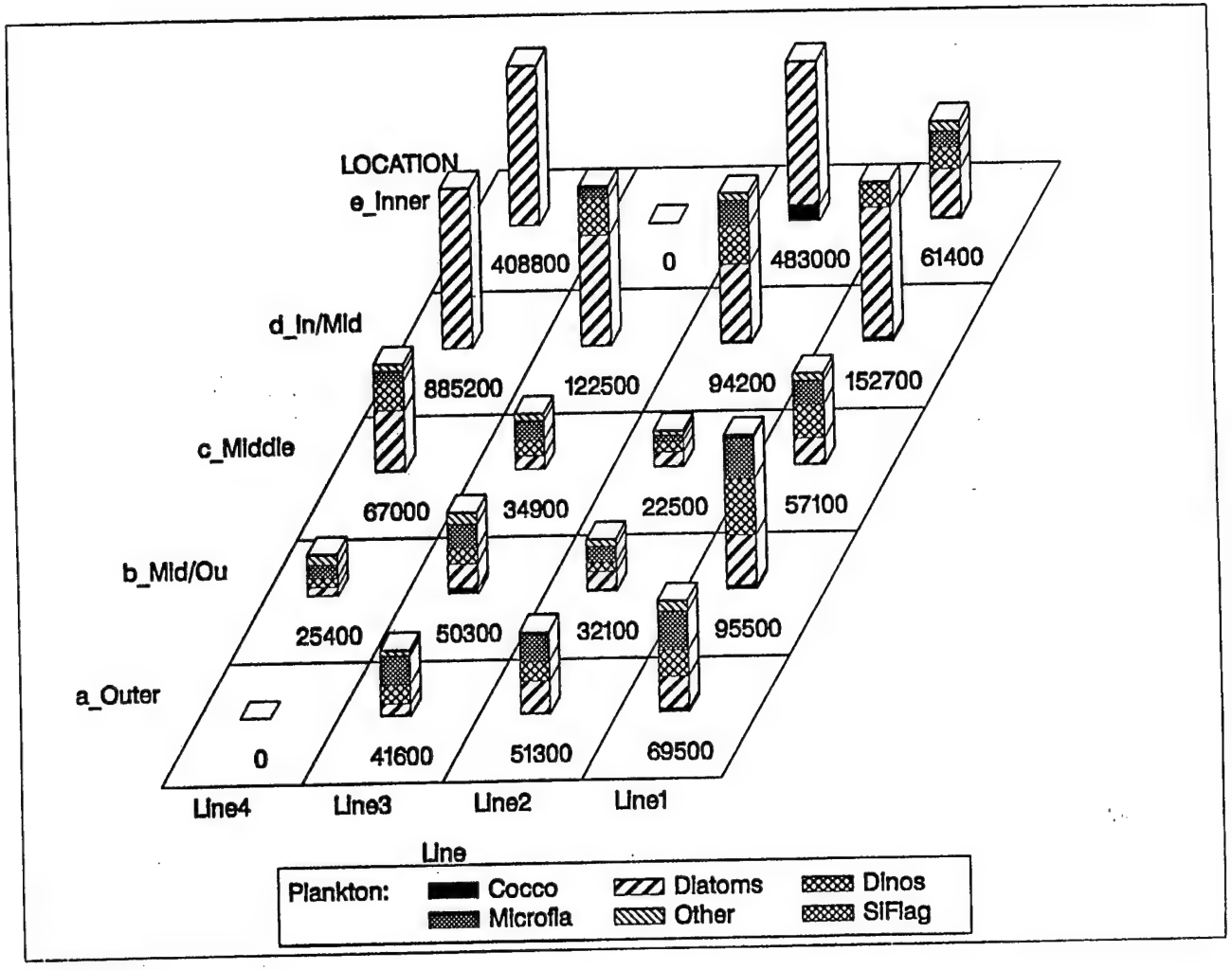

Figure 32. August 1992 (H02) Louisiana shelf surface phytoplankton distributions and abundances. Plot normalized for outer shelf to 100,000 cells L^{-1}.

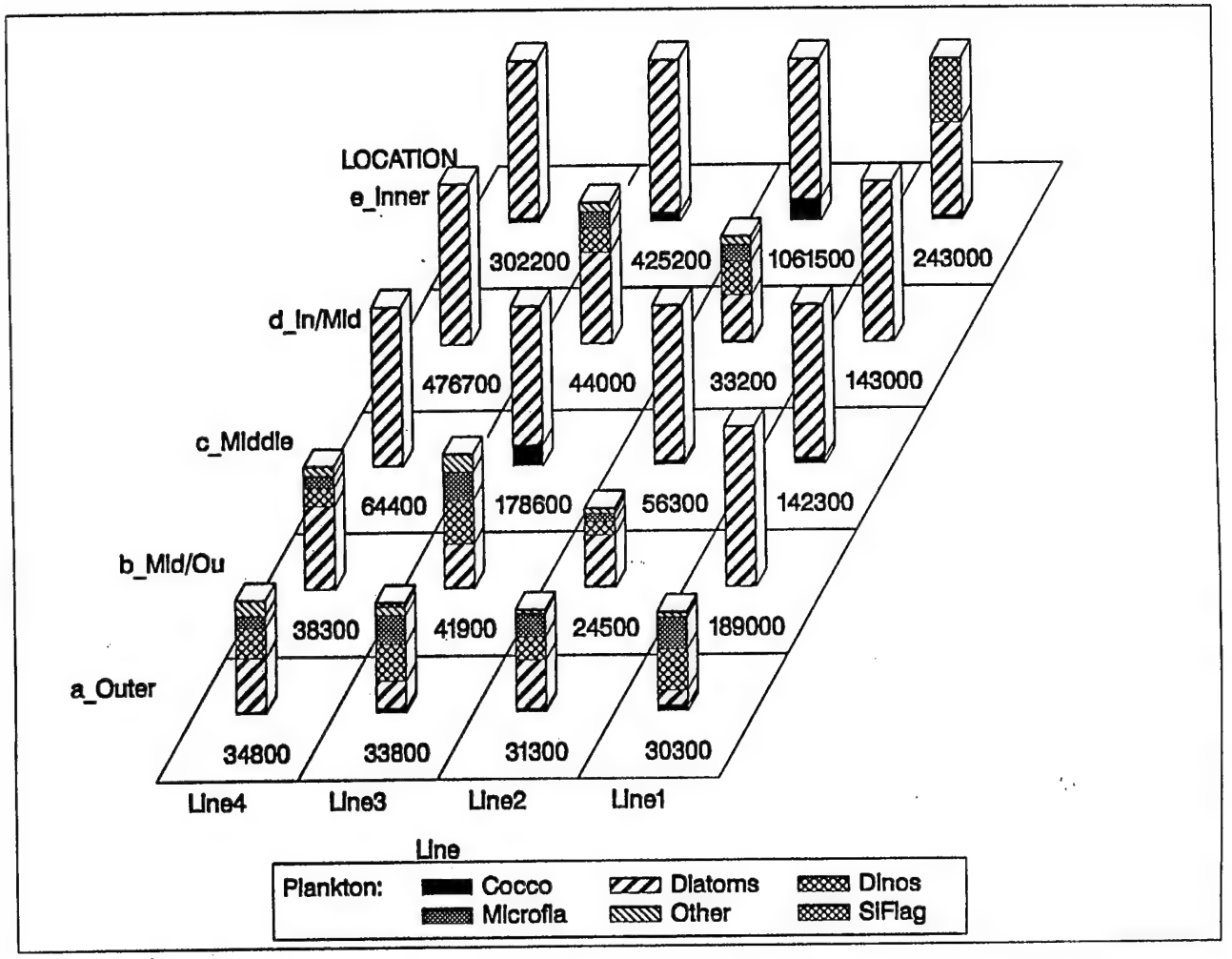

Figure 33. August 1992 (H02) Louisiana shelf chlorophyll maximum phytoplankton distributions and abundances. Plot normalized for outer shelf to 50,000 cells L^{-1}.

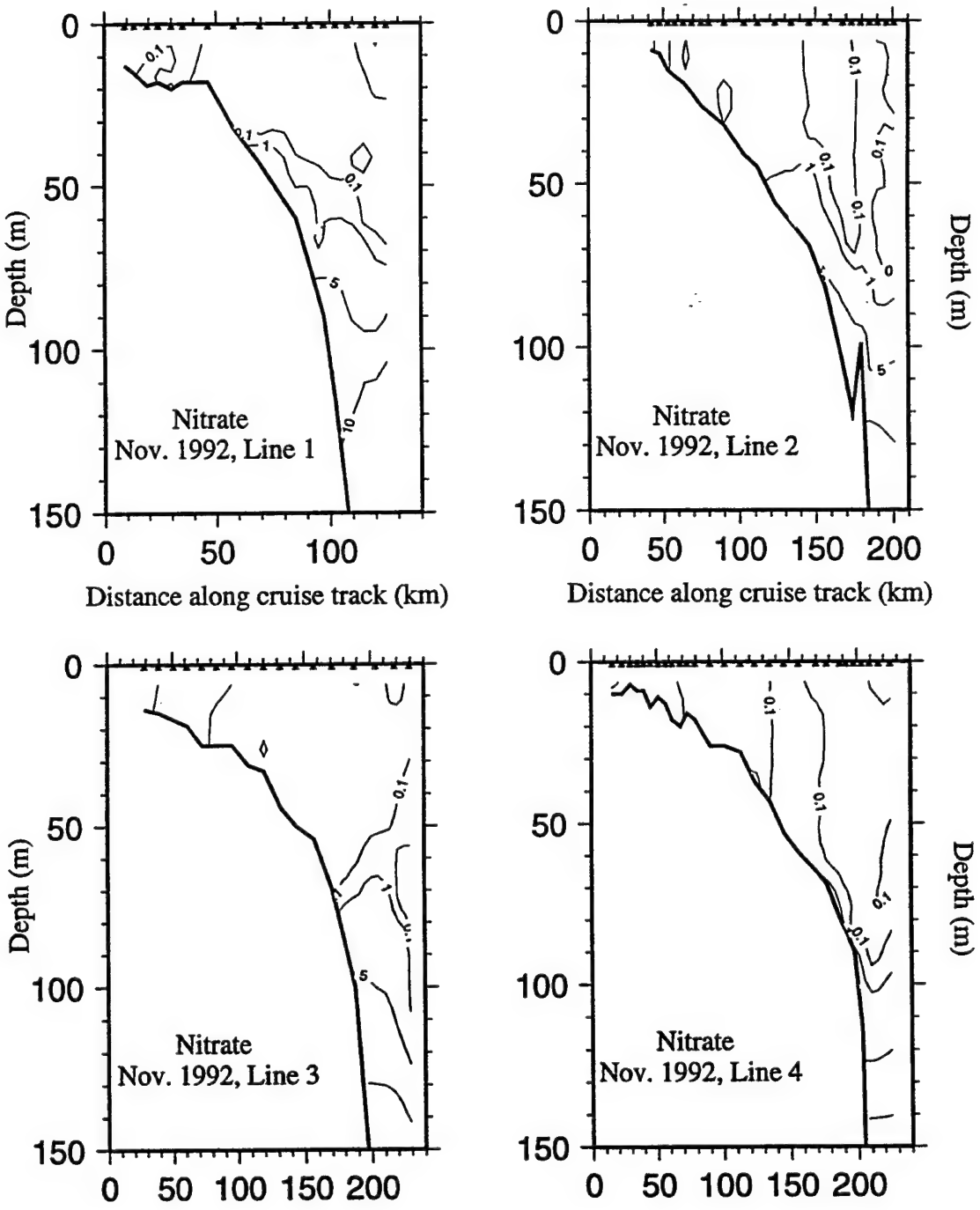

Figure 34. Vertical sections of nitrate concentration (μmol L^{-1}) for Lines 1-4 during November 1992 (H03).

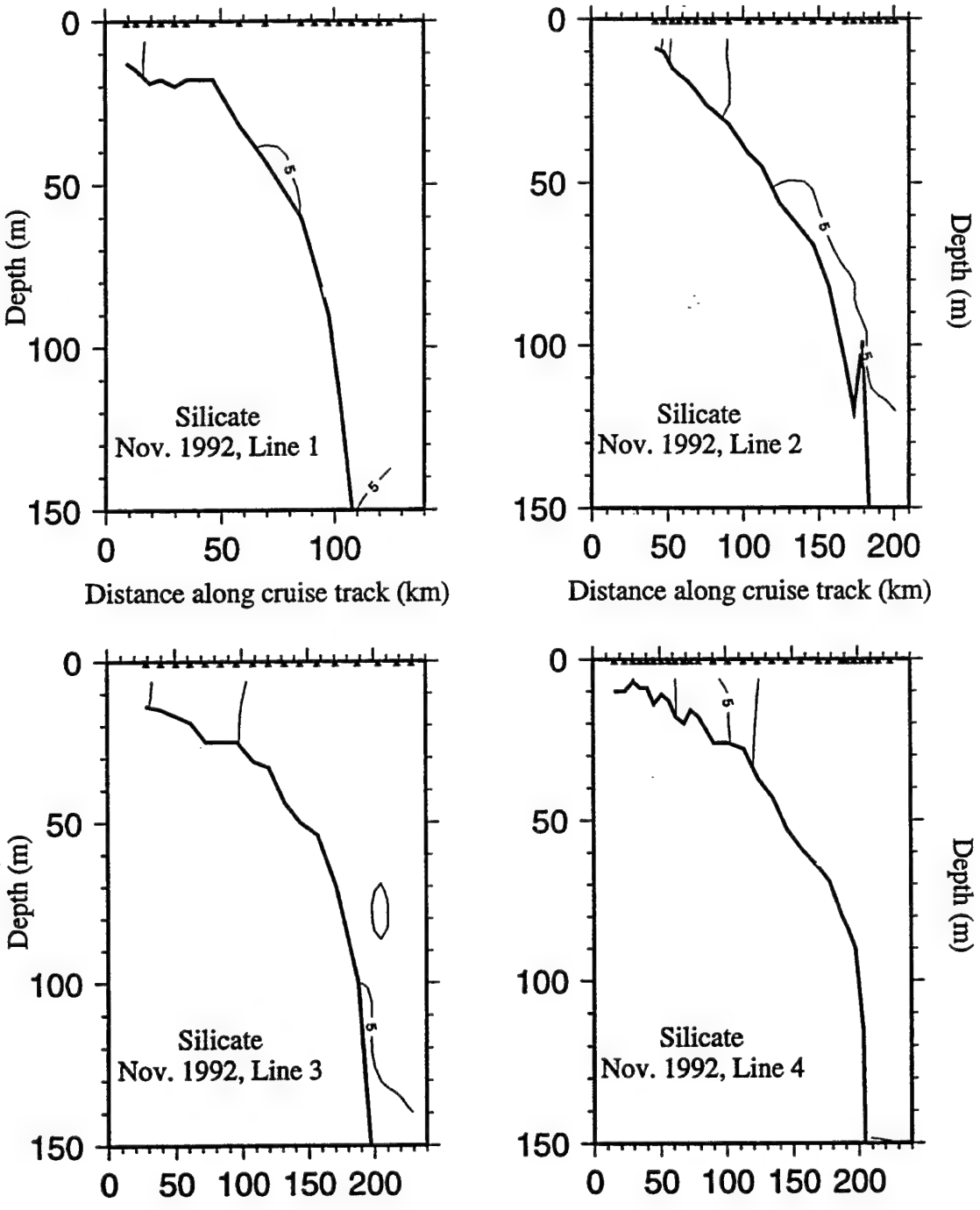

Figure 35. Vertical sections of silicate concentration (μmol L^{-1}) for Lines 1-4 during November 1992 (H03).

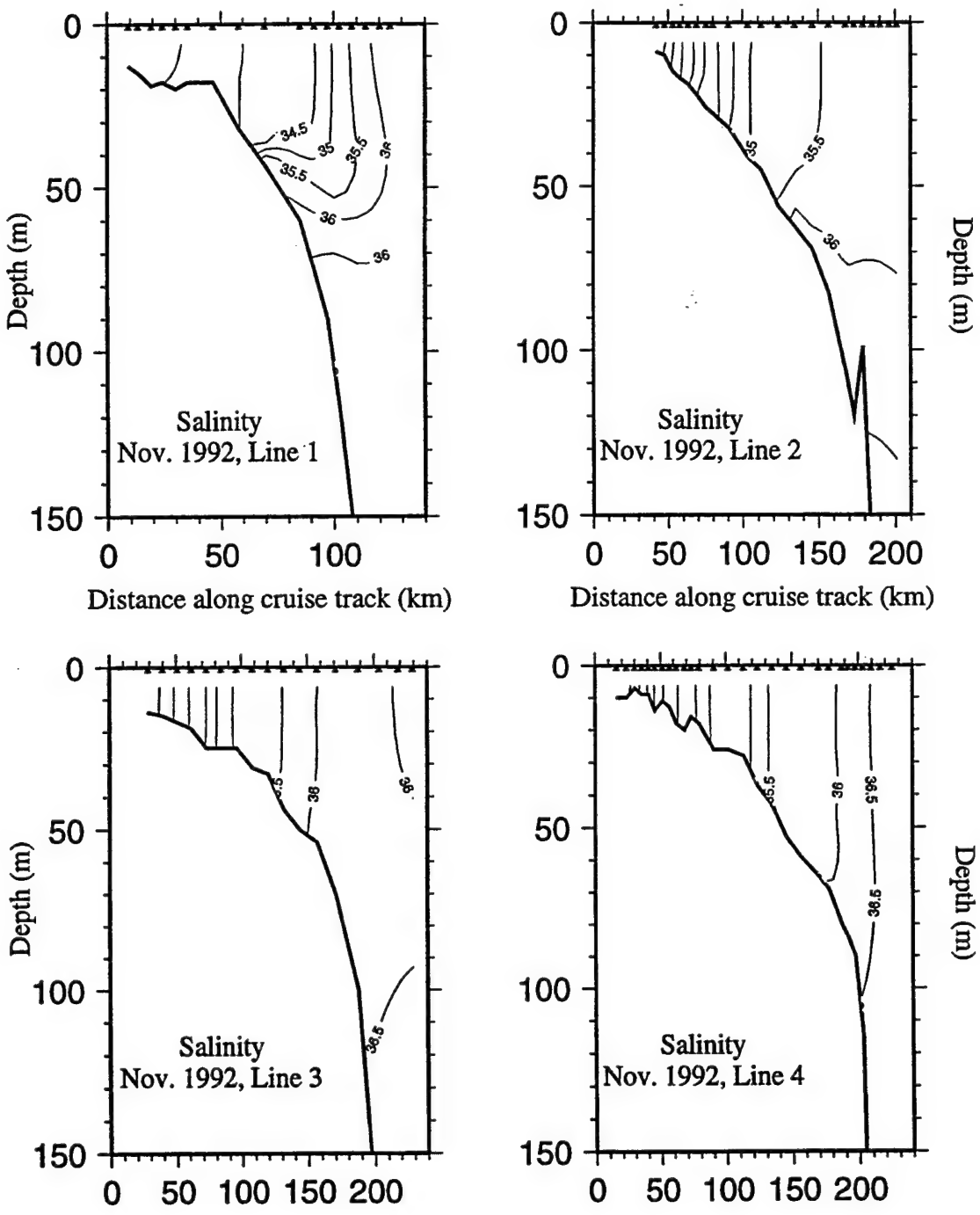

Figure 36. Vertical sections of salinity
for Lines 1-4 during November 1992 (H03).

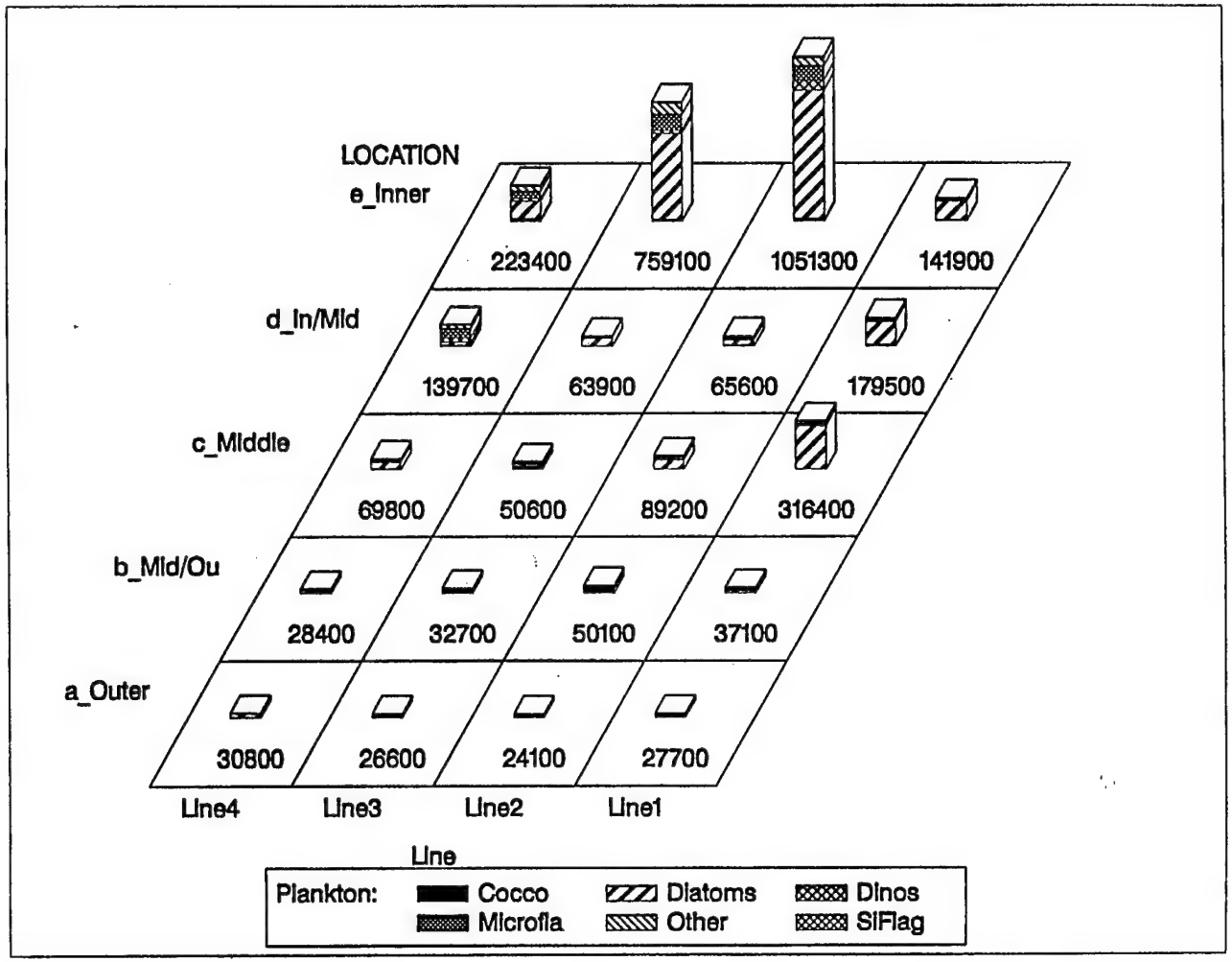

Figure 37. November 1992 (H03) Louisiana shelf surface phytoplankton distributions and abundances.

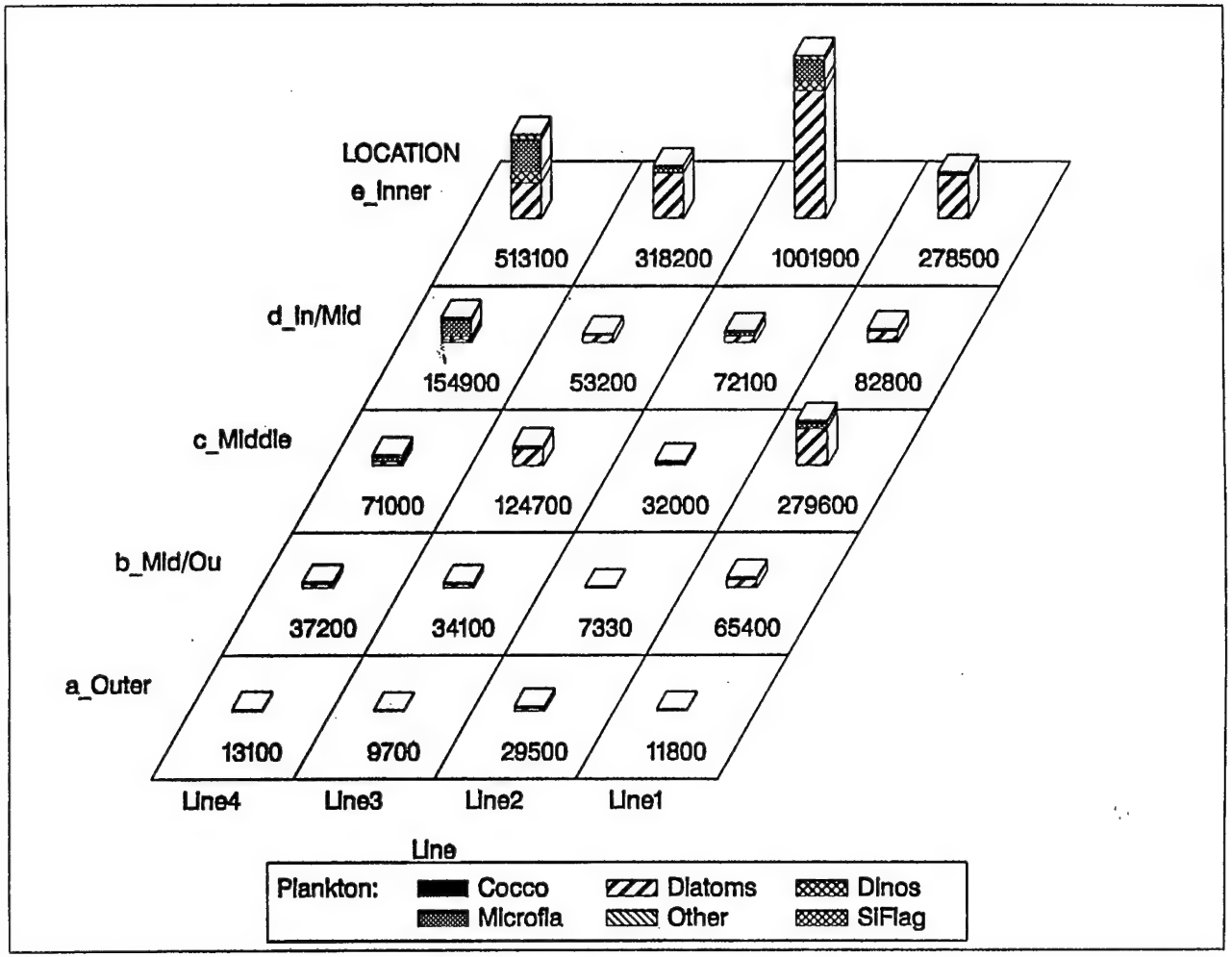

Figure 38. November 1992 (H03) Louisiana shelf chlorophyll maximum phytoplankton distributions and abundances.

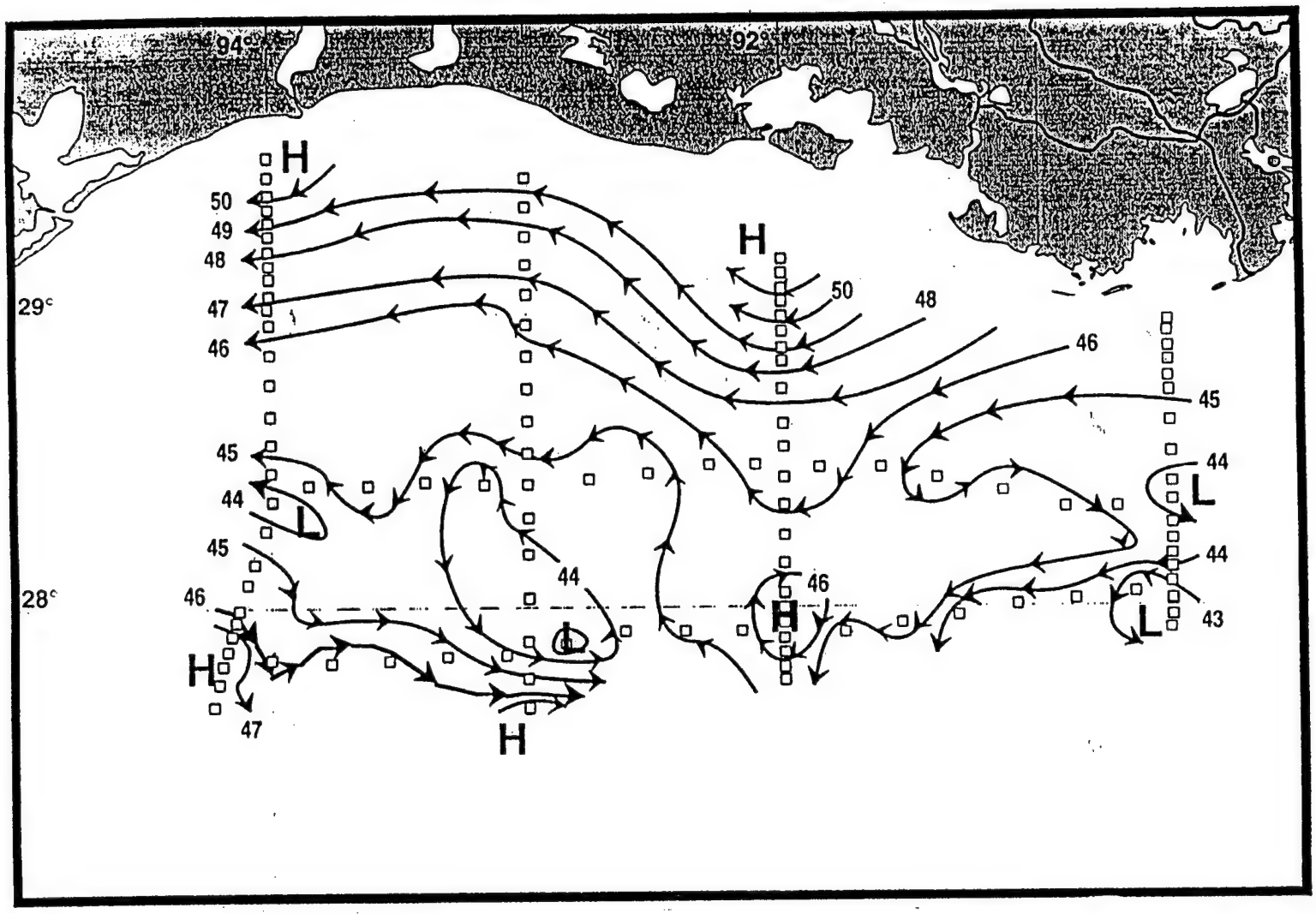

Figure 39. November (H03) geopotential anomaly for the Louisiana shelf for 3 over 160 decibars in dynamic centimeters (after Jochens and Nowlin 1994).

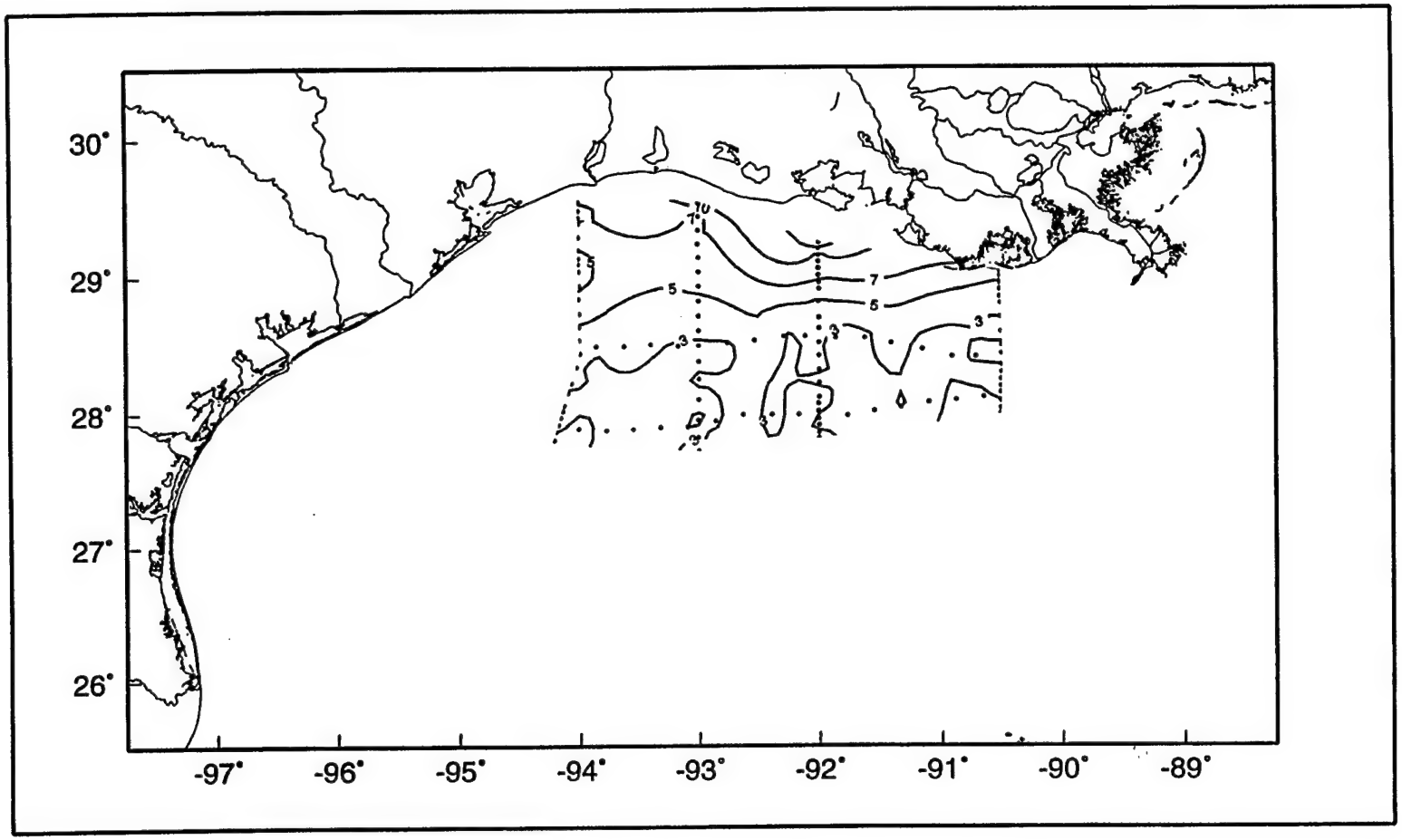

Figure 40. Surface silicate concentrations (μmol L^{-1}) on the Louisiana shelf during November 1992 (H03).

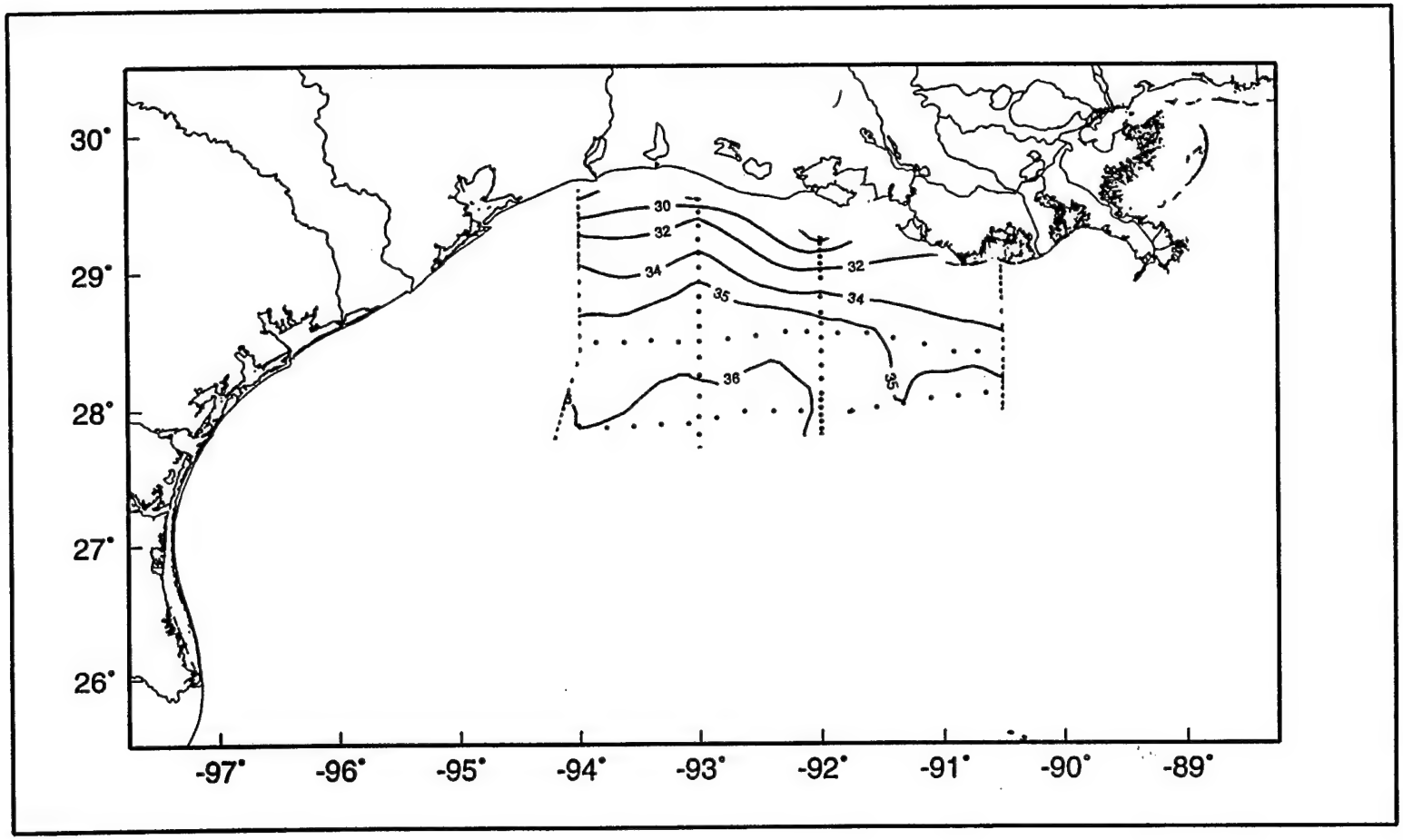

Figure 41. Surface salinity on the Louisiana shelf during November 1992 (H03).

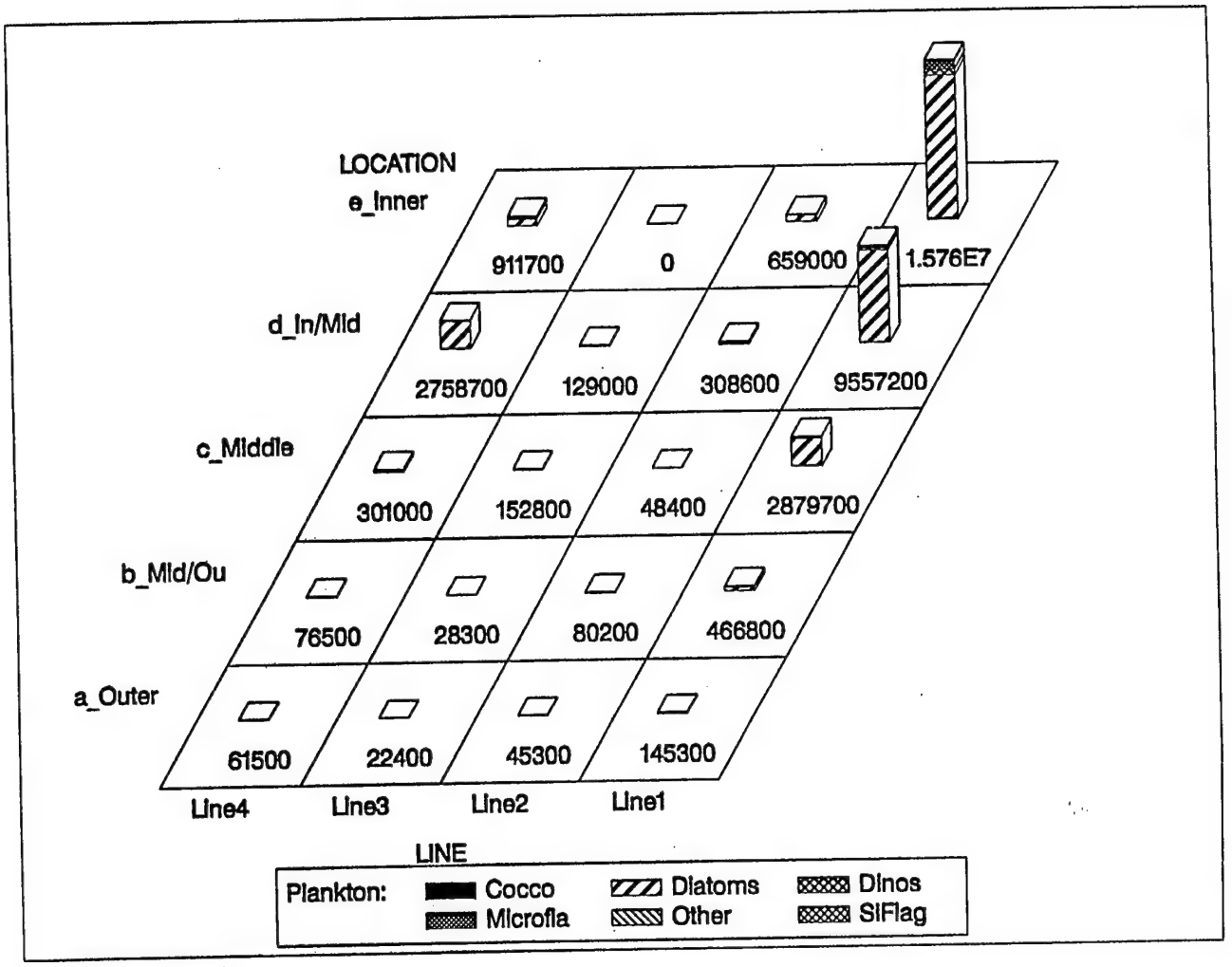

Figure 42. May 1993 (H05) Louisiana shelf surface phytoplankton distributions and abundances.

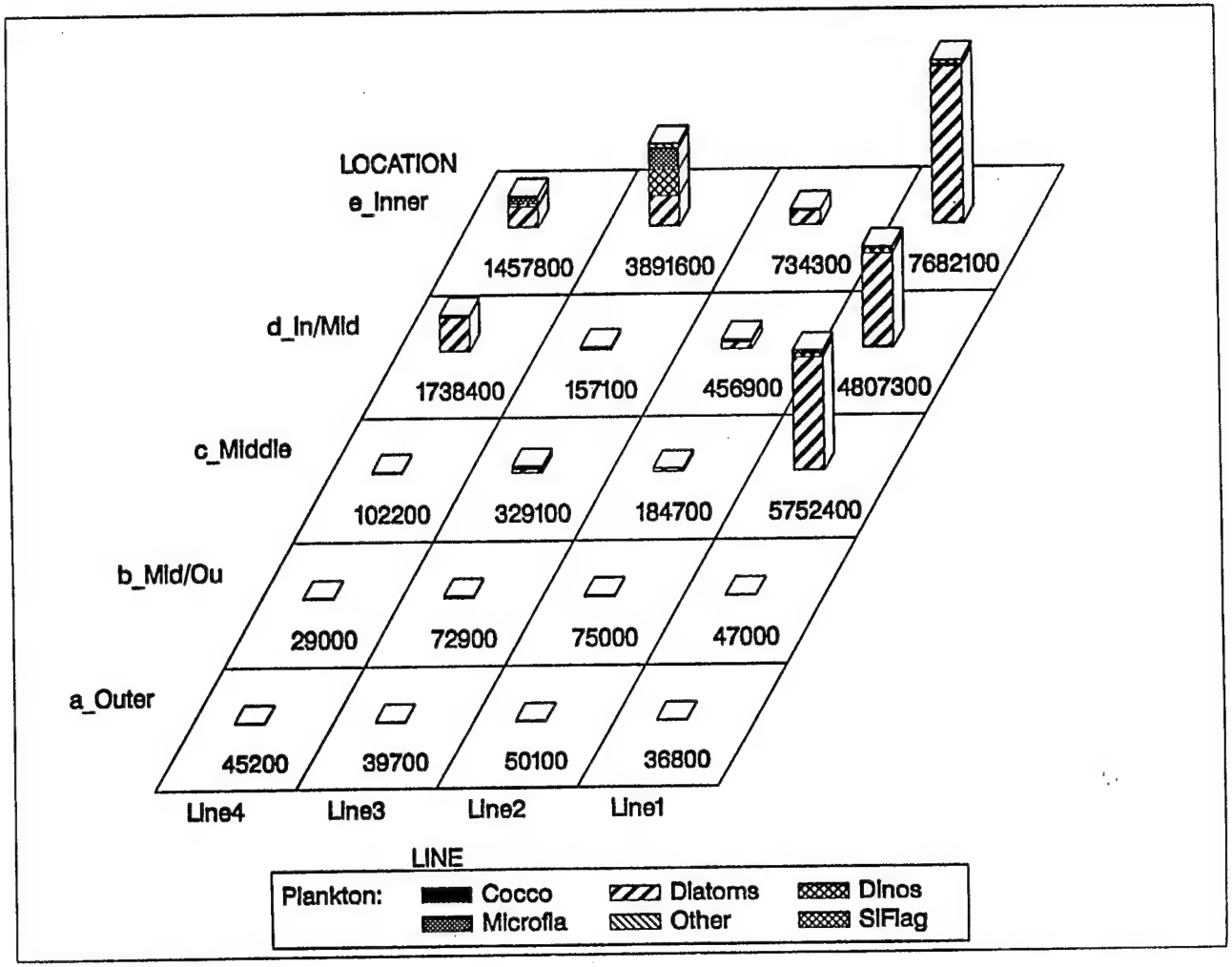

Figure 43. May 1993 (H05) Louisiana shelf chlorophyll maximum phytoplankton distributions and abundances.

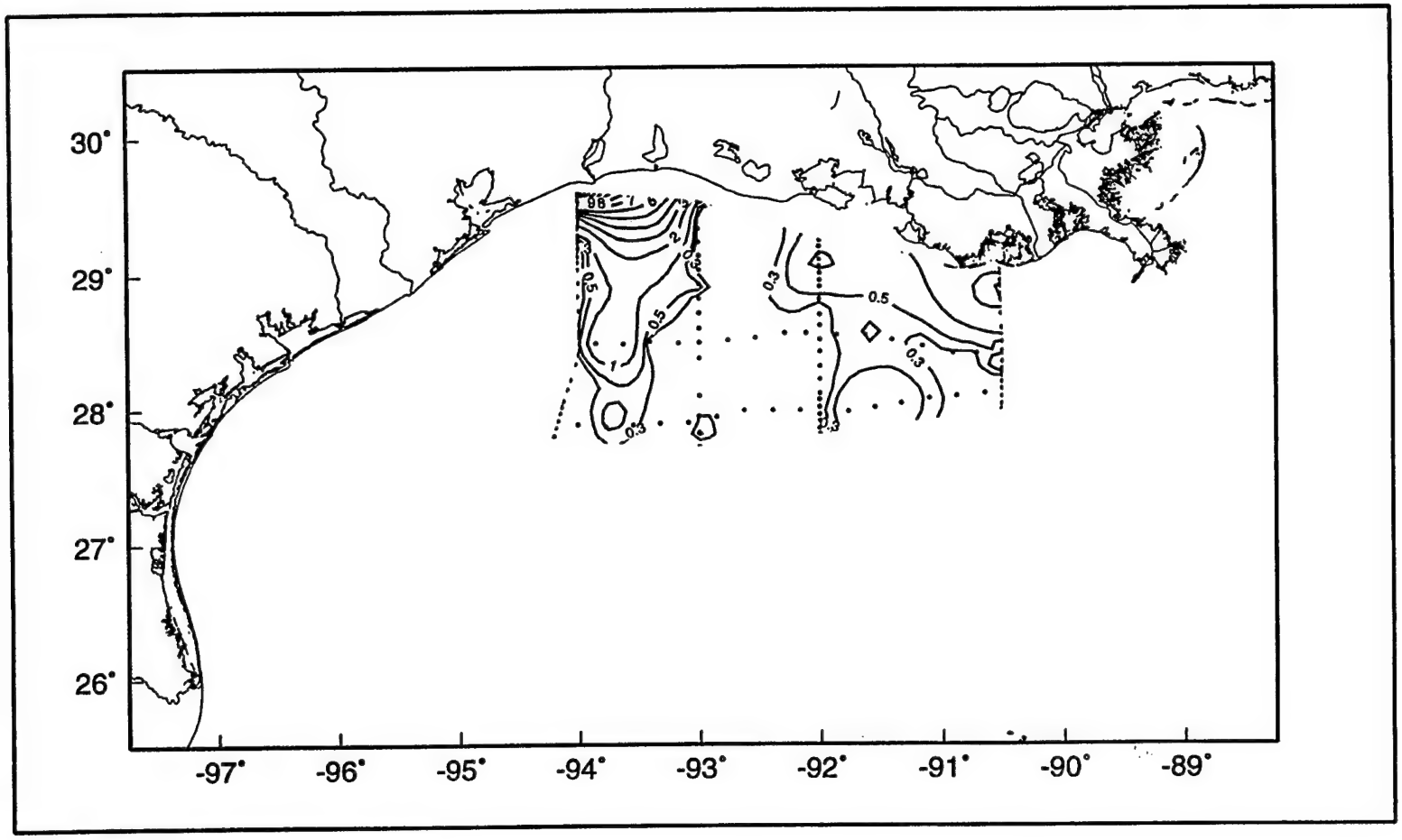

Figure 44. Surface nitrate concentrations (μmol L^{-1}) on the Louisiana shelf during May 1993 (H05).

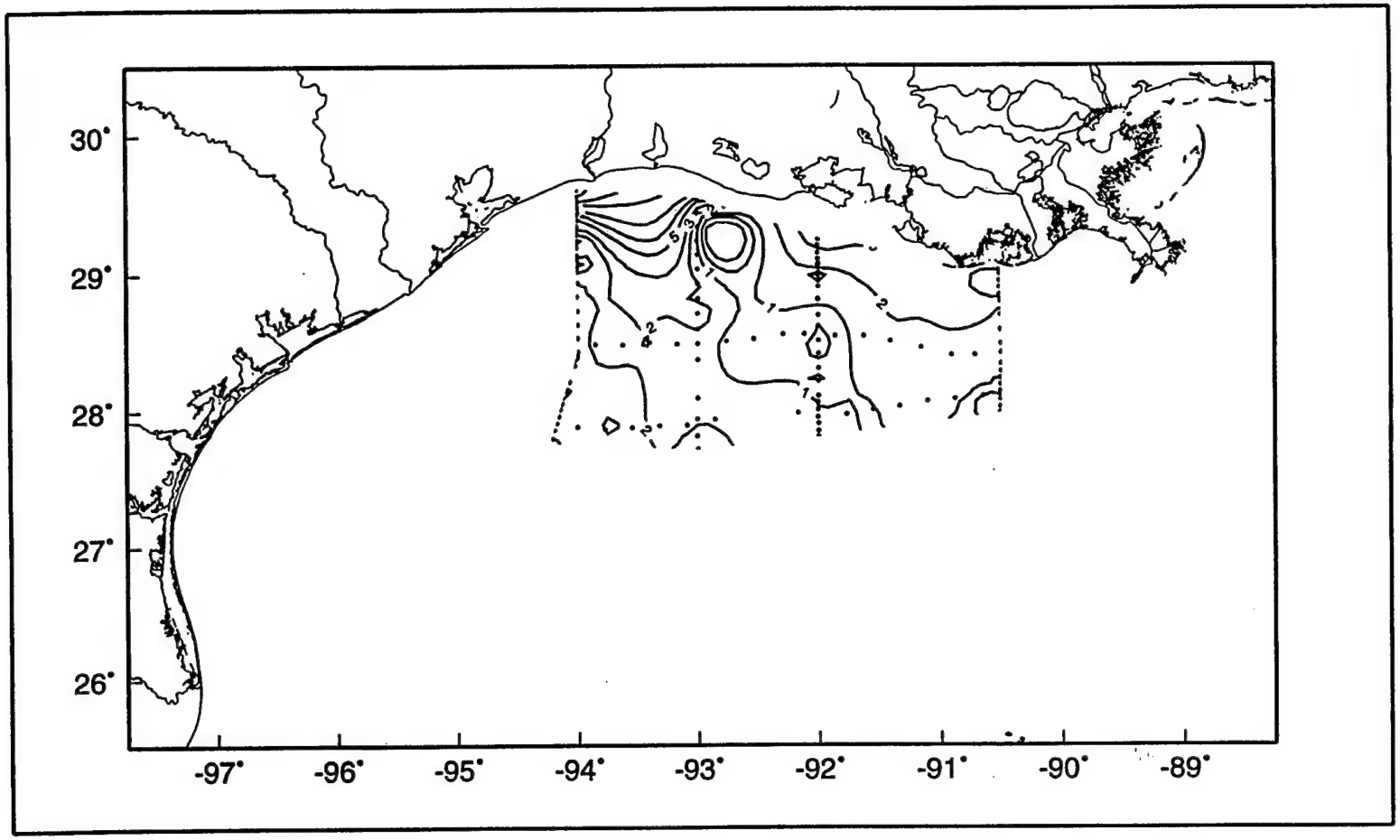

Figure 45. Surface silicate concentrations (µmol L^{-1}) on the Louisiana shelf during May 1993 (H05).

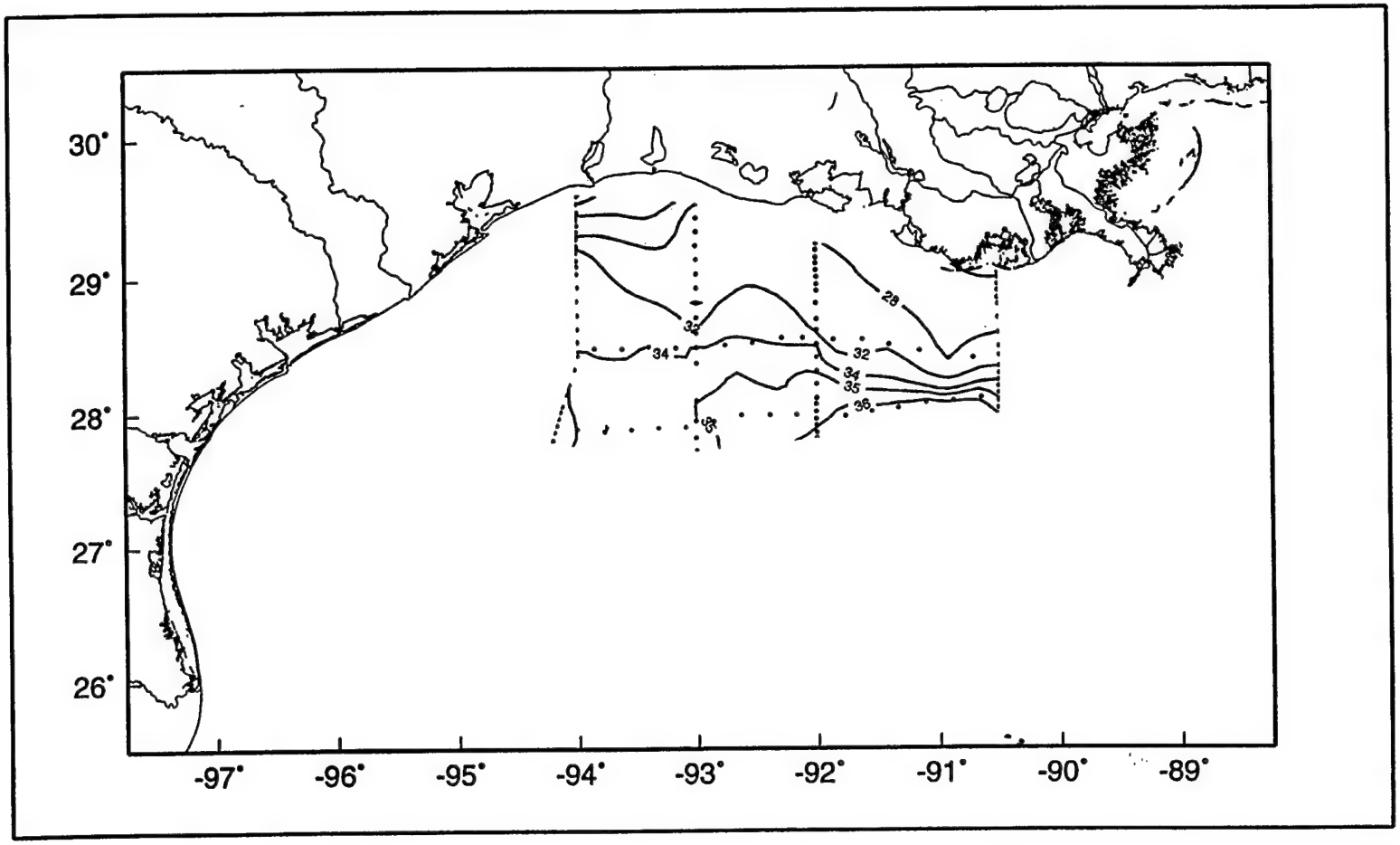

Figure 46. Surface salinity on the Louisiana shelf during May 1993 (H05).

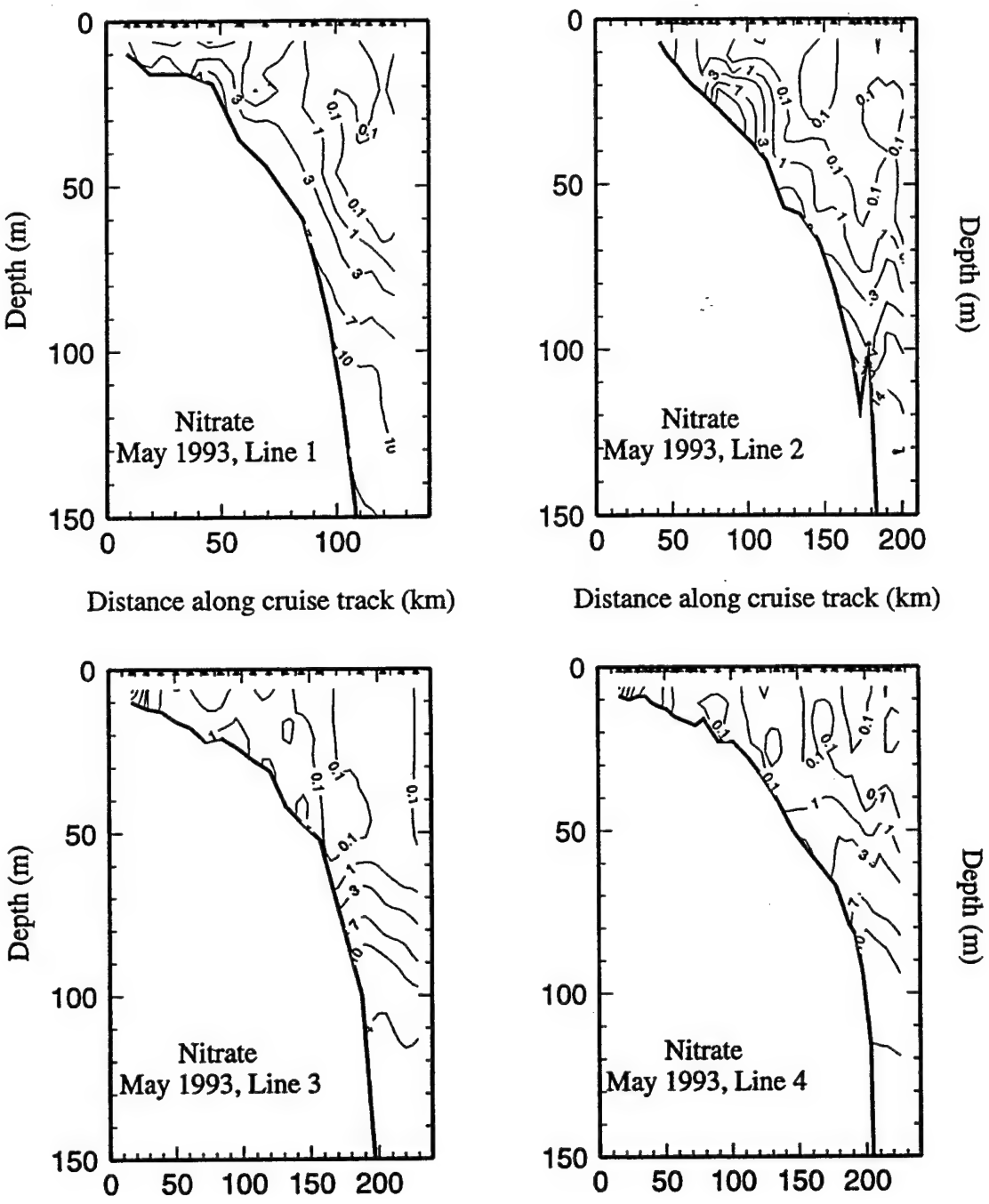

Figure 47. Vertical sections of nitrate concentration (μmol L^{-1}) for Lines 1-4 during May 1993 (H05).

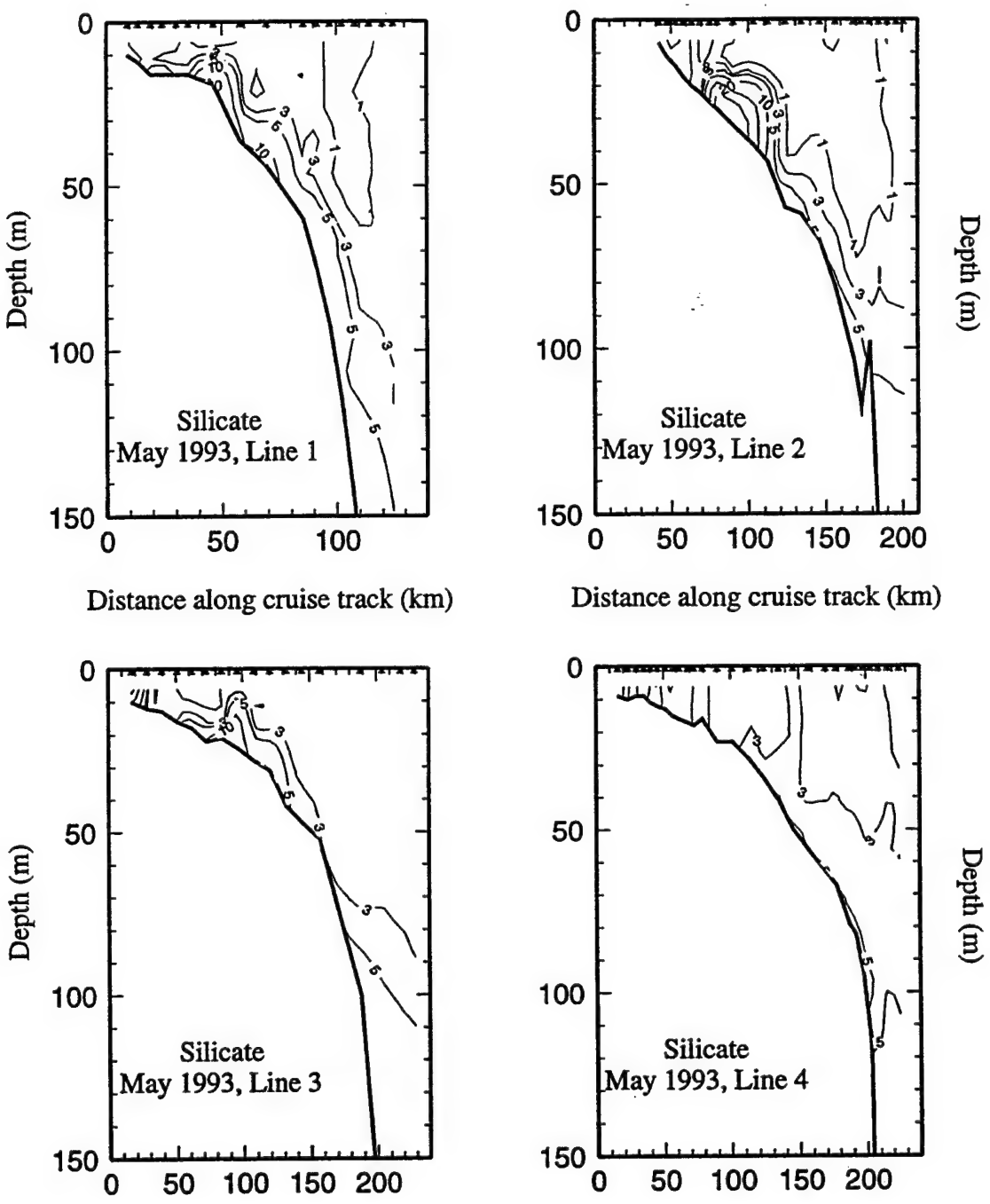

Figure 48. Vertical sections of silicate concentration (µmol L^{-1}) for Lines 1-4 during May 1993 (H05).

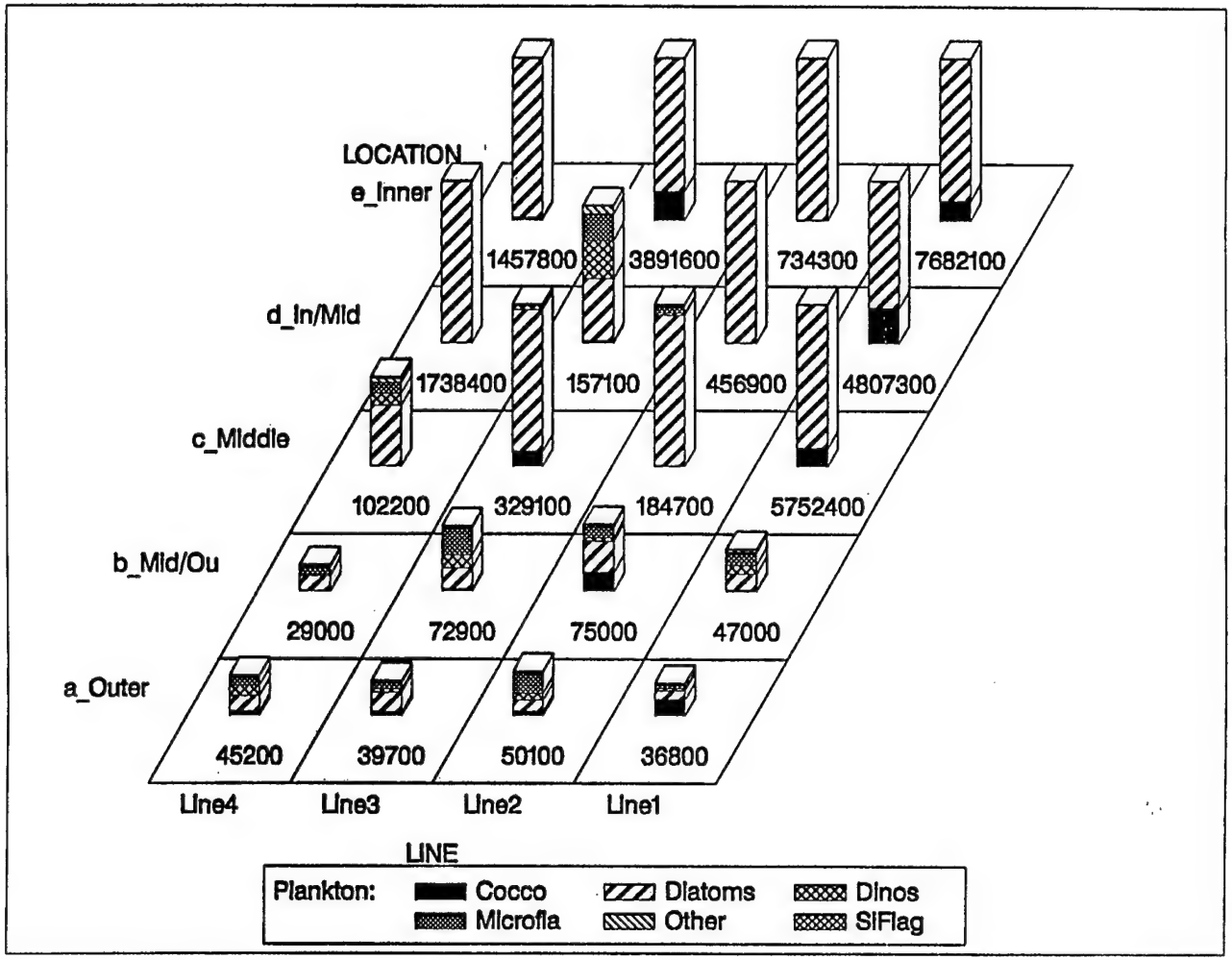

Figure 49. May 1993 (H05) Louisiana shelf surface phytoplankton distributions and abundances. Plot normalized for outer shelf to 184,700 cells L^{-1} on Line 2.

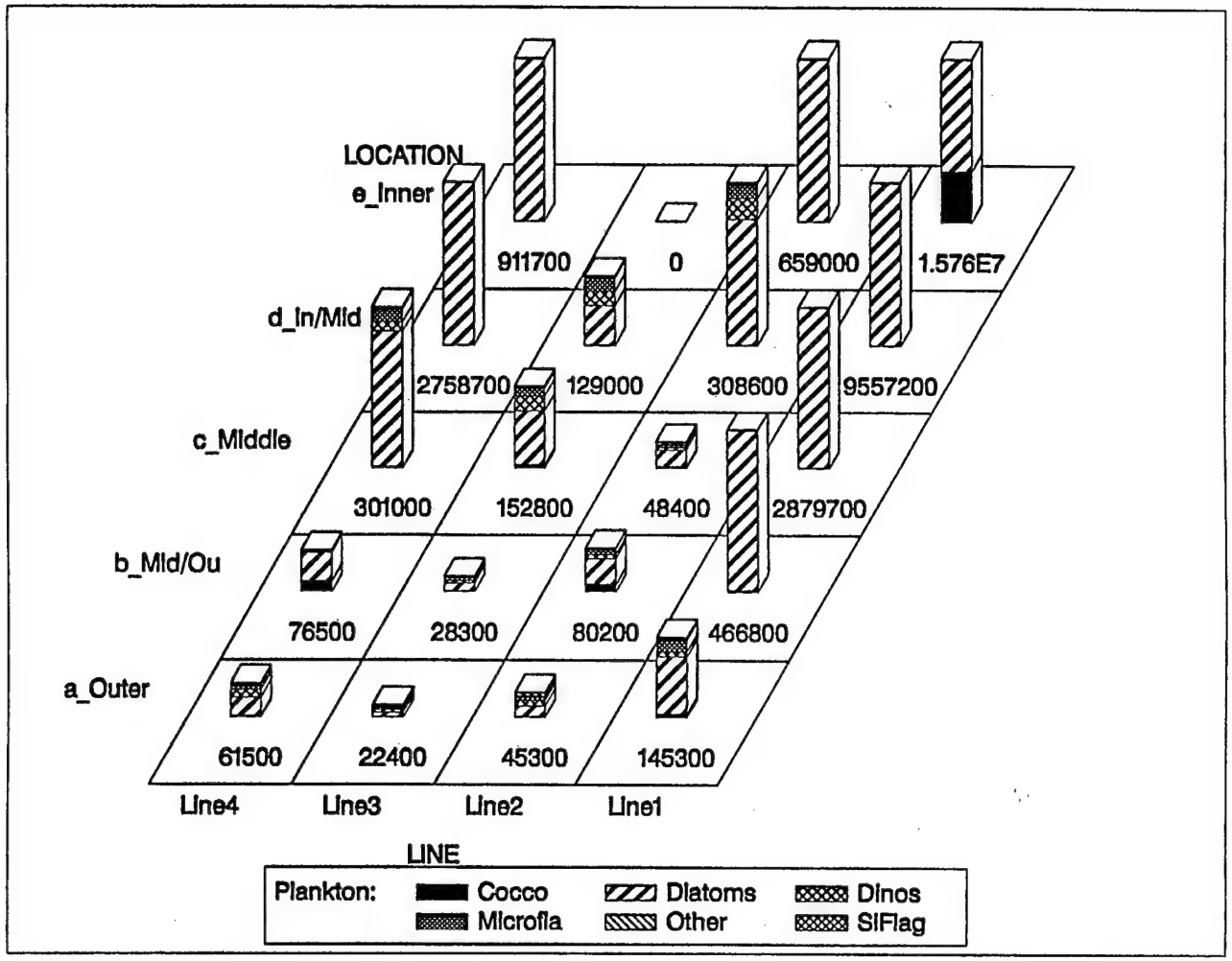

Figure 50. May 1993 (H05) Louisiana shelf chlorophyll maximum phytoplankton distributions and abundances. Plot normalized for outer shelf to 300,000 cells L^{-1}.

APPENDIX A

Phytoplankton Diversity in Relation to Coastal Physical Processes

by

Paula S. Bontempi
and
Denis A. Wiesenburg

Institute of Marine Sciences
University of Southern Mississippi
Stennis Space Center, MS 39529

Final Report

Prepared for

Department of the Navy
Office of Naval Research
800 North Quincy Street
Arlington, Virginia 22217-5000

Contract No. N00014-93-1-0513

Report No. IMS-97-01

February 1997

Modeling the Phytoplankton Distributions on the Texas-Louisiana Shelf

by

Changsheng Chen
Department of Marine Sciences
University of Georgia

Subcontract No. RR50905F

Model Part of Final Report

1. Introduction (Note: Objectives/Model in section of introduction)

The Louisiana-Texas (LATEX) shelf is well-known for its high biological productivity associated with the unique physical environment (Riley 1937; Sklar and Turner 1981). Primary production on the LATEX shelf has been observed to be closely tied to the seasonal discharge of the nutrient-rich fresh water from the Mississippi and Atchafalaya River (MAR) system at the coast, upwelling associated with the Loop Current eddies at the shelf break, and local wind and tidal mixings (Lohrenz *et al.* 1990; Bierman *et al.* 1994; Sahl *et al.* 1993; Neuhard 1994). An interdisciplinary field program conducted during May 1993 over the LATEX shelf has shown a high level of primary production in the inner shelf, which was strongly linked to the unusual large freshwater discharge from the MAR system (Figs. 1 and 2). The averaged freshwater flux was about 32,867 m^3/s at the Mississippi River and 14,721 m^3/s at the Atchafalaya River, which was about 10,000 m^3/s (Mississippi River) and 6,000 m^3/s (Atchafalaya River) larger than the maximum discharges averaged over the sixty two-year records from 1930 to 1992 (Wiesenburg *et al.* 1994; Dinnel and Wiseman 1986).

Hydrographic data, taken from the May 1993 interdisciplinary survey over the LATEX shelf, has shown a relatively strong low-salinity (or density), surface-bottom frontal zone near 20 to 40-*m* isobaths along the shelf (Figs.1 and 2). In addition to a high biomass concentration of nitrate and chlorophyll *a* near the coast, nitrate concentrations showed a distinct maximum value at the bottom within the low-salinity front that was located at 20 to 30-*m* isobaths on Sec.1 and at 20 to 40-*m* isobaths on Sec. 2 (Fig. 2). Such a bottom-rich nitrate pattern extended offshore to a region of deeper than 60 *m* on Sec.1, the section between the Mississippi and Atchafalaya Rivers. However, the maximum dome of nitrate, observed on Sec. 2 west of the Atchafalaya River, seemed to isolate from the outer shelf source.

High nitrate concentrations observed near the bottom on the middle shelf may result from the interaction of biological and physical processes associated with dynamics of the low-salinity front. In view of biological processes, the benthic regeneration may become important in the middle shelf where no significant input of nutrients from river water exists (Flint and Kamykowski 1984; Rowe *et al.* 1975). The possible presence of bottom nepheloid layers on the middle shelf, as a consequence of suspension of sediment due to tidal and wind mixing, would supply nutrients from benthic regeneration and zooplankton excretion near the bottom (Shideler 1975; Kamykowski and Bird 1981; Neuhard 1994). Since the maximum dome of nitrate was observed near the bottom within the low-salinity front, physical processes associated with the front formation and cross-front secondary circulation may become critically important in the generation of the bottom-rich nitrate pattern on the middle shelf. However, the detailed relationship of such a biological pattern with dynamics of the low-salinity front on the LATEX shelf has not been well explored yet.

Objective of this research was to study numerically the ecosystem over the inner Louisiana-Texas (LATEX) shelf, with a focus on interactions of biological and physical processes associated with river discharges and wind forcing. Special emphasis was placed on the model simulation of biological productions observed during the spring 1993 LATEX interdisciplinary survey.

We have applied a fully coupled physical and biological model to the LATEX shelf. This coupled model was developed by Franks and Chen (1996). To better understand the basic dynamic processes that control the cross-shelf distribution of biological production, as a first step, we have simplified our modeling experiments to a two dimensional (so-called 2-D) problem involving a cross-shelf slice of the LATEX shelf in which the along-shelf variation for all independent variables was ignored. Although the contribution of along-isobath advection from the Mississippi River was ignored in such a simple model, the model results have shown in a reasonable agreement with observed biological data and also provided us new level of understanding the

fundamental physical and biological mechanisms responsible for the cross-shelf distribution of nutrients, phytoplankton, zooplankton over the inner LATEX shelf where river discharge was a dominant physical forcing.

2. Coupled Physical and Biological Model (Note: Modeling efforts in section of methods)

2. 1. Physical Model

The physical model used in this study is a modified version of the three-dimensional (so-called 3-D) coastal ocean circulation model developed originally by Blumberg and Mellor (1987). This model incorporates the Mellor and Yamada (1974 and 1982) level 2.5 turbulent closure scheme to provide a realistic paramterization of vertical mixing that has been found critically important for coastal mixing and cross-shelf circulations (Wright and Loder 1985; Chen and Beardsley 1995; Chen *et al.* 1995). A free surface is coupled with this model, which allows simulation of surface wave propagation such as tides and long gravity waves. Time variable river/dam and onshore intake/outflow discharges also are included in the model for the study of buoyancy-driven circulations caused by river discharges.

A σ-coordinate transformation is used in the vertical and a curvilinear coordinate system in the horizontal, which allow a smooth representation of irregularly variable bottom topography and real coastal geometry. To improve the computational efficiency, the model incorporates a semi-implicit scheme for time-stepping of the barotropic mode (Casulli 1990). A modification of the stability functions made by Galperin *et al.* (1988) was recently included in the Blumberg and Mellor model. An updated version of this model was described in detail in Blumberg (1994) and Chen and Beardsley (1995). A brief description of the 2-D version of this model is given here to provide a systematic understanding of how biological and physical models were coupled.

The model consists of momentum, continuity, temperature, salinity, and density equations:

$$\frac{\partial u}{\partial t}+u\frac{\partial u}{\partial x}+w\frac{\partial u}{\partial z}-fv=-\frac{1}{\rho_o}\frac{\partial p}{\partial x}+\frac{\partial}{\partial z}(K_m\frac{\partial u}{\partial z})+F_u \qquad 2.1$$

$$\frac{\partial v}{\partial t}+u\frac{\partial v}{\partial x}+w\frac{\partial v}{\partial z}+fu=\frac{\partial}{\partial z}(K_m\frac{\partial v}{\partial z})+F_v \qquad 2.2$$

$$\frac{\partial p}{\partial z}=-\rho g' \qquad 2.3$$

$$\frac{\partial u}{\partial x}+\frac{\partial w}{\partial z}=0 \qquad 2.4$$

$$\frac{\partial \theta}{\partial t}+u\frac{\partial \theta}{\partial x}+w\frac{\partial \theta}{\partial z}=\frac{\partial}{\partial z}(K_h\frac{\partial \theta}{\partial z})+F_\theta \qquad 2.5$$

$$\frac{\partial s}{\partial t}+u\frac{\partial s}{\partial x}+w\frac{\partial s}{\partial z}=\frac{\partial}{\partial z}(K_h\frac{\partial s}{\partial z})+F_s \qquad 2.6$$

$$\rho_{total}=\rho_{total}(\theta,s) \qquad 2.7$$

where u, v, and w are the x, y, z velocity components, θ the potential temperature, s the salinity, p the pressure, f the Coriolis parameter, g' the gravitational acceleration, K_m the vertical eddy viscosity coefficient, and K_h the thermal vertical eddy friction coefficient. F_u, F_v, and F_θ represent the horizontal momentum and thermal diffusion terms. ρ and ρ_o are the perturbation and reference density, which satisfy

$$\rho_{total} = \rho + \rho_o \qquad . \qquad 2.8$$

The cross-shelf streamfunction is defined as

$$\psi = -\int_{-H(x)}^{z} u dz \qquad 2.9$$

where $H(x)$ is the water depth. The vertical eddy viscosity and diffusion coefficient were calculated using the second-order turbulent closure scheme (level 2.5) developed by Mellor and Yamada (1974 and 1982). Under the boundary layer approximation where the shear production of turbulent energy can be neglected except in the vertical, the eddy viscosity can be calculated through the closure turbulent kinetic energy and turbulent macroscale equations. A detailed description of the turbulent closure scheme, which was used in our 2-D model, can be seen in Chen and Beardsley (1995).

2.2. Biological Model

The biological model is a simple nutrient (N), phytoplankton (P) and zooplankton (Z) model (Franks *et al.* 1986) in which dissolved nutrients are taken up by the

phytoplankton following Michaelis-Menten kinetics and phytoplankton are grazed by zooplankton with an Ivlev functional response:

$$\frac{\partial P}{\partial t}+u\frac{\partial P}{\partial x}+w\frac{\partial P}{\partial z}=\frac{V_m N}{k_s+N}f(I_o)P-ZR_m(1-e^{-\lambda P})-\varepsilon P+\frac{\partial}{\partial z}(K_p\frac{\partial P}{\partial z}) \qquad 2.10$$

$$\frac{\partial Z}{\partial t}+u\frac{\partial Z}{\partial x}+w\frac{\partial Z}{\partial z}=(1-\gamma)ZR_m(1-e^{-\lambda P})-gZ+\frac{\partial}{\partial z}(K_z\frac{\partial Z}{\partial z}) \qquad 2.11$$

$$\frac{\partial N}{\partial t}+u\frac{\partial N}{\partial x}+w\frac{\partial N}{\partial z}=-\frac{V_m N}{k_s+N}f(I_o)P+\gamma ZR_m(1-e^{-\lambda P})+\varepsilon P+gZ+\frac{\partial}{\partial z}(K_p\frac{\partial N}{\partial z}) \qquad 2.12$$

where

$$N+P+Z=N_T\ , \qquad 2.13$$

and N_T is the total amount of nutrients (μ *mole* $N\ l^{-1}$), V_m the maximum phytoplankton growth rate; k_s the half-saturation constant of phytoplankton, R_m the maximum grazing rate of phytoplankton by zooplankton, λ the grazing efficiency of phytoplankton by zooplankton, γ the fraction of ingested phytoplankton unassimilated by zooplankton, ε the phytoplankton death rate, g the zooplankton death rate. The phytoplankton depends on incident irradiance I_o though the function $f(I_o)$ that we have taken to be linear:

$$f(I_o)=I_o e^{-k_{ext}z}, \qquad 2.14$$

where k_{ext} is the diffuse attenuation coefficient for irradiance. The detailed description for coupling of physical and biological models can be seen in Franks and Chen (1996).

2.3. Boundary Conditions

In the absence of surface and bottom heat fluxes, the surface and bottom boundary conditions are

$$\left.\begin{aligned}&\frac{\partial\theta}{\partial z}=\frac{\partial s}{\partial z}=\frac{\partial P}{\partial z}=\frac{\partial Z}{\partial z}=\frac{\partial N}{\partial z}=0,\quad w=\frac{\partial\eta}{\partial t}+u\frac{\partial\eta}{\partial x}\\&K_m(\frac{\partial u}{\partial z},\frac{\partial v}{\partial z})=(\tau_{sx},\tau_{sy})/\rho\end{aligned}\right\}\quad at\quad z=\eta(t,x) \qquad 2.15$$

and

$$\left.\begin{aligned}&\frac{\partial\theta}{\partial z}=\frac{\partial s}{\partial z}=\frac{\partial P}{\partial z}=\frac{\partial Z}{\partial z}=\frac{\partial N}{\partial z}=0,\quad w=-u\frac{\partial H}{\partial x}\\&K_m(\frac{\partial u}{\partial z},\frac{\partial v}{\partial z})=(\tau_{bx},\tau_{by})/\rho\end{aligned}\right\}\quad at\quad z=-H(x) \qquad 2.16$$

where $(\tau_{sx}, \tau_{sy}) = C_d \sqrt{u_s^2 + v_s^2}\,(u_s, v_s)$ and $(\tau_{bx}, \tau_{by}) = C_d \sqrt{u_b^2 + v_b^2}\,(u_b, v_b)$ are the x and y components of surface and bottom stresses. u_s and v_s the x and y components of the surface wind velocity, while u_b and v_b the x and y components of the bottom friction velocity. The drag coefficient C_d is determined by matching a logarithmic bottom layer to the model at a height z_{ab} above the bottom, i.e,

$$C_d = \max\left(k^2 / \ln(\frac{z_{ab}}{z_o})^2 , \quad 0.0025 \right) \qquad 2.17$$

where z_o is the bottom roughness parameter, taken here as z_o=0.001 m.

The fresh water was injected into the model domain from the coastal boundary as a single point source. The volume transport was defined as the flux per unit length, *i.e.*:

$$U_o(t) = - \int_{-H(x)}^{\eta} u dz \qquad 2.18$$

The nutrient concentration of the fresh water N_f was specified at the mouth of the river.

A gravity wave radiation boundary condition plus a sponge layer was specified at the open boundary to allow waves to propagate out of the computational domain with minimum reflection (Chapman 1985). A barotropic K_1 tidal elevation of 0.14 m was added at the open boundary to investigate effects of tidal mixing on spatial distribution of biological production.

2.4. Initial Conditions

To simplify the model problem and focus on how the oceanic mixing affects the formation of the low-salinity front and associated biological production, we ignored the cross-shelf gradient of the background physical and biological variables. It is consistent with our assumption that any horizontal gradients of water masses and biological production should develop during simulation as a result of physical process or physical and biological coupling.

Initial distributions of temperature and salinity were simply given by a vertically linear function with a temperature of 25.5° C and a salinity of 36.2 at the surface and 7.5° C and 34.9 at the bottom of 500 m. The surface and bottom values of temperature and salinity used in the model were based on the observed hydrographic data taken at the 500-*m* isobath during the May 1993 interdisciplinary LATEX survey.

Initial distributions of biological state variables *P*, *Z*, and *N* were given by an analytical steady-state solution of the *P-Z-N* model (Franks *et al.* 1986; Franks and Chen 1996). Since any biological variables were independent of temperature in the *PZN* model and nor was k_{ext} allowed to vary across the shelf in our present modeling experiment, the initial *P*, *Z*, and *N* were horizontally uniform across the shelf (Fig. 4).

2.5. Biological Parameters

The choice of biological parameters is listed in Table 1. Because there were a wide range of values for some biological parameters, we first ran the model with an initial set of parameters and then conducted some sensitivity analyses over ranges of parameters. Descriptions and discussions of our initial choices for biological parameters are given here.

Table 1: Parameters for the biological model

Parameter	Description	Value
V_m	maximum phytoplankton growth rate	1.38 d^{-1}
k_s	half-saturation constant	1 μ *mole* $N\,l^{-1}$
R_m	maximum grazing rate	0.5 d^{-1}
g	zooplankton death rate	0.2 d^{-1}
λ	Ivlev constant for grazing	0.5 (μ *mole* $N\,l^{-1}$)$^{-1}$
ε	phytoplankton death rate	0.1 d^{-1}
γ	unassimilated fraction by zooplankton	0.3
k_{ext}	diffuse attenuation coefficient	0.1 m^{-1}
N_T	initial total amount of nutrient	10 μ *mole* $N\,l^{-1}$

Based on profiles of observed nitrate concentrations on the outer LATEX shelf obtained from the May 1993 interdisciplinary survey, the total amount of nutrients was initially given as N_T =10 μ *mole* $N\,l^{-1}$. The maximum phytoplankton growth rate V_m was chosen as 1.38 d^{-1} in our model. This value was estimated from recent observational data in the surface water at a shallower station (near the 20-*m* isobath) west of the Atchafalaya River (Brown 1994). The diffuse attenuation coefficient k_{ext} = 0.1 m^{-1} was used for our model, which was calculated from the 1% light depths reported in Neuhard (1994) for spring.

Half saturation constant k_s for phytoplankton is a very species-specific parameter. Considering that over 300 species of phytoplankton were identified on the LATEX shelf, the estimation of this value from the literature is fairly general compared to the identified overall species. According to Lalli and Parsons (1993), k_s ranges from 0.01 to 0.1 for oligotrophic waters and from 0.5 to 2.0 for eutrophic coastal water. The value of k_s =1.0 was chosen in our model, which represented a mean value of oligotrophic middle-shelf water and eutrophic near-coastal water.

The maximum zooplankton grazing rate R_m and grazing efficiency of phytoplankton by zooplankton λ are variable parameters, which were reported to vary in a range of 0.16 to 1.5 d^{-1} and 0.1 to 2 μ *mole* $N\,l^{-1}$ (McAllister 1970; Frost 1972; Checkley 1980; Franks *et al.* 1986). Fahnenstiel *et al.* (1992) described the mean zooplankton grazing rate for several different types of phytoplankton in the Gulf of Mexico. The zooplankton grazing rates on the dominant phytoplankton species were described further in Fahnenstiel *et al.* (1995). The mean grazing value of R_m =0.5 d^{-1} and the grazing efficiency of λ = 0.5 were initially used in our model.

The assimilated fraction of phytoplankton by zooplankton (1-γ) is heavily influenced by the amounts of ingested phytoplankton and produced faeces. The efficiencies range from 30 to 80 %, while the majority is between 60 and 70 % (Raymont 1980; Franks *et al.* 1986). γ was chosen as 0.3 in our model, which represented an

assimilated efficiency of 70 % . This value was determined based on Franks *et al.* (1986) and Fuhrman (1992).

Phytoplankton and zooplankton death rates (ε and *g*) were derived from Franks *et al.* (1986). $\varepsilon = 0.1\ d^{-1}$ was used for our model, which gave an *e*-folding life time scale of 10 days for phytoplankton. A wide range of values for *g* were used in previous modeling studies (Steele 1974; Steele and Frost 1977; Steele and Henderson 1981; Franks *et al.* 1986; Franks and Chen 1996). The value of *g* used in those models ranged from 0.07 to 1.75 d^{-1}. Franks *et al.* (1986) chose $g = 0.2\ d^{-1}$ based on observational evidences of zooplankton death rate under the condition of no food (Checkley 1980; Dagg 1977). The same value for *g* was used for our model, which represented an *e*-folding life time scale of five days for zooplankton.

2.6. Design of Numerical Experiments

A schematic of numerical experiments of our coupled physical and biological model is shown in Fig. 3. The model domain featured a section cut from north to south across the LATEX shelf near the Atchafalaya River. The bottom topography along the section was taken from the hydrographic survey data and smoothed for our modeling purposes. The water depth was 20 *m* at the coast, gradually increased to 200 *m* at the shelf break, and then rapidly dropped to 500 *m* at the outer edge of the slope. Non-uniform grids were used in the horizontal. The horizontal resolution was 2 *km* within the region from the coast to 60 *km* off the slope, and then linearly increased to 20 *km* over an interval of 20 grid points outside the domain of interest. A uniform grid was used in the vertical. The vertical resolution in the σ coordinate system was 0.0167 (61 points in the vertical), which corresponded to a vertical resolution of 8.3 *m* in the deep region at the 500-*m* isobath and 0.3 *m* near the coast at the 20-*m* isobath.

The model was run as an initial value problem for a spring flooding case of the Atchafalaya River. The model was forced by a constant river discharge of 8,000 m^3/s at the coast. The outflow from the river contained a nitrate concentration of 20 $\mu\ mole\ N\ l^{-1}$.

The water quality data, measured in Morgan City, LA at the head of the Atchafalaya Bay, showed that the nitrate concentration of freshwater discharge at the Atchafalaya River ranged from 77 to 100 μ *mole* $N\,l^{-1}$ during April 28 and June 3, 1993. However, the nitrate concentration, measured at the northernmost station on Sec. 2 during the May 1993 LATEX interdisciplinary survey, was only about 14 μ *mole* $N\,l^{-1}$. It suggests that the nitrate concentration of the riverine water significantly decreased when the water was carried out onto the inner shelf from the Atchafalaya Bay. Since the main focus in this study was on the interaction of physical and biological processes with a simple 2-D model approach, we have chosen the nitrate concentration for the freshwater flux based on the extrapolated value from two closed points at the northernmost stations on Sec. 2.

The river discharge of the Atchafalaya River in 1993 was about 14,000 m^3/s in April and May and reduced to about 8,300 m^3/s in June. Observations showed that large amounts of fresh water were turned westward and flowed along the coast like a coastal trapped wave (Wiesman and Kelly 1994; Wiesman and Garvine 1995). Therefore, the actual offshore transport of fresh water on the 3-D shelf was much smaller than the flux measured in the river. As for as a 2-D model was used, we chose a reduced river transport to best resolve the location of the low-salinity front within the onset time scale of the Atchafalaya riverine plume.

The steady and variable winds were added into the model to examine effects of wind mixing and advections on the spatial distribution of biological production and plankton patches. Winds were imposed at the surface at the end of the 30th day when the density front was fully developed. A diurnal tidal forcing also was included later to estimate the contribution of tidal mixing on biological production.

We also used the physical part of the coupled model to study numerically the physical mechanism controlling the cross-shelf distribution of near-inertial oscillations on the LATEX shelf. A paper written based on model results was recently accepted by Journal of Geophysical Research (Chen and Xie 1996). Lagrangian studies of neutral-

density particle trajectories were conducted to examine the physical processes controlling the cross-frontal exchanges of water masses and marine organisms. Since the results were already reported to the ONR last year as a progress report, we have not included them in this report.

3. Model Results

3.1. Structure of the Density Front and Currents (Note: G: Modelling Results in section of "Results")

The model was first run prognostically as an initial problem forced only by the constant river discharge. A density (low-salinity) front formed after 10 model days (Fig. 5a). This front was intensified and moved offshore with time as the total amount of fresh water on the inner shelf increased. A typical inner-shelf density field was fully developed at the 30th model day, which created a stronger density frontal zone with a width of 30 *km* between 20 to 50-*m* isobaths (Fig. 5d). Large cross-shelf density gradients within the frontal zone generated a strong along-shelf current, which flowed westward with a maximum of about 160 *cm/s* at the surface at the 45-*m* isobath (Fig. 5e).

The cross-shelf current was characterized with a multiple cell circulation pattern that was developed with the evolution of the density front (Fig. 5c and f). When the density front just formed on the 10th model day, the cross-shelf circulation consisted of two cells: a clockwise cell on the inshore side of the front and a counterclockwise cell on the offshore side of the front. Multiple circulation cells were developed on the 25th day as a result of increasing freshwater discharge. Three significant cells were found within the frontal zone over a distance of about 50 *km*. Such a pattern remained unchanged as the density front moved slowly offshore with time (Fig. 5f).

The cross-shelf circulation on the offshore side of the front was characterized by a weak counterclockwise current, which flowed offshore in the deep region and returned to the onshore direction near the surface. On the inshore side of the front was a clockwise current, which flowed onshore near the bottom and offshore near the surface. The

maximum value of the cross-shelf current near the river was about 10 *cm/s*. The vertical velocity reached 0.02 *cm/s* within the frontal zone where multiple circulation cells were located.

3.2. Cross-Shelf Distributions of *P*, *Z*, and *N*

Fig. 6 shows the color images of *P*, *Z* and *N* at the end of the 30th model day for the case with only the constant river discharge. The biological field was significantly modified from their initial conditions. A maximum of phytoplankton biomass concentrations (about 14 to 15 μ *mole* $N\,l^{-1}$) developed throughout the whole water column close to the mouth of the river. A phytoplankton patch with a high biomass concentration of 7 to 8 μ *mole* $N\,l^{-1}$ formed at the outer edge of the density front, which stretched downward from the surface to the depth of about 20 *m*. Biomass concentrations of phytoplankton were lower within the frontal zone between 20 to 60-*m* isobaths. The mean value of concentrations was only about 0.1 μ *mole* $N\,l^{-1}$. Relatively high phytoplankton concentrations also were found in the upper 15 *m* on the outer shelf outside the frontal zone.

Phytoplankton distributions were reflected directly by the dissolved nutrient distributions, which showed lower values throughout the whole water column in the inner-shelf region about 7 to 20 *km* away from the coast, and in the upper 10 *m* at the outer edge of the density front and on the outer shelf outside the frontal zone. The maximum value of nutrient concentrations was found in the upper 10 *m* over a region of 7 *km* from the coast, which was consistent with lower phytoplankton concentrations over there. A high nutrient concentration dome developed near the bottom within the frontal zone between 20- and 40-*m* isobaths. The maximum value of nutrient concentrations in the dome was about 12 μ *mole* $N\,l^{-1}$. Distributions of the nutrients predicted by our model closely resembled those observed from the May 1993 LATEX interdisciplinary survey (see Fig. 1).

Distributions of the nutrients outside the frontal zone about 90 *km* away from the coast was characterized by a tongue-like structure. Dissolved nutrients, ranging from 6 to 11 μ *mole* $N\,l^{-1}$, were pumped from the deep region and extended upward to the surface at the outer edge of the frontal zone, which resulted in a large gradient of the nutrients at the edge of the density front between inner-shelf low-salinity and outer-shelf saline waters.

Zooplankton populations had their maxima of about 8 to 10 μ *mole* $N\,l^{-1}$ in the region between 10 and 30 *km* away from the coast. A patch with an immediate high biomass of 3 to 4 μ *mole* $N\,l^{-1}$ also was found at the outer edge of the density front, which corresponded to the high biomass concentration of phytoplankton in that region. It should be pointed out here that no swimming and other behaviors of zooplankton were included in the present model. Since no zooplankton data were available from the May 1993 LATEX interdisciplinary survey, it was difficult to check our model for zooplankton prediction. For this reason, we will focus our discussions on nutrients and phytoplankton here.

3.3. Nutrient Uptake and Regeneration

Nutrient uptakes by phytoplankton were defined by the first term on the right-side of the phytoplankton equation (2.10), which were controlled by the maximum phytoplankton growth rate, the incident irradiance, the half-saturation constant, and the biomass concentration of phytoplankton and nutrients. The regeneration of nutrients was defined as the sum of zooplankton excretion, and phytoplankton and zooplankton death rates on the right-side of the nutrient equation (2.12). Franks and Chen (1996) calculated the fraction of new nutrient production to total nutrient production by a *f*-ratio defined as the ratio of the difference between the nutrient uptake and regeneration to the nutrient uptake, *i.e.*, (uptake – regeneration)/uptake. They defined the nutrient uptake as total production, and regenerated nutrients as recycled production. In this way, the new production equaled the difference between uptaked and regenerated nutrients. We adopted their definition in the present study.

The right panel of Fig. 6 shows the nutrient uptake and regeneration as well as the *f*-ratio estimated based on the biomass concentration of *P*, *Z*, and *N* at the end of the 30th day. The highest nutrient uptakes of about 5 μ *mole* $N\,l^{-1}$ were found throughout the whole water column within a relatively wide region near the coast, and also in the upper 10 *m* at the outer edge of the density front. Between these two high nutrient uptake zones was a wider region characterized with a very low uptake rate. The mean value of nutrient uptakes in that region was about 0.5 μ *mole* $N\,l^{-1}$ near the surface and decreased down to 0.01 μ *mole* $N\,l^{-1}$ near the bottom.

Cross-shelf distributions of the nutrient regeneration were similar to those of nutrient uptakes and zooplankton biomass. The highest regeneration of 4 μ *mole* $N\,l^{-1}$ was found throughout the whole water column in a region between 10 and 30 *km* away from the coast. An immediate high regeneration patch, ranging from 1 to 2.5 μ *mole* $N\,l^{-1}$, also was found in the upper 15 *m* at the outer edge of the density front. Between these two regions was a dome-like region characterized with a very low regeneration rate. The value of nutrient regeneration in this area was about 0.01 near the bottom and increased up to 0.5 near the surface.

Using Franks and Chen (1996)'s definition described above, we also calculated the *f*-ratio across the shelf. The results also showed two high new production regions: one near the coast and another at the outer edge of the density front. The first was wider at the surface and became narrower with depth. The second was limited to the upper 15 *m*, widest at the surface and extended downward like an tongue. The maximum new production rate in these two regions was about 1.0 to 1.5 μ *mole* $N\,l^{-1}$. Between these two high production zones was a wider region with a very low new production. This region occupied a large portion of the frontal zone, suggesting that the bottom-rich nutrient pattern found within the frontal zone was caused by the interaction of physical and biological processes rather than biological production itself.

3.4. Comparisons with Observations

A data set for nitrate and chlorophyll *a* was taken from bottles samples during the May 1993 interdisciplinary survey on the LATEX shelf. The horizontal resolution of these samples was about 5 to 10 *km* in nitrate and about 20 to 30 *km* in chlorophyll *a*. The data taken on Sec. 2, the closest section to the Atchafalaya River, were used for comparison with our model results. The distribution of observed nitrates near the bottom agreed both qualitatively and quantitatively with model results in the inner shelf within the frontal zone (Fig. 8a). The distribution of observed chlorophyll *a* near the surface also agreed well with model results in the inner shelf within the frontal zone (Fig. 8b). Poor agreement was found on the outer shelf for both nitrate and phytoplankton. The basic patterns of predicted and observed nitrates were the same on the outer shelf. However, the concentration of predicted nutrients was higher than observations. Similarly, the predicted phytoplankton biomass concentration on the outer shelf was too high compared with the observed chlorophyll *a* data.

Poor agreements in phytoplankton over the outer shelf were probably in part due to the poor sample resolution and missing of sinking behavior of phytoplankton. Since the chlorophyll *a* samples were taken with a separation scale of about 30 *km* between 35- and 55-*m* isobaths, the observation failed to resolve the high biomass patch of phytoplankton at the outer edge of the density front.

A sinking speed of 1 $m\ d^{-1}$ was specified for phytoplankton on the 30th model day. The inclusion of such a constant sinking velocity resulted in a subsurface phytoplankton maximum outside the density frontal zone, which provided a much better comparison between model results and observations. In addition, the model results with sinking showed very little influences on the distribution of phytoplankton in the inner shelf. This suggests that the sinking was not prerequisite for the formation of high phytoplankton zone near the river and the patch at the outer edge of the density front.

The increase of nutrient concentrations near the bottom between 20 to 40-*m* isobaths, found in the sinking case on the end of the 35th day, resulted from the evolution of nutrients with time but with nothing related to sinking of phytoplankton.

3.5. Wind Effects

The synoptic-scale meteorological field on the LATEX shelf in spring and summer was dominated by a southeasterly wind. Such a wind filed, however, was intermittently altered with the air frontal passages associated with low-pressure cells (Chen *et al.* 1996). The typical time scale of a frontal passage was about 5 to 7 days. In general, the wind was southeastward during the first 2 to 3 days and then reversed to become northwestward after the front passed. Although some efforts were made to examine oceanic responses of the LATEX shelf to local and global winds (Cochrane and Kelly 1986; Chen *et al.* 1996; Lewis and Reid 1985), effects of the wind on biological production have not well explored in the inner LATEX shelf.

To examine the contribution of the wind on biological production, we added the surface wind stress into the model at the end of the 30th day, at a time after the density front fully developed and the bottom-rich nutrient pattern formed within the frontal zone. Three types of the wind forcing were considered: (1) upwelling-favorable winds, (2) downwelling-favorable winds, and (3) variable winds associated with frontal passages. The wind direction was defined by the degree from which the wind blew and was measured clockwise from north. The upwelling-favorable wind referred to the wind blowing eastward along the shelf, while the downwelling-favorable wind referred to the wind blowing westward. The magnitude of the wind was specified as 5 *m/s* for all three cases.

Upwelling-favorable winds. When a constant upweling-favorable wind started blowing at the surface, the density and current fields were destroyed. As a result, the buoyancy-induced, along-shelf westward current significantly weakened over the shelf, especially near the coast where the current reversed to the east as the same direction as wind. The density front was pushed away from the coast by an offshore, near-surface Ekman transport, and in turn the deep denser water flowed onto the shelf in the subsurface through the bottom (Fig. 8a). This process resulted in a single circulation cell

across the shelf, with a relatively strong upwelling near the coast, a narrow offshore flow near the surface, and a compensate onshore flow in the deep region.

The biological field also was altered with the response to the change of the physical field. The wind tended to speed up the offshore (onshore) migration of phytoplankton and nutrients in the upper layer (in the lower layer from the mid-depth to the bottom). This process significantly reduced (increased) the horizontal (vertical) gradient of biological production. As a result, a long lens of high phytoplankton biomass formed in the upper 10 *m* within the low-salinity water (Fig. 8b). The dome-like bottom-rich nutrient pattern, which was originally located on the 20 to 40-*m* isobaths, was stretched shoreward to the coast (Fig. 8c).

Downwelling-favorable winds. In this case, the wind drove oceanic dense water onshore in the upper layer and hence enhanced vertical mixing in the frontal zone. As a result, the density contours became straight lines intersected with the surface and the bottom.

The wind-enhanced turbulent mixing also produced the vertically uniform structure of phytoplankton and nutrients over the shelf. The region of high phytoplankton biomass near the coast, which was originally narrower near the surface and wider near the bottom, became much uniform in both the vertical and horizontal. The patch of the high phytoplankton biomass, formed at the outer edge of the density front, extended downward to a depth of 40 *m* near the bottom. The bottom-rich nutrients between 20- and 40-*m* isobaths were mixed up to the surface and led to vertically-uniform bars within the frontal zone.

Variable winds. The variable wind used in this study was specified as a sinusoid function with a period of 5 days. The wind started blowing eastward at the end of the 30th day and reversed to become westward at the 32.5th day. The maximum of eastward wind (upwelling-favorable) occurred at 31.25 days, 30 hours after the wind started, while the

westward wind (downwelling-favorable) reached its maximum at 33.75 days, 90 hours after the wind blew.

Similar to the case with the constant upwelling wind, the varying wind stress during the period of upwelling also tended to speed up the offshore movement of low-salinity water in the upper layer and the onshore movement of dense water in the deep region. This process resulted in the tilted density front towards the offshore direction (Fig. 9a). A broad high biomass patch of phytoplankton was found near the coast, which was wider near the surface and became narrower with depth (Fig. 9b). The bottom-rich nutrient pattern was shrunk in the vertical and stretched shoreward in the horizontal (Fig. 9c).

When the wind reversed to become westward, both physical and biological fields responded rapidly. The density, phytoplankton, and nutrients became vertically uniform near the coast just one day after the wind reversed (Fig. 9d, e, f). However, since the duration of downwelling wind was too short to mix biological variables in the region deeper than 20 *m*, the bottom-rich nutrient pattern still existed within the frontal zone, though its size significantly reduced (Fig. 9f).

Time evolution of the biological field under different wind forcings also was examined. For example, time sequences of N and P at the surface and bottom at a location with 5 *km* away from the coast are shown in Fig. 10 for upwelling, downwelling, and variable winds. In the upwelling case, nutrients at the surface decreased to 9 μ *mole* $N\,l^{-1}$ in the first one and half days and then rapidly increased up to 15.5 μ *mole* $N\,l^{-1}$ in the rest of times. Correspondingly, the phytoplankton at the surface rapidly increased up to 1.7 μ *mole* $N\,l^{-1}$ in the first two days, and then decreased again in the rest of times. Time series of nutrients and phytoplankton at the bottom were very similar to that at the surface, except for smaller amplitudes and phase shifts.

Enhanced vertical mixing due to downwelling winds caused an increase (a decrease) in nutrients (phytoplankton) during all the time, even though the growth rate

was much smaller than that in the upwelling case. N was up to 14 μ *mole* $N\,l^{-1}$ at the end of the 35th day, while P dropped close to zero after 5 days. The variation of P and N in the variable wind case was very similar to those in the upwelling and downwelling cases, even though the duration of upwelling and downwelling winds in this case was shorter.

3.6. Tidal Effects

Tides were weak on the LATEX shelf (Reid and Whitaker 1981). Previous observations of sea surface elevation near the coast showed that the most significant tidal constituents in this region were diurnal tides. Ried and Whitaker (1981) numerically simulated the astronomical tides in the Gulf of Mexico. By tuning the model to best fit the available coastal tidal data, they provided the cotidal charts of semidiurnal and diurnal tides in the entire Gulf. The cotidal charts for diurnal O_1 and K_1 showed that, at the central LATEX shelf, the amplitude of the tidal elevation was about 14 *cm* at the 500-*m* isobath and then increased up to 18 *cm* at the coast. Based on this information, we added tidal forcing into the model by specifying a barotropic K_1 tidal elevation with an amplitude of 14 *cm* at the southern open boundary.

The inclusion of diurnal tidal forcing didn't change the distribution of biological field (Fig. 11). The weak tidal mixing did reduce the biomass concentration near the bottom where a high nutrient dome was located. The phytoplankton was a tittle enhanced near the coast, and also the region of maximum zooplankton biomass was horizontally shrunk near the surface.

3.7. Sensitivity Analyses

Our model results are quite robust in a qualitative aspect with regard to a good agreement with observations for nutrients and phytoplankton on the onshore side of the density front. Basic distribution patterns of N and P kept similar within and outside the frontal zone under a wide range of biological parameters, even though the values of biomass concentrations were sensitive to parameters. We have run the model with a range of the maximum growth rate of phytoplankton V_m, the maximum grazing rate R_m, the

grazing efficiency of phytoplankton by zooplankton λ, the half-saturation constant of phytoplankton k_s; the fraction of ingested the fraction of ingested γ, and the nutrient concentration of freshwater discharge N_f. Some of these results are shown in Fig.12 for examples.

Previous studies in the Gulf of Mexico suggested that the maximum phytoplankton growth rate ranged from about 0.1 to 3.0 d^{-1} (Fahnenstiel *et al.* 1992; Fahnenstiel *et al.* 1995; Brown 1994; Bierman *et al.* 1994). Bierman *et al.* (1994) applied a preliminary mass balance model to study primary productivity and dissolved oxygen in the Mississippi River plume over the inner LATEX shelf. They found that maximum growth rates at ambient temperatures can be up to 3.0 d^{-1} due to high water temperature during summer. The growth rate significantly reduced due to nutrient and light limitations, and the actual specific growth rates ranged between 1.0 d^{-1} and 1.2 d^{-1} in the inner shelf near the Mississippi Delta. These values were closed to the observed value (1.38 d^{-1}) found by Brown (1994) at the measurement station west of the Atchafalaya River. Based on these data, we suggest here that maximum phytoplankton growth rates over the inner LATEX shelf range between 1.0 d^{-1} and 1.4 d^{-1}.

While the maximum phytoplankton growth rate V_m reduced to 1.0 d^{-1}, basic patterns of the biological field within and outside the density frontal zone remained similar at the end of the 30th model day. However, the variation tendency of P and N near the coast was significantly modified. The time at which the maximum nutrients and phytoplankton occurred delayed about 5 days compared with the case with $V_m = 1.38\ d^{-1}$ (Fig. 12b).

Another example can be seen for the grazing efficiency of phytoplankton by zooplankton λ. Previous studies suggested a range of λ between 0.1 and 2 μ *mole* $N\,l^{-1}$ in the inner LATEX shelf (Fahnenstiel *et al.* 1995). While λ increased up to 0.8, the evolution of phytoplankton, zooplankton and nutrients showed little changes near the coast and inside the frontal zone (Fig. 12c).

Basic patterns of the biological field were insensitive to the increasing values of nitrate concentration of freshwater water discharges. While N_f increased from 20 μ *mole* $N\,l^{-1}$ up to 40 μ *mole* $N\,l^{-1}$, the basic patterns of P, Z, and N kept unchanged, even though the values of biomass concentration significantly increased (Fig. 12d). We also ran the model with even big values of N_f (for example, N_f = 60 μ *mole* $N\,l^{-1}$) and found that the resulting patterns of P, Z, and N just liked the enlarged pictures of those with smaller N_f.

3.8. Discussions

Similar to observations, the model predicted a dome-like pattern of nitrate with a maximum concentration near the bottom within the frontal zone. The fact that this dome was located in the region with a very low new production rate of nutrients suggests that occurrence of such a pattern was closely related to the interaction of biological and physical processes.

Model-predicted cross-shelf circulation after 20 model days was characterized with a surface-intensified offshore current near the coast and multiple cells inside the frontal zone (Fig. 5f). Cross-shelf currents were very weak near the bottom, even in the frontal zone where multiple cells existed. In addition to recycled and new productions of nutrients through biological processes, the model shows that nutrients in the frontal zone was supported physically by two sources: (1) horizontal advection from the river discharge and (2) advection- and diffusion-induced upward nutrient flux outside the frontal zone on the shelf. Mutiple cells in the frontal zone acted like a retention zone that recirculated the nutrients in the vertical and also restricted marine organisms from cross-frontal exchanges. However, since these cells were not completely closed in the vertical, especially near the bottom and surface, parts of marine organisms might settle down near the bottom in the weak flow region as they were advected along instantaneous streamlines from the river into the frontal zone.

The e-folding vertical scale of light efficiency was about 10 *m* in our model. The limitation restricted the efficient utilization of nutrients by phytoplankon to the upper 10

m euphotic zone. Since the uptake rate of nutrients by phytoplankton was larger near the surface than near the bottom, the nutrients were rapidly utilized by phytoplankton when they were advected to the upper layer from either the outside sources or recirculations by multiple cells. Therefore, no high concentration dome was possible to form near the surface in the frontal zone where cross-shelf currents were dominated by multiple cells.

A relatively longer time of about 25 to 30 days was found to form a high concentration dome of nutrients in the weak flow region near the bottom inside the frontal zone. This supports the settle-down mechanism of nutrients by the cross-shelf secondary circulation in the frontal zone. Physical processes caused formation of large concentration of nutrients in the weak current region within the frontal zone, and then biological processes limited the increase of nutrients in the upper euphotic zone and hence led to the bottom-rich nutrient pattern.

It should be pointed out here that our present model ignored the along-shelf advecton of nutrients from the Mississippi Rivers. In spite of this, our 2-D model successfully re-produced the basic observed patterns of nutrients and phytoplankton in the inner LATEX shelf where the Atchafalaya River discharge was dominant. This suggests that the 2-D model has captured the basic dynamics of biological and physical processes in that particular region.

3.9. Conclusions

A simple 2-D coupled physical and biological model of the plankton has captured the main features of phytoplankton and nutrients over the inner LATEX where the river discharge was a dominant physical forcing. The model re-produced a well-defined high concentration dome of nutrients near the bottom within the frontal zone. The model also predicted a high concentration patch of phytoplankton that was developed near the surface at the outer edge of the density front.

The model results were in a reasonable agreement with field measurements taken from the May 1993 interdisciplinary survey on the LATEX shelf. The formation of bottom-rich nutrient pattern in the frontal zone was probably caused by the interaction of physical and biological processes associated with the settle down mechanism of nutrients through the cross-shelf secondary circulations and spatial variation of nutrient uptakes and regenerations.

Estimates of nutrient uptakes and regenerations from the coupled model showed that the uptakes and regenerations were higher in the whole water column near the coast and in the upper layer at the outer edge of the density front. The maximum value of nutrient uptakes was about 5 μ *mole* $N\,l^{-1}$. The maximum value of nutrient regenerations was about 3.5 to 4.0 μ *mole* $N\,l^{-1}$ near the coast and 1.5 to 2 μ *mole* $N\,l^{-1}$ at the outer edge of the density front. The new production of nutrients also was high near the coast and in the upper 10 *m* at the outer edge of the density front. Most of the region inside the frontal zone, especially near the bottom, was characterized with low nutrient uptakes and regenerations as well as low new productions.

Cross-shelf distributions of the biological field were significantly modified by upwelling-favorable wind through the Ekman transport mechanism. The downwelling-favorable wind tended to enhance the vertical mixing and caused more vertically uniform pattern of nutrients, phytoplankton, zooplankton. Modification of the biological field due to variable winds associated with air frontal passages depended on the amplitude and duration of winds. Tidal mixing was too weak to make a contribution to the basic distribution of biological productions within the frontal zone over the inner LATEX shelf.

Acknowledgments

Modeling studies were supported by the ONR grants under subcontract number RR50905F to University of Georgia (C. Chen). We want to think Liusen Xie for assistance in routine runs of model experiments, and also Paul Bobntempi for providing information about the biological parameters used in the model. Physical and biological data used in this study were kindly provided by the LATEX A Program at Texas A&M University. LATEX A program was supported by the Minerals Management Services of the U.S. Department of the Interior, under OCS contract number 14-35-0001-30509.

Literature Cited

Blumberg, A.F., 1994. A primer for ECOM-si. Technical Report of HydroQual, Inc., 66p.

Blumberg, A. F., and G. L. Mellor, 1987. A description of a three-dimensional coastal ocean circulation model. In: *Three-Dimensional Coastal Ocean Model*, N. S. Heaps (Ed), *Coastal and Estuarine Sci.*, **4**, 1-16.

Bierman, V. J. Jr., N. N. Rabalais, S. C. Hinz, R. E. Turner, and W. J. Wiseman, Jr, 1994. A preliminary mass balance model of primary productivity and dissolved oxygen in the Mississippi River plume/inner gulf shelf region. *Estuaries*, **17**, 886-899.

Brown, S. L., 1994. Microzoplankton grazing along the northwestern continental shelf of the Gulf of Mexico. M.S. thesis. University of Texas at Austin. 124pp.

Casulli, V., 1990. Semi-implicit finite-difference methods for the two-dimensional shallow water equations. *J. Computational Physics*, **86**, 56-74.

Chapman, D. C., 1985. Numerical treatment of cross-shelf open boundaries in a barotropic coastal model. *J. Phys. Oceanogr*, **15**, 1060-1075.

Checkley, D. M., 1980. The egg production of a marine planktonic copepod in relation to its food supply: laboratory studies. *Limnol. Oceanogr.*, **25**, 430-446.

Chen, C. and R. Beardsley, 1995. Numerical study of stratified tidal rectification over finite-amplitude banks. part I: symmetric banks. *J. Phys. Oceanogr.*, **25**, 2090-2110.

Chen, C., R. Beardsley, and R. Limeburner, 1995a Numerical study of stratified tidal rectification over finite-amplitude banks. Part II: Georges Bank. *J. Phys. Oceanogr.*, **25**, 2111-2128.

Chen, C., R. Reid, and W. D. Worth, Jr., 1996. Near-inertial oscillations over the Texas-Louisiana shelf. *J. Geophys. Res.*, **101**, 3509-3524.

Chen, C. and L. Xie, 1996. Numerical studies of near-inertial oscillations over the Louisiana-Texas shelf. *J. Geophys. Res*, accepted.

Cochrane, J. D. and F. J. Kelly, 1986. Low-frequency circulation on the Louisiana-Texas shelf. *J. Geophys. Res.*, **88**, 2615-2620.

Dagg, M., 1977. Some effects of patchy food environments on copepods. *Limnol. Oceanogr.*, **22**, 99-107.

Dinnel, S. P., and W. J. Wiseman, Jr, 1986. Fresh water on the Louisiana and Texas shelf. *Continental Shelf Res.*, **6**, 765-784.

Fahnenstiel, G. L., M. H. Marcowitz, M. J. McCormick, D. G. Redalje, S. E. Lohrenz, H. J. Carrick, and M. J. Dagg, 1992. High growth and microzoplankton grazing loss rate for phytoplankton populations from the Mississippi River plume region. In: *Nutrient Ehanced Coastal Ocean Productivity Publication Number TAMU-SG-91-109*. Sea Grant Program TAMU Calveston, Texas, 111-116.

Fahnenstiel, G. L., M. J. McCormick, G. A. Lang, D. G. Redalje, S. E. Lohrenz, M. H. Marcowitz, B. Wagoner, and H. J. Carrick, 1995. Taxon-specific growth and loss rates for dominant phytoplankton populations from the northern Gulf of Mexico. *Mar. Ecol. Prog. Ser.*, **117**, 229-239.

Flint, R. W. and D. Kamykowski, 1984. Benthic nutrient regeneration in south Texas coastal waters. Estuarine, *Coastal and Shelf Sci.*, **18**, 221-230.

Franks, P. J. S., and C. Chen, 1996. Plankton production in tidal fronts: a model of Georges Bank in summer. *J. Mar. Res.*, in press.

Franks, P. J.S. Wroblewski, and G. R. Flierl, 1986. Behavior of a simple plankton model with food-level acclimation by herbivores. *Mar. Biol.*, **91**, 121-129.

Frost, B. W., 1972. Effects of size and concentration of food particles on the feeding behavior of the marine planktonic copepod Calanus pacificus. Limnol. Oceanogr. **17**, 805-815.

Fuhrman, J., 1992. Bacterioplankton roles in cycling of organic matter: the microbial food web. In: *Primary Productivity and Biogeochemical Cycle in the Sea*, P. G. Falkowski and A. D. Woodhead, eds., Plenum Press, New York, 361-384.

Galperin, B., L. H. Kantha, S. Hassid, and A. Rosati, 1988. A quasi-equilibrium turbulent energy model for geophysical flows. *J. Atm. Sci.*, **45**, 55-62.

Kamykowsji D. and J. L. Bird, 1981. Phytoplankton associations with the variable nepheloid layer on the Texas continental shelf. Estuarine, *Coastal and Shelf Sci.*, **13**, 317-326.

Lalli, C. M. and T. R. Parsons, 1993. The effects of nutrients on growth rates. In: *Biological Oceanography - An Introduction*, Pergamon Press, New York, p. 63.

Lewis, J. K. and R. O. Reid, 1985. Local wind forcing of a coastal sea at subinertial frequencies. *J. Geophys. Res.*, **94**, 8163-8178.

Lohrenz, S. E., M. J. Dagg, and T. E. Whitledge, 1990. Enhanced primary production at the plume/oceanic interface of the Mississippi River. *Continental Shelf Res.*, **10**, 639-664.

MaAllister, C. D., 1970. Zooplankton rations, phytoplankton mortality and the estimation of marine production. In: *Marine food chains.* J. H. Steele (ed). Berkley: University of California Press.

Mellor, G. L. and T. Yamada, 1974. A hierarchy of turbulence closure models for planetary boundary layers. *J. Atm. Sci.*, **33**, 1791--1896.

Mellor, G. L. and T. Yamada, 1982. Development of a turbulence closure models for geophysical fluid problem. *Rev. Geophys. Space Phys.*, **20**, 851-875.

Neuhard, C. A., 1994. Phytoplankton distributions across the Texas-Louisiana shelf in relation to coastal physical processes. MS thesis. Texas A&M University, pp205.

Raymont, J. E. G. (Ed), 1980. *Plankton and productivity in the oceans*: *vol.2*: *zooplankton*, Pergamon Press, New York.

Reid, R. O. and R. E. Whitaker, 1981. Numerical model for astronomical tides in the Gulf of Mexico: theory and application. *Technical report of the department of oceanography*, Texas A&M University, College Station, TX 77843, 115pp.

Riley, G. A., 1937. The significance of the Mississippi River drainage for biological conditions in the northern Gulf of Mexico. *J. Mar. Res.*, **1**, 60-74.

Rowe, G. T., C. H. Clifford, K. L. Smith Jr., 1975. Benthic nutrient regeneration and its coupling to productivity in coastal waters. *Nature*, **225**, 215-217.

Sahl, L. E., W. J. Merrell, and D. C. Biggs, 1993. The influence of advection on the spatial variality of nutrient concentrations on the Texas-Louisiana continental shelf. *Continental Shelf Res.*, **13**, 233-251.

Shiderler, G. L., 1975. Development of the benthic nepheloid layer on the south Texas continental shelf, western Gulf of Mexico. *Mar. Geol.*, **41**, 37-61.

Sklar, F. H. and R. E. Turner, 1981. Characteristics of phytoplankton off Barataria Bay in an area influenced by the Mississippi River. *Contr. Mar. Sci.*, **24**, 93-106.

Steele, J. H., 1974. The Structure of Marine Ecosystems. Cambridge, Harvard University Press, 128pp.

Steele, J. H. and B. W. Frost, 1977. The structure of plankton communities. *Phil. Trans. R. Soc. Lond.* **280**, 485-534.

Steele, J. H. and E. W. Henderson, 1981. A simple plankton model. *Am. Nat.*, **117**, 676-691.

Wiseman, W. J. Jr. and F. J. Kelly, 1994. Salinity variability within the Louisiana coastal current during the 1982 flood season. *Estuaries*, **17**(4), 732-939.

Wiseman, W. J. Jr. and R. W. Garvine, 1995. Plumes and coastal currents near large river mouths. *Estuaries*, **18**(3), 509-517.

Wiesenburg, D. A, and L. E. Sahl, 1994. A comparison of hydrographic conditions on the Texas-Louisiana shelf in August 1992 and 1993. The 1994 Ocean Sciences Meeting, ***EOS***, *Trans.*, **75** (3), 65.

Wright, D. G. and J. W. Loder, 1985. A depth-dependent study of the topographic rectification of tidal currents. *Geophys. Astrophys. Fluid Dyn.*, **31**, 169-220.